METEOROLOGY HYDROLOGY AND WATER MANAGEMENT
IMGW-PIB Science Journal since 2013

VOL. 8 | ISSUE 2 | 2020

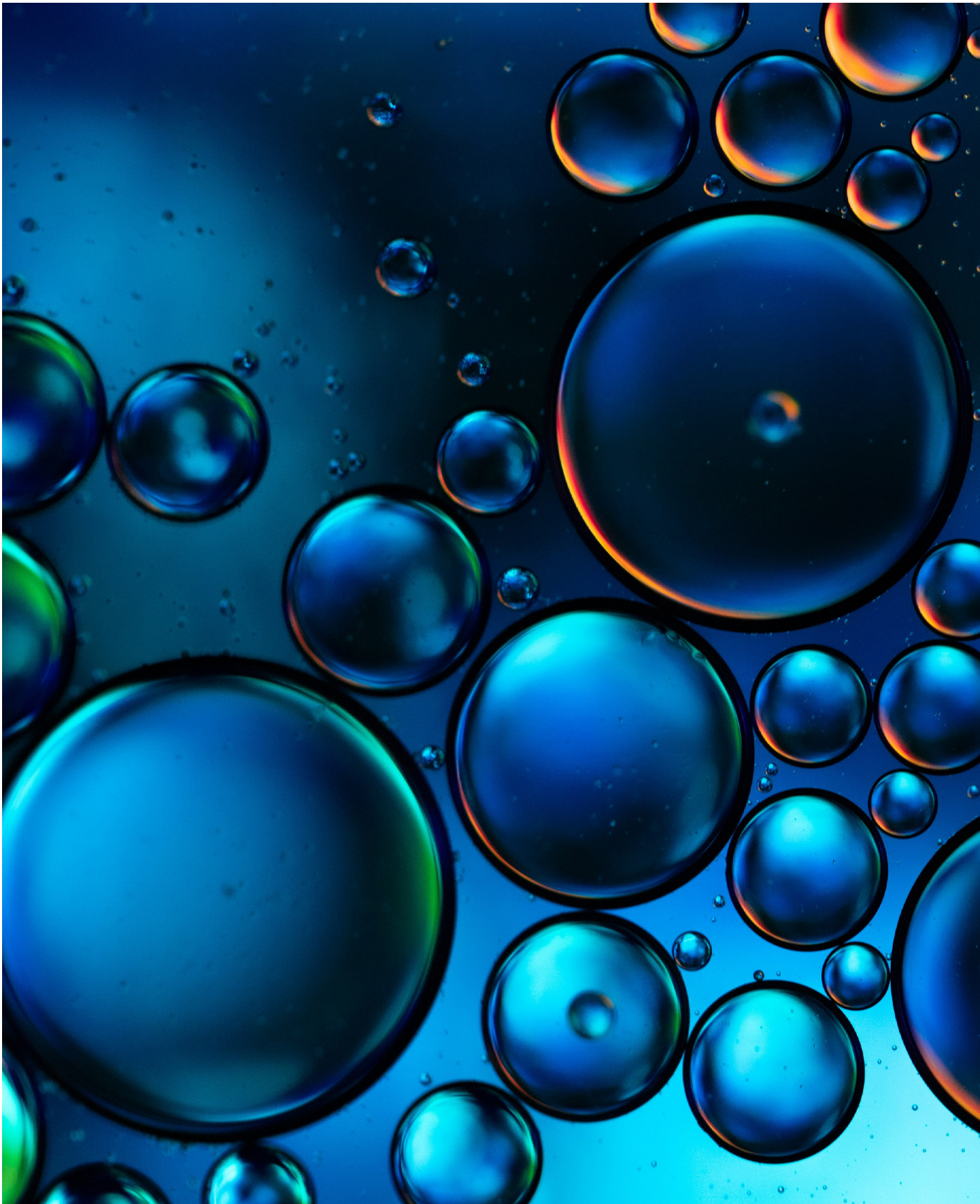

ISNN 2299-3835 | POLISH INSTITUTE OF METEOROLOGY AND WATER MANAGEMENT – NATIONAL RESEARCH INSTITUTE

Dear audience,

it was a tough year, marked by the struggle of the world community with the global COVID-19 pandemic. Lockdown and communication restrictions also affected the scientific community at that time. Against all odds, we managed to keep the work going and publish new issues of the MHWM magazine.

MHWM would like to thanks to authors and reviewers. Thank you for trust, support and understanding. It is you who determine the quality and brand recognition of the magazine. That is why we invite again to publish new articles in the MHWM magazine and promote our content among colleagues from the world of science.

We would like to thank members of the Advisory Board: Mr. Kazimierz Banasik, Mr. Christian Bernhofer, Mr. Günter Blöschl, Mr. Dawei Han, Mr. Ni Jinren, Mr. Zbigniew Kundzewicz, Mr. Henny van Lanen, Mr. Artur Radecki-Pawlik and Mr. Paweł Wielgosz, for supporting the magazine and promoting it on the international publishing arena. We invite you to further cooperation and look forward to your remarks and comments on the Journal's Publishing Policy. We want to work even more closely with you to improve the image and quality of the magazine.

Words of appreciation to colleagues from the Editorial Board team who, in the difficult circumstances of remote work and despite accumulating official duties, ensured a friendly and professional working atmosphere. Thanks to your commitment, we can look into the future with hope and set new goals and challenges.

Next few years will be a time of rebuilt. The global economy has to recover from the recession. This is a big chance for science to play a key role in this process. We must re-trust the scientific authorities and undertake ambitious tasks for a better future. An extremely important element of this post-COVID order will be to deal with challenges posed by global warming and climate change. Science, and in particular such fields as Earth Sciences and Environmental Engineering, must return to the arena of international discussions about the future of our planet and the human species.

Best regards

Prof. Mariusz Figurski
Editor in Chief
Director of Centre of Numerical Weather Prediction IMGW-PIB

MHWM – Meteorology Hydrology and Water Management is issued by
Polish Institute of Meteorology and Water Management
– National Research Institute
01-673 Warsaw, Podleśna 61, Poland
www.imgw.pl
ISNN 2299-3835

MHWM EDITORIAL OFFICE
Institute of Meteorology and Water Management – National Research Institute
01-673 Warsaw, Podleśna 61, Poland
T: +48 22 56 94 510 | E: mhwm@imgw.pl

SWOT analysis of the Institute of Meteorology and Water Management – National Research Institute in the context of World Meteorological Organization Reform adopted during its 18th Congress

Tomasz Walczykiewicz
Institute of Meteorology and Water Management – National Research Institute, Podleśna 61, 01-673 Warszawa, Poland,
e-mail: tomasz.walczykiewicz@imgw.pl

Janusz Filipiak
University of Gdańsk, Faculty of Oceanography and Geography, Jana Bażyńskiego 8, 80-309 Gdańsk, Poland

DOI: 10.26491/mhwm/124787

ABSTRACT. This article is an analysis of how the World Meteorological Organization (WMO) constituent bodies governance reform (WMO Reform) can affect the activities of the Polish National Hydrological and Meteorological Service. The analysis employs the SWOT (Strengths, Weaknesses, Opportunities, Threats) model. The World Meteorological Congress is the highest authority of the World Meteorological Organization, whose findings guide the operations of the WMO and the National Meteorological and Hydrological Services (NMHSs) globally. During the 18th Congress, in June 2019, discussions covered the routine operations of the WMO and its Secretariat, the status and development prospects of all the Organization's research and technical programs, and the Organization's budget for the 18th financial period beginning in 2020. The key actions of the Congress, however, were the election of the WMO senior officers and final approval (after thorough discussion) of the WMO Reform of its governance structure. The purpose of the Reform is to ensure better preparation of the organization for the challenges of the present and future, such as climate change and its impact, the growing number and intensity of extreme weather events, environmental degradation, and increasing urbanization. The tasks of the National Hydrological and Meteorological Service in Poland are performed by the Institute of Meteorology and Water Management – National Research Institute (IMGW-PIB), in accordance with the provisions of the Water Law.

KEYWORDS: Meteorology, hydrology, WMO, reform, analysis.

SUBMITTED: 3 February 2020 | **REVISED:** 20 April 2020 | **ACCEPTED:** 29 June 2020

1. INTRODUCTION

The World Meteorological Organization (WMO) is an intergovernmental organization of 193 members based in Geneva. It was established in 1950 as a transformation of the International Meteorological Organization (IMO) that had been founded in 1873. The treaty establishing the organization was signed on October 11, 1947 (Convention 1947), and took effect on March 23, 1950. In commemoration, this date is celebrated annually as World Meteorological Day. Since March 17, 1951, WMO has been a specialized agency of the United Nations with the mission to standardize, improve, and exchange meteorological information and to support climatological, hydrological, oceanographic, and environmental studies. The main task of the WMO is to organize and coordinate the activities of meteorological services of various countries, by unifying meteorological observation methods and disseminating weather forecasts. Every four years the World Meteorological Congress, the WMO's supreme governing body, meets in Geneva. Its findings guide the operations of WMO and the National Meteorological and Hydrological Services (NMHS) throughout the world. During the 18th Congress in June 2019, routine topics of discussion included the operations of the WMO and its Secretariat, the status and development prospects of all the Organization's research and technical programs, and the Organization's budget for the 18th financial period beginning in 2020. The key points of the Congress, however, were (1) the election of the WMO Secretary General, President, three Vice-Presidents, and members of the Executive Council for new four-year terms of office; and (2) a final thorough discussion and approval of the WMO constituent bodies governance reform (WMO Reform). The Reform is intended to ensure better preparation of WMO and its members and their National Hydrological and Meteorological Services for the challenges of the present and future, such as climate change and its impacts, the growing number and intensity of extreme weather events, environmental degradation, and increasing urbanization.

Poland, one of the founding members, has belonged to the WMO since 1947. The tasks of the National Hydrological and Meteorological Service in Poland are performed by the Institute of Meteorology and Water Management – National Research Institute (IMGW-PIB). The statutory responsibility of the IMGW-PIB is to monitor atmospheric and hydrological processes with sufficient coverage to support forecasting and early warning of threats to public safety, health, and life of citizens and property. The agency also conducts long-term, complex research in the areas of meteorology, hydrology, water management, and oceanography, directed toward steady improvement in forecasting complex atmospheric and hydrological phenomena and their consequences. IMGW-PIB also monitors Poland's climate. Under the Water Law Act (July 2017) this institution includes the National Meteorological & Hydrological Service (PSHM). As a result, it maintains the national observational-measurement network, the data exchange and archiving system, as well as meteorological and hydrological forecasting offices. Meteorological and hydrological monitoring is financed principally from the state budget. An interesting question is how the WMO Reform is likely to affect the activities of the Polish NMHS.

2. TASKS OF THE INSTITUTE OF METEOROLOGY AND WATER MANAGEMENT – NATIONAL RESEARCH INSTITUTE, WITHIN THE FRAMEWORK OF WMO

The tasks of the IMGW-PIB include meteorological and hydrological measurements and observations conducted through the observational network, including:

a) 63 synoptic stations;
b) 200 climatological stations (including evaporation measurements);
c) 659 precipitation stations;
d) 862 water gauge stations (including coastal, limnological, and hydrometric measurements);
e) 3 aerological measurement stations;
f) POLRAD meteorological radar network, which consists of 8 radar stations;
g) PERUN lightning detection and location network consisting of 12 stations;
h) satellite data assimilation station;
i) additional dedicated measurement networks, i.e. 23 evapotranspiration stations, 9 radiation stations, radioactive contamination measurements, etc.

The above measurements and observations are carried out continuously, to the extent and with the frequency appropriate for a given type of station, as specified by WMO standards as well as regulations and methodologies used in PSHM. The basic tasks of PSHM also include maintenance, ongoing repair and failure removal, servicing and reconstruction, expansion, reconstruction, and disassembly of the basic measurement and observation network as well as a system for collecting, processing, and exchanging data.

Real-time analyses of the hydrological and meteorological situation are carried out, supporting preparation and dissemination of forecasts and warnings. Additional important tasks are to prepare meteorological and hydrological information, bulletins, hydrological and meteorological yearbooks of PSHM, as well as other dedicated assessments. All these tasks are carried out by closely cooperating meteorological and hydrological forecasting offices and supporting teams.

In preparing forecasts, the Institute uses, among others, the COSMO[1] and ALADIN[2] models, participating actively through its representatives in the work of these consortia. Activities related to hydrological and hydraulic modeling in the field of flood hazards and drought assessment are part of the EU's water policy context (Directive 2000/60/EC). Optimal cooperation of PSHM with public administration bodies in reducing the effects of dangerous phenomena occurring in the atmosphere and the hydrosphere, in turn, requires conducting educational activities in the field of hydrology, meteorology, and oceanology. These activities are aimed at increasing the effectiveness of hazard protection. The development of PSHM is supported by appropriate IMGW-PIB methodological departments. To ensure the data exchange and access required for hydrological and meteorological protection, IMGW-PIB belongs to other international organizations such as EUMETSAT[3], EUMETNET[4] and ECOMET[5]. It should be emphasized that from the point of view of state policy it is important in Poland that meteorological and hydrological protection is provided jointly by the same institution, which is neither global nor pan-European. In other large European countries like Spain, Germany, and France, these tasks are divided between different institu-

[1] www.cosmo-model.org
[2] www.umr-cnrm.fr/aladin/
[3] www.eumetsat.int
[4] www.eumetnet.eu
[5] www.ecomet.eu

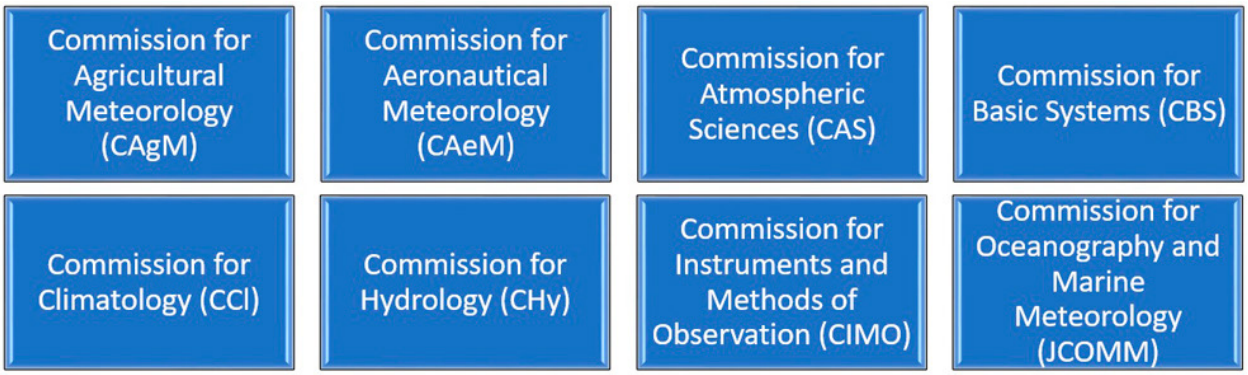

Fig. 1. Former WMO Technical Commissions.

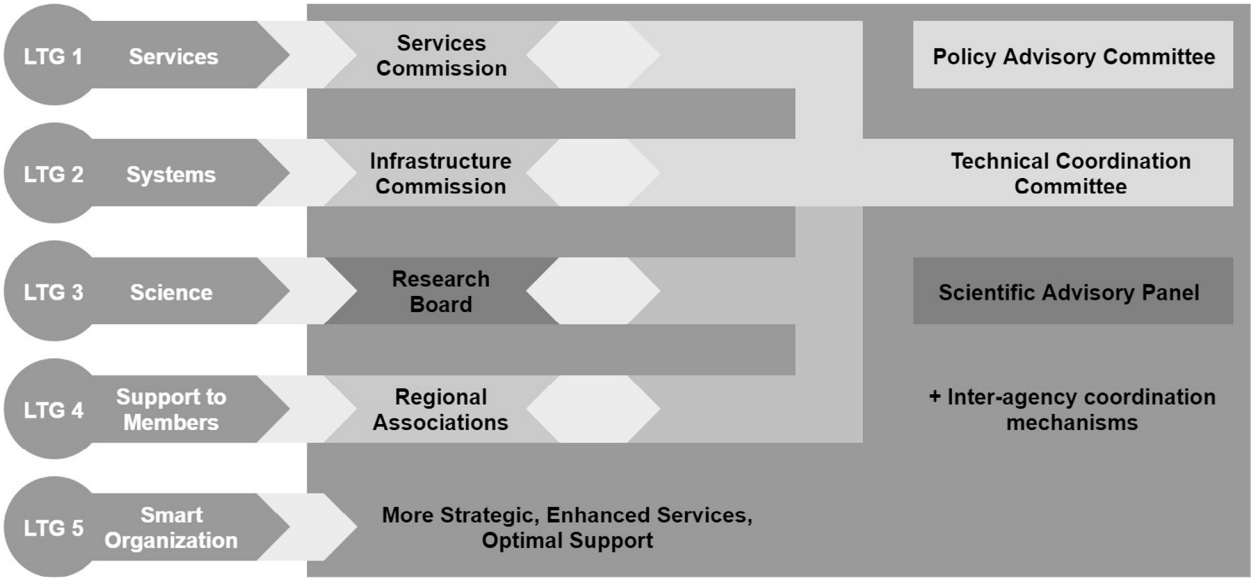

Fig. 2. The new WMO organizational structure (adapted from WMO documentation).

tions. From the point of view of WMO reform, the Polish solution is important and can be treated as an advantage.

3. BASIC DIRECTIONS OF WMO REFORM

3.1. THE MAIN ACHIEVEMENTS

The WMO Strategy for 2020-2023[6] captures the WMO future activities in the form of five Long-Term Goals (LTG) described as follows:

- LTG 1. Better serve societal needs.
- LTG 2. Enhance Earth system observations and predictions.
- LTG 3. Advance targeted research.
- LTG 4. Close the capacity gap.
- LTG 5. Strategic realignment of WMO structure and programs.

Simplifying, the first three goals are dedicated to the development of the following domains: services, infrastructure, and science. The fourth objective refers to regional aspects, while the last one concerns further systematization and improvement of the effectiveness of WMO operations. The implementation of the Strategic Plan will be carried out by means of an Operational Plan, which describes in detail the allocation of budget funds for specific projects.

The WMO Congress approved, after detailed analysis, all final guidelines that had been forwarded in the previous months by the Executive Council, in particular the Working Group on Strategic Planning and the Task Force on Reform. The debate on the final shape of the Reform lasted until the last day of Congress, as the scale of planned changes generated many uncertainties, and sometimes even imperfections requiring refinement during the Congress's activity.

The finally-approved Reform of the WMO affects each of its constituent bodies. Only the geographical division into six associations has been virtually unchanged, but their tasks have been thoroughly reformulated in ways that significantly improve the concentration and distribution of resources allocated to tasks at regional and sub-regional levels.

In reference to the new management structure and strategic plan, in line with the WMO Reform approved, the existing eight WMO Technical Commissions have been replaced by two more coordinated commissions to streamline work and maximize the effects of their activities.

The Commission for Observation, Infrastructure and Information Systems is intended to contribute to the development and implementation of globally coordinated systems for the acquisition, processing, transmission, and dissemination of Earth system observations and standardization related to each stage

[6] https://www.wmo.int/aemp/sites/default/files/d06_Att1_wmo-sp-2020-2023-scheme-29-Nov-2017.pdf

of this value chain (meteorological and hydrological value chain). This Commission was also entrusted with coordinating the production and use of forecasting models as well as developing and implementing good practices of data and information management for all WMO programs and related areas of application and services.

The Commission for Weather, Climate, Water and Related Environmental Services and Applications will contribute to the development and implementation of globally harmonized weather-related services and applications to climate, water, oceans, and the environment to enable informed decision-making and the realization of socio-economic benefits by all end-user groups in society.

The WMO Executive Council (EC) will invariably take care of all the work related to the coordination of activities of individual newly-appointed WMO constituent bodies and will ensure the development and control of mechanisms for effective cooperation between them. All new bodies will be subordinate to the EC (or cooperate with it). The organization of this process will be assisted by its Technical Coordination Committee (TCC), which includes: presidents and vice presidents of technical committees, presidents of regional associations, head of the Research Council, and heads of programs sponsored and co-sponsored by WMO.

The Research Board will translate WMO's strategic goals and decisions of the Congress and EC into overarching research priorities, and ensure the implementation and coordination of research programs. The Scientific Advisory Panel (SAP) will, in turn, develop opinions and recommendations for Congress and the EC on matters relating to WMO research strategies and optimal scientific directions to support the development of the organization's mandates in the fields of weather, climate, water, and related environmental issues, such as social aspects. The EC was composed of representatives primarily from the meteorological community. The SAP, in turn, is a group of independent scientific authorities with internationally recognized status.

The diagram of the new WMO organizational structure, including Long Term Goals is shown in the figure below.

The Joint WMO-IOC Collaborative Board (IOC: UNESCO's Intergovernmental Oceanographic Council) will in turn coordinate the joint development, integration, and implementation of activities related to oceanographic and meteorological observations at sea, data management and information, services, modeling and forecasting systems, as well as research. Several activities formerly coordinated by the JCOMM (Joint WMO and IOC Committee on Oceanography and Marine Meteorology) have been transferred to the newly established WMO technical commissions.

The Policy Advisory Committee (PAC) is a group of selected EC members as well as SAP and TCC heads, which, under the direction of the WMO President, is to shape the vision of developing the organization's political and financial strategies. The Policy Advisory Committee (PAC) shall advise the EC on any matters concerning the strategy and policy of the Organization submitted to it by the EC.

WMO, in the context of the Reform, is beginning to attach much greater importance to: (1) strengthening the coordination of actions combating the effects of global climate change; (2) improving operational hydrological services; and (3) improving monitoring and forecasting of hydrological phenomena. Two groups were established under the EC to coordinate these activities: a Climate Coordination Panel and a Hydrological Coordination Panel.

The Hydrological Assembly, which was first convened during the 18th Congress, will become a regular event accompanying every Congress. It is intended to be a forum for exchanging views among Hydrological Advisers of Permanent Representatives of WMO countries.

3.2. HYDROLOGY

A special dialogue on water during the EC-70 in June 2018 and an extraordinary Commission of Hydrology (CHy) session in February 2019 were the first steps toward a consensus about how best to manage hydrological affairs in the reformulated WMO. The Hydrological Assembly held during the Congress led to consolidated views on how to engage the wider community and strengthen cooperation with partners. The Assembly also developed ways to organize hydrological activities more effectively in WMO and to increase participation of the hydrological community in the new WMO governance structure. The discussions resulted in formulation of eight long-term ambitions that will inform the development of water-related WMO activities. These include: (1) no one is surprised by a flood; (2) everyone is prepared for drought; (3) climate and meteorological data support the food safety program; (4) high-quality data supports learning; (5) science provides a solid foundation for operational hydrology; (6) we have thorough knowledge of the world's water resources; (7) sustainable development is supported by hydrological information; (8) water quality is known. These ambitions are expected to lead to increased involvement and participation of a broad hydrological community in WMO activities to improve knowledge-based decision making.

During the Assembly, the discussion panel 'Hydrology for sustainable development and peace' concluded with the following findings:

1. Water is a key factor for life, environmental protection, and sustainable development.
2. Several stressors affect the water cycle, affecting water resources distribution and availability, which are especially sensitive to climate change, population growth, and water quality.
3. The UN system lacks one strong political voice for water, and WMO should take a more active coordination and leadership role, focusing on its mandate in operational hydrology.
4. There is market potential for extending hydrological data and services. WMO can contribute to achieving a balance between specific needs and general social interest.
5. The collection, management, and sharing of data is essential for the development of relevant hydrological products.
6. Data and knowledge are of fundamental importance in the decision-making process, especially in international and transboundary waters.
7. Water quality and quantity issues should be addressed in a comprehensive manner.
8. A dialogue with all users is necessary to articulate their needs, discuss them, and then include them throughout the entire value chain.

An extremely long discussion was undertaken to redefine the concept of operational hydrology. The consensus definition is as follows: "Operational hydrology is the regular measurement, collection, processing, archiving and distribution of hydrological, hydrometeorological and cryospheric data in real-time as well as generating analyses, forecasts and warnings that inform about water resource management and support water-related decisions across the entire spectrum of time and spatial scales. Operational hydrology requires capacity building and scientific and technical progress and innovation in the areas of observation, standards and data services, modeling, prediction, hydro computer science and decision support, training and information activities." The anno-

tation to the definition states that "this data includes, inter alia, precipitation; air temperature and humidity; water levels of streams, lakes, deltas and estuaries; flow; snow and ice cover, water equivalent; river and lake ice; glacier mass balance; reservoir reserves; soil moisture; groundwater and ground freezing; evaporation and evapotranspiration; water temperature; sediment dynamics; water and sediment quality and other related variables, including in the context of global change. Global change is expressed in various aspects, such as land-use change, socio-economic dynamics, climate variability and changes at various scales".

3.3. CLIMATOLOGY

Upon the failure of the Global Framework for Climate Services[7] management structure, Intergovernmental Board for Climate Services (IBCS), it became necessary to reformulate this body with a new, much more effective mechanism. For this reason, it was decided to establish a fairly wide Climate Coordination Panel (including representatives of associations, IPCC, technical committees, PACs, and the Research Council), which, under the leadership of the First Vice President of WMO, will review the extensive WMO activities related to climatological issues.

A preliminary version of the Manual on High Quality Global Data Management Framework for Climate was adopted. It is an annex to the Technical Regulations (basic WMO documentation on standard and recommended procedures), which is to enable national services to effectively develop and exchange high-quality climate data based on integrated infrastructure at global, regional, and national levels. Based on that document, the assumptions of the open-source reference system for climate and hydrological data management will be built on the basis of proven climate data management practices (specifically the Climate Data Management System described in WMO No. 1131). The long-term observing stations initiative is being continued and 23 additional stations were added to the current 117 stations. It may be important for the Polish service to submit several candidates from Polish stations.

The Congress adopted a methodology for cataloging dangerous meteorological phenomena, recommending the services to adapt it in their work on cataloging and archiving data. The results of the methodology test phase in RA VI confirmed the great utility of the method.

3.4. METEOROLOGY

The Congress focused on various initiatives related to meteorological applications. In the field of general meteorology, WMO's unchanging vision of development of the Impact-Based Forecast and Warning Systems should be emphasized.

An important item on the agenda was the adoption of several interdependent concepts: GMAS (Global Multi-Hazard Alerting System[8], WCM (WMO Coordination Mechanism) and SWFP (Severe Weather Forecasting Program), which will provide support from WMO for the development of a global information system on hazardous phenomena, which in turn will improve the coordination of humanitarian operations conducted by United Nations agencies, especially in the poorest countries. Although the European Meteoalarm managed by EUMETNET under the EMMA[9] program is cited as an example, GMAS is planned as a warning system for many threats, not only from the weather. The implementation of GMAS is also an opportunity to emphasize the irreplaceable role of national services in issuing alerts (the so-called single authoritative voice). It was recommended that Technical Committees develop guides to the procedures and mechanisms for effective support from national services of the national disaster risk management system, with emphasis on: institutional coordination in the areas of risk information and impact assessment; detection, monitoring, analysis, and forecasting of hazards and possible consequences; disseminating warning and advisory information and supporting national response and recovery plans. The WMO long-term plan for the development of aviation meteorology was accepted, which coincided with the assumptions of the future operation of ICAO, expressed in the GANP (Global Air Navigation Plan) (ICAO 2016) document.

3.5. OCEANOGRAPHY

In view of the approaching Decade of Ocean Knowledge for Sustainable Development 2021-2030 announced by the United Nations (UN Decade of Ocean Science for Sustainable Development), the Congress adopted the principles of a framework of close cooperation with UN agencies, international organizations, governmental institutions, the academic community, and the private sector. The provisions of the framework refer to five specific tasks posed to this cooperation: (1) construction of advanced deep ocean observation systems, (2) implementation of new technologies in ocean biochemical measurements, (3) concentration of ocean models resolution, (4) new methods for assimilating coupled data, and (5) conducting focused observation and modeling campaigns. Member State services were called upon to adopt and implement the provisions of all resolutions related to the marine environment. Member State services have been encouraged to actively support the United Nations Ocean Conference 2020 event in February 2020 in New York.

3.6. OBSERVATION, TRANSMISSION, AND PROCESSING SYSTEMS

The key WMO initiative, WIGOS-WMO Integrated Global Observing System (IMGW-PIB 2016) is entering a fully operational phase. The Congress acknowledged that despite significant financial and technical problems, WIGOS has reached a sufficient level of maturity that it can be recognized as operational on January 1, 2020. At the same time, WIGOS is becoming part of the basic structure of WMO's operations. The priorities of the operational phase include slightly modified terms, with the following status indicated for the pre-operational phase 2016-2019:

1. National implementation of WIGOS;
2. Supporting a culture of compliance with WIGOS technical regulations;
3. Implementation of GBON (Global Basic Observing Network)[10] and RBON (Regional Basic Observing Network);
4. Operational implementation of the WIGOS data quality monitoring system;
5. Operationalization of WIGOS Regional Centers;
6. Further development of OSCAR (Observing Systems Capability Analysis and Review Tool)[11].

4. SWOT ANALYSIS IN THE CONTEXT OF THE WORLD METEOROLOGICAL ORGANIZATION REFORM

SWOT analysis is used to analyze the internal and external environments of an organization, as well as to analyze a project or business approach. It is used universally as a tool for

[7] https://gfcs.wmo.int/
[8] www.wmo.int/gmas/
[9] www.eumetnet.eu/activities/forecasting-programme/current-activities-fc/emma/
[10] www.wmo.int/pages/prog/www/wigos/GBON.html
[11] www.wmo-sat.info/oscar/

the first stage of strategic analysis. It supports use of available information to develop an action strategy based on strengths and opportunities, while eliminating or reducing weaknesses and threats (Szałata, Zwoździak 2011).

SWOT analysis consists of dividing information into four groups:

- S (Strengths) – everything that is an asset or advantage;
- W (Weaknesses) – everything that is a weakness, barrier, or defect;
- O (Opportunities) – everything that creates a chance for favorable change;
- T (Threats) – anything that creates a danger of adverse change.

Strengths, weaknesses, opportunities, and threats of IMGW-PIB in the context of World Meteorological Organization Reform are identified below. They were classified according to their impact on IMGW-PIB as either 1 = weak impact, or 2 = strong impact.

STRENGTHS

- Joint solution and unified structure
  The advantage of the Polish approach to the field of hydrological and meteorological services is the combination of tasks in the fields of meteorology, hydrology, to some extent oceanography, meteorological protection of civil aviation, and research into a single institution. This allows for better coordination of work, economic efficiency, and better management of the joint technical service (2-strong impact).
- Hydrology and water resources are included in the activity
  Before the Congress, there was great concern about the fate of hydrology at WMO in connection with the reorganization plans and the liquidation of the hydrology commission. It was thought that the liquidation of the hydrology commission would lower the rank of hydrology in WMO and would hinder cooperation in the field of hydrology in the fields of measurement, modeling, and forecasting. Meanwhile, the Commission for Weather, Climate, Water and Related Environmental Services and Applications will have a broad scope in its competencies that also provides water services. In this respect, the role of hydrology is to create analyses for integrated water resources management, taking into account their quantity and quality. In this regard, IMGW-PIB also maintains methodological departments for the study and research of water resources. This solution should be used as a potential opportunity in the WMO activity forum (2-strong impact).
- Cooperation in Disaster Risk Reduction (DRR)
  The successful contribution of WMO to disaster risk reduction[12], climate change adaptation (CCA), and increased resilience is based on coordinated and collaborative initiatives between the WMO Members. It should be emphasized that in addition to its statutory activities, the Polish NHMS, IMGW-PIB actively participates in complementary work focusing on reducing the risk of natural and technological hazards. The main directions include: (1) National Platform for Disaster Risk Reduction at IMGW during the Hyogo decade (Hyogo 2007); (2) training and education policy; (3) completed research and implementation projects.
  IMGW-PIB recording and statistics of emergency alerts supports the observation that the number of extreme weather events dangerous to human health and life and the material losses associated with them is greatly increasing. The Institute of Meteorology and Water Management – National Research Institute, participates in the process of identification of meteorological and hydrological risks and hazards, analyses of these threats, and distribution of warnings about their possible occurrence. IMGW-PIB is a good example of a broader involvement of the national hydrometeorological service in activities to reduce natural and technological hazards. In this regard, it may also be part of the WMO forum, which is actively involved in DRR aspects (1-weak impact).
- Research activities
  In addition to activities related to the tasks of the National Hydrological and Meteorological Service, the Institute also conducts scientific research that provides significant support in the development of this institution.

IMGW-PIB scientific and research and implementation work focuses on the following problems:

In the field of hydrology – developing modern computer models for forecasting water flows in mountain rivers and streams, with particular emphasis on flood and low-pressure conditions; assessment of the size and variability of surface water resources over time under the influence of climatic and anthropogenic factors; study of hydrological processes in small experimental and representative catchments.

In the fields of meteorology and climatology – improving numerical methods for meteorological and agrometeorological forecasts; the use of remote sensing, satellite and radar data to determine parameters of the atmosphere and to detect extreme phenomena (e.g., forecasting the amount of precipitation or maximum wind speeds); diagnosis and forecasting of Poland's climate along with an assessment of changes under the influence of natural and anthropogenic factors; modeling of air pollution transport.

In the field of oceanology – research and forecasting of hydrological and meteorological conditions on the southern Baltic coast; improvement of measurement methods and chemical laboratory analyses used in testing the quality of marine waters (2-strong impact)

- Institute staff
  The institute's strength is having qualified staff in the fields of meteorology, hydrology, climatology, computer science engineering and water management. It is a good basis for implementing the provisions of the 18th Congress (2-strong impact).

WEAKNESSES

- Uncertainty of financial stability
  Dangerous hydrological and meteorological phenomena are intensifying, indicating the need for optimal (from the point of view of the security of Poland and its inhabitants) development of the system for monitoring and forecasting of these phenomena by the National Hydrological and Meteorological Service. The implication is that sufficient funding must be restored to maintain this system and further develop it. It should be explained here that the reduction of PSHM funding in recent years (2014-2018) caused significant limitations on the collection of measurement and observation data on the state of the atmosphere and hydrosphere and their contribution to a central historical database, which has been kept by IMGW-PIB since 1919. Further funding limitations may critically affect the effectiveness of research on climate change in Poland, international cooperation, and IMGW-PIB participation in relat-

[12] https://www.undrr.org/

ed research projects. Moreover, ensuring minimum cooperation in connection with the new WMO organizational structure requires guaranteeing sound preparation and strengthening of the staff. The development prospects for PSHM require the stabilization of IMGW-PIB financing as soon as possible, especially in the field of PSHM. Stabilization of financing will require restoring the full amount of funding defined in the applications for co-financing of PSHM submitted by IMGW-PIB in previous years and maintaining it predictably thus enabling planning of activities and investments in the long term (at least several years) (2-strong impact).

- Status of implementation and management of the WMO-WIGOS program
  Another challenge for PSHM will be full implementation of WMO-WIGOS (WMO Integrated Global Observing System), occupying one of the key places among the WMO activity development plans for the coming years. The goal of the system is to support initiatives taken as part of WMO, e.g., GAW – Global Atmosphere Watch. As part of the WIGOS system, it is assumed that PSHM will provide a coordinated and comprehensive observation system that economically and sustainably provides WMO members with data for the development of weather forecasts, climate change, water resources, and environmental observations. Expectations for the WIGOS system are directed toward timely, long-term series of measurement and observation data of appropriate quality, subject to quality control, and well documented.. The implementation of quality management procedures is required for better use of existing and future measurement and observation capabilities. It is crucial for national services to maintain the updated status of the network they manage in the OSCAR portal. It is also crucial in this case to properly identify all types of measurement platforms by applying and maintaining the appropriate WIGOS identifiers from the WSI (WIGOS Station Identifier) system. WSI is a system for assigning a unique identifier, applicable to all types of observation stations, irrespective of the owner, which allows registering a substantially unlimited number of stations in WIGOS. In many countries there are no standard identifiers in existing 5-digit allowed ranges and no additional stations can be registered. Implementation of the WSI is mandatory in accordance with WIGOS technical regulations. Only data from properly identified stations can be exchanged. In case there are platforms managed by institutions other than national services in a given country or region, the Congress has identified the possibility of not properly identifying such stations. To improve the process of assigning WSI, a Resolution was adopted enabling the relevant institutions (e.g., atmospheric chemistry monitoring agencies, etc.) to acquire relevant WIGOS IDs, except for the need to refer to relevant national services. The full integration of the observation network under the responsibility of the national services and the partner will not occur until the problem is resolved (1-weak impact).

OPPORTUNITIES

- Modernization projects
  An extremely important factor that will affect the overall operation of IMGW-PIB including PSHM is the necessary modernization and development of the flood monitoring and warning system. As part of the loan financed by the World Bank, it assumes, among other things, a significant increase in the number of automatic measuring stations, modernization of measuring equipment currently used at PSHM stations, and modernization of field crew equipment. These steps will undoubtedly improve the effectiveness of the monitoring and warning system against dangerous hydrological and meteorological hazards. However, it will require an increase in the number of service employees and qualified staff servicing new devices, technical solutions, and models. It will be necessary to improve the competence of the staff responsible for processing and analyzing data and results from numerical models to ensure high quality forecasts and warnings. In the longer term, organizational changes to enable optimal operation of existing and new infrastructure purchased as a result of the loan will also be considered (2-strong impact).
- Implementation of Global Basic Observing Network
  The Congress adopted the concept of creating GBON, i.e. the Global Basic Observing Network, to secure an adequate, global-wide contribution of data to numerical forecasting systems. So far, not all associations can guarantee such a contribution. GBON is to become an operational network from July 1st, 2021. Considering e.g. the development of EUMETNET initiative METEOALARM, aimed at the exchanging of meteorological warnings, it seems that the European region is quite well prepared to implement the concept of GBON (1-weak impact).
- Cooperation with national air carrier
  Great possibilities are inherent in the agreement initiated several months earlier between WMO and the International Air Transport Association (IATA). Under it, both institutions are to support IATA affiliated airlines in the development of the AMDAR system. Although it is another challenging task, the agreement opens the possibility of cooperation with the Polish national air carrier LOT Polish Airlines (1-weak impact).

THREATS

- Need for appropriate financial expenditure regarding data policy
  The progress in science and technology significantly improves our collective ability to generate decision-supporting data, products and services for governments, businesses, and citizens. The Geneva Declaration adopted during the 18th Congress encourages cooperation in the field of data exchange, emphasizing the importance of public-private partnership. Data from the Institute of Meteorology and Water Management, National Research Institute, are available via the ICT system at: http://dane.imgw.pl/ and at www.pogodynka.pl. Data that cannot be disclosed by the above methods can be provided upon request. The WMO Congress underlined the need for innovative approaches and incentives to enable fair and equitable access to data, including the rapidly accumulating non-traditional data from all sectors. Inevitably, approaching full openness in the field of data policy, as mandated by the amended EU Directive (Directive (EU) 2019/1024), will require appropriate financial expenditure and organizational solutions to ensure it.
  Meeting this need will require, among other things:
  a) Standardization and development of IT tools used in meteorological and hydrological protection as well as in the management, processing, and collection of hydrological and meteorological information.
  b) Development of IT systems used to make data available to the public (e.g., dane.imgw.pl portal, SOK – Customer Service System or IMGW-PIB Monitor – the portal visualizing the operational meteorological and hydrological data).

c) Improvement and development of meteorological and hydrological information forms, along with standardized publication of observation results measurements, and statistical studies as part of international exchange in accordance with WMO standards (data replicator from IMGW-PIB database resources to the OSCAR/Surface platform according to technical requirements outlined by WMO – as part of WIGOS) (1-weak impact).

- The ability to provide and finance high qualified staff for new tasks

  Modernization projects will require an increase in the number of service employees and qualified staff servicing new devices, technical solutions, and models. These are usually very narrow specializations in which it is difficult to find specialists. It will be necessary to improve the competence of the staff responsible for processing and analyzing data and results from numerical models in order to ensure high quality forecasts and warnings. In the longer term, organizational changes to enable optimal operation of existing and new infrastructure purchased because of the modernization will also be considered. (2-strong impact).

5. CONCLUSIONS

The World Meteorological Congress adopted dozens of international law acts that set the framework for national services. In view of the fundamental changes in the management structure at WMO, the Polish National Meteorological and Hydrological Service will have to reconsider its contribution to the development of WMO by appointing relevant, competent representatives to the newly established Technical Commissions. The Congress has reformulated the means of developing and implementing many international, regional, and national processes that frame the activities of the national services. The reform process is scheduled for the next dozen or so months, during which time several important sessions will take place, in which active participation is a key task of the Polish service.

The following conclusions and recommendations are derived from the SWOT analysis:

- It is necessary to take advantage of the opportunities associated with modernization projects, which will strengthen the position and contributions of IMGW-PIB in Disaster Risk Reduction.
- IMGW-PIB financial stability and long-term sustainability of financing will ensure the ability to recruit and finance highly qualified staff for new tasks.
- Implementation and management of the WMO-WIGOS program will allow for better IMGW-PIB communication in various areas of WMO operations.

The opportunities resulting from the organizational structure and tasks performed by the Polish service in the fields of hydrology, meteorology, and related research works should be maximized. Finally, it is worth emphasizing that the unpredictable events associated with the COVID-19 pandemic can have a significant impact on the financing of hydro-met services, and may also have impacts on modernization and the organization of work.

REFERENCES

- Convention, 1947, Konwencja dotycząca Światowej Organizacji Meteorologicznej podpisana w Waszyngtonie dnia 11 października 1947 r. ratyfikowana zgodnie z ustawą z dnia 30 grudnia 1949 roku
- Directive (EU) 2019/1024 of the European Parliament and of the Council of 20 June 2019 on open data and the re-use of public sector information, EUR-Lex, Brussels
- Directive 2000/60/EC of the European Parliament and of the Council of 23 October 2000 establishing a framework for Community action in the field of water policy, Official Journal L 327, 22/12/2000 P. 0001 – 0073, EUR-Lex, Brussels
- GWP, 2011, Global Water Partnership Central and Eastern Europe, 2011, What is IWRM?, available online at https://www.gwp.org/en/GWP-CEE/about/why/what-is-iwrm/ (data access 02.08.2019)
- Hyogo, 2007, United Nations International Strategy for Disaster Reduction, Hyogo Framework for Action 2005-2015, Geneva, Switzerland 2007, available online at https://www.unisdr.org/we/inform/publications/1037 (data access 09.08.2019)
- ICAO, 2016, 2016-2030 Global Air and Navigation Plan, International Civil Aviation Organization, Montreal, Quebec, Canada, available online at https://www.icao.int/airnavigation/Documents/GANP-2016-interactive.pdf (data access 10.08.2019)
- IMGW-PIB, 2016, Metody kontroli jakości dla polskiej Państwowej Służby Hydrologiczno-Meteorologicznej, vol. 9, IMGW-PIB, Warszawa
- Szałata Ł., Zwoździak J., 2011, SWOT analysis as a basic tool in environmental management (in Polish), Rocznik Ochrona Środowiska, 13 (2), 1105-1113
- Water Law, 2017, Ustawa z dnia 20 lipca 2017 r. Prawo Wodne, Dz.U. z 2017 r. poz. 1566, 2180, z 2018 r. poz. 650, 710

Simulating the influence of doubled CO_2 on the water budget over West Africa using RegCM4.7

Mojisola Oluwayemisi Adeniyi
University of Ibadan, Department of Physics, Ibadan, Oyo State, Nigeria, e-mail: mojisolaadeniyi@yahoo.com

DOI: 10.26491/mhwm/124787

ABSTRACT. This paper simulates the responses of water budget components to doubled CO_2 (2 × 378 ppm) concentration in the atmosphere with atmospheric and oceanic surface warming of 2°C. Simulations employed version 4.7 of the Regional Climate Model of the International Centre for Theoretical Physics (ICTP). Two six-year experiments were each repeated twice with the same model physics and parameterizations. The control experiment held the CO_2 concentration at 378 ppm (no warming), while the other experiment specified doubled CO_2 concentration and warming. The results showed a positive response (60-100% increase) to doubled CO_2 for precipitation, runoff, and storage terms in Sierra Leone, Burkina Faso, Guinea Bissau, and the ocean area between 3 and 13°N. However, there was a negative response (up to 60%) for northern Senegal, southern Mali, and northern Nigeria. The reductions in water fluxes were observed mostly on the leeward side of the highlands. Evapotranspiration showed a negative response (1-20%) to doubled CO_2 on the land north of 20°N. Burkina Faso and southern Mali responded oppositely to doubled CO_2, despite their spatial proximity.

KEYWORDS: Water budget, doubled CO2, runoff, precipitation, evapotranspiration, West Africa.

SUBMITTED: 28 June 2019 | **REVISED:** 27 May 2020 | **ACCEPTED:** 10 July 2020

1. INTRODUCTION

Water scarcity prevails over West Africa during the dry season due to lack of rainfall, because rainfall is the major resource for replenishing the ground water. The state of water availability affects all the sectors which are highly dependent on water, namely agriculture, industry, and households (Van Beek et al. 2011; Byeon 2014). Besides lack of rainfall, other factors such as variability and changes in climate, urbanization, and population growth have the potential to further intensify water scarcity, especially during the dry season (Short et al. 2012; Mikovits et al. 2014, 2017; Zeisl et al. 2018). The importance of water has drawn the attention of climate scientists to the water budget of regions under warming climate (North et al. 1995; Friesen et al. 2005; Becker et al. 2011). Local and regional area share the impacts of global warming (North et al. 1995; Becker et al. 2011), in particular, its impact on the water budget of such regions (Friesen et al. 2005). Water availability varies over space and time (Postel et al. 1996), so annual assessments of water availability will underestimate water stress, because periods with surpluses and deficits of water will tend to cancel out. Likewise, global averages of water availability may misrepresent the real situation of water availability in some local areas or regions where there might be water surpluses or deficits (Meigh et al. 1999). These considerations necessitate assessment of water availability for small areas and short time scales; these analyses have been conducted for West Africa. Anyadike (1992) used moisture regimes to delineate hydrological regions over West Africa, while Arnault et al. (2016) studied the process of precipitation recycling over the West African region using Weather Research and Forecasting (WRF). In the same vein, Diallo et al. (2014) used version 4 of the Regional Climate Model (RegCM4) to study the water budget over the West African monsoon region using various lateral boundary conditions. In addition, Meynadier et al. (2010) analysed the water budget over West Africa, while Friesen et al. (2005) analysed the water budget over the Volta basin in West Africa. Over a still smaller area, Ledger (1975) analysed the water budget of exceptionally wet areas of Sierra Leone.

Changes in greenhouse gas (GHG) emissions have been blamed for most of the changes in the climate of all regions and the globe (Zhuang et al. 2007). Understanding of the influence of doubled CO_2 emission on water surplus or deficit of any area will inform policy on proper adaptation strategies against the inevitable changes. The influence of increasing GHG concentrations on the local water budget over West Africa has not been studied using regional climate models (RCM). Adeniyi et al. (2019) reported the spatial variation of changes in precipitation, temperature, and wind as a result of changes in the levels of GHG in the atmosphere resulting from 1.5°C ocean and atmosphere warming. The study did not consider water budgets over West Africa. Diallo et al. (2014) also did not consider the influence of CO_2 increases under global warming. It is necessary to study the water budget over West Africa with its components such as evapotranspiration, precipitation, runoff, and storage under GHG concentration increase (warming) using an RCM. This paper aims at simulating the response of the water budget components to doubled CO_2 (2×378 ppm) under 2°C ocean and atmosphere warming over West Africa using RegCM4.7.

Table 1. Model set up, parameterizations and data.

Model parameter	Set up, parameterizations and data
Dynamics	Hydrostatic core
Map projection	Normal Mercator
Planetary boundary layer	Holtslag et al. (1990)
Cumulus parameterization	Tiedtke (Tiedtke 1996) on land and Kain-Fritsch (Kain, Fritsch 1990; Kain 2004) on ocean
Microphysics parameterization	Subgrid Explicit Moisture Scheme (SUBEX; Pal et al. 2000)
Land surface scheme	Biosphere-Atmosphere Transfer Scheme – BATS (Dickinson et al. 1993)
Radiation parameterization	The National Center for Atmospheric Research (NCAR), Community Climate System Model (CCM3) (Kiehl et al. 1998)
Ocean flux parameterization	Zeng et al. (1998)
Time step	2.5 minutes
Initial and lateral boundary conditions	Era Interim 0.75 Reanalysis data sets (Dee et al. 2011)
Soil moisture initialization	European Space Agency – Climate Change Initiative (ESA-CCI) data (Dorigo et al. 2017; Gruber et al. 2017, 2019)
Topography data	Global 30 Arc-Second Elevation topography dataset (Danielson 1996; Verdin, Greenlee 1996)
Oceanic boundary condition	Six hourly updated, Optimum Interpolated (OI) SST weekly SST data (Reynolds et al. 2002)
Lake model	Hostetler et al. (1993)
Reference CO_2 level	378 ppm
Model duration	1 January, 2001 – 1 January, 2007
Realization 1	1 January, 2001 – 1 January, 2007
Realization 2	1 July, 2000 – 1 January, 2007

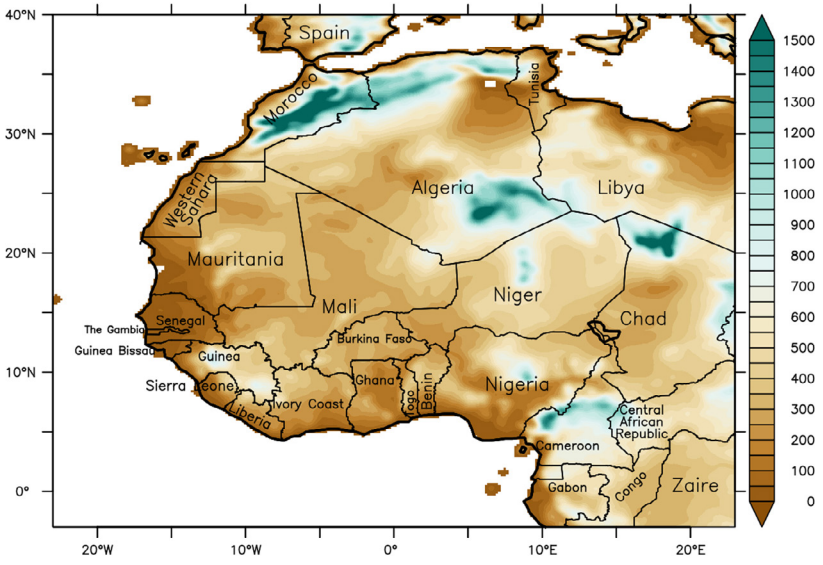

Fig. 1. Topography of the simulation domain (m above sea level) including the country names.

2. MODEL SET-UP

The hydrostatic core in version 4.7 of the RegCM (RegCM4.7) of the International Center for Theoretical Physics is used in this study. Control and doubled CO_2 experiments with two repetitions each were done to investigate the influence of doubled CO_2 on water balance over West Africa. The reference CO_2 concentration in the control simulations is 378 ppm, while it is 378×2 = 756 ppm in the CO_2 doubling experiment. Giorgi et al. (2012) give the detailed description of the RegCM4 mod-

el. The two sets of experiments used the same set of model physics and parameterizations. The simulations were done on 20 km × 20 km grids with a total of 250 × 250 = 62,500 grid points and 23 vertical levels (sigma coordinates) over West Africa. The domain is centred on longitude 0°E and latitude 20°N (Fig. 1). The domain cartographic projection, model physics, parameterization schemes, and data used in this study are listed in Table 1.

The schemes used for radiation, lateral boundary condition, boundary layer, explicit moisture, ocean flux, and pressure gradient flux in this study are in line with Adeniyi (2017). Adeniyi (2019b) reported good performance of cumulus parameterization schemes by Tiedtke (Tiedtke 1996) and Kain-Fritch (Kain, Fritsch 1990) over West Africa.

3. DATA AND METHODOLOGY

3.1. EVALUATION DATA

The performance of RegCM4.7 in simulating the water budget components over West Africa is evaluated using precipitation, runoff, evapotranspiration, and storage from ERA5 reanalysis data[1] on 25 km × 25 km grids. In addition, simulated precipitation and potential evapotranspiration are evaluated using observed gridded precipitation and potential evapotranspiration from Climate Research Unit (CRU) 4.02 time series, respectively (Harris et al. 2014). The CRU data are station data interpolated on a 0.5 × 0.5 degrees grid. These data are re-gridded to the same grid (0.18 × 0.18 degrees grid) with the simulations before comparison.

3.2. WATER BUDGET

The water budget equation used in this study is adapted from Healy et al. (2007). It is given as equation (1a, b):

$$PRE = RO + EVA \tag{1a}$$

$$PRE = RO + EVA + \Delta S \tag{1b}$$

where: *PRE* is precipitation, *RO* is runoff, *EVA* is evapotranspiration and *ΔS* is change in storage. The water budget components are direct output of RCMs except Δ*S*. The water budget equation equates the inflow and outflow of water in a particular location at a particular period. Precipitation is the main inflow (input) in equation 1. Evapotranspiration is the amount of moisture loss into the atmosphere through evaporation and transpiration from the soils, surface-water bodies, and plants. Runoff is the total flow of water out of the location and change in storage is the additional water added or removed from the soil water storage to balance equation 1a. Equation 1a does not always achieve closure, this is achieved by introducing the change in storage term in equation 1b.

Required water for evapotranspiration is calculated by subtracting the actual evapotranspiration from potential evapotranspiration (Adeniyi 2019a). Potential evapotranspiration is the amount of evapotranspiration that would occur if a sufficient water source were available. The required water for evapotranspiration indicates the amount of water required to make up for the potential evapotranspiration in form of irrigation. Evaluation of simulated water budget components is carried out during the summer (June-September, JJAS), which is the period of precipitation over the whole of West Africa. Changes in the water budget components are also considered during summer. In addition, intra-annual consideration of changes in water budget components is done at some locations for further investigation.

Climate models generally represent reality imperfectly and are bound to have biases because of the assumptions they make in simulating atmospheric phenomena. Each model has internal variability which is a source of uncertainty. There is also model uncertainty, which can be as a result of structural deficiencies and parameterization errors in the model. The boundary conditions data used for simulations can also introduce errors into the simulations (Kerkhoff et al. 2014). Bias corrections are usually done to remove model uncertainties. These are mainly based on two assumptions: constant bias and constant relation (Kerkhoff et al. 2014). It is well documented that biases cancel out when changes are calculated as scenario minus control (Buser et al. 2009; Liu et al. 2014) with the assumption of constant bias. With constant relation also, biases cancel out when percentage change is calculated as follows:

$$CTRL * CF = CTRL_C \tag{2}$$

$$CO_2 * CF = CO_{2_C} \tag{3}$$

Equations (2) and (3) represent the correction of control (*CTRL*) and doubled CO_2 experiments using a correction factor *CF*.

The simulated difference between *CTRL* and CO_2 experiments is given by the equation:

$$CO_{2_C} - CTRL_C = CO_2 * CF - CTRL * CF = (CO_2 - CTRL)CF \tag{4}$$

Percentage difference/change based on corrected simulations is given by the equation:

$$\frac{(CO_2 - CTRL)CF}{CTRL * CF} * 100 = \frac{(CO_2 - CTRL)}{CTRL} * 100 \tag{5}$$

Similarly, percentage difference/change based on uncorrected simulations is given by the equation:

$$\frac{(CO_2 - CTRL)}{CTRL} * 100 \tag{6}$$

The two percentage differences are the same (equations 5 and 6 are equal since the correction factor cancels out), so it does not matter if the simulation output is corrected or not once percentage difference is used (Funk et al. 2012).

4. RESULTS AND DISCUSSION

4.1. EVALUATION OF SIMULATED WATER BUDGET COMPONENTS

Figure 2 shows the comparison of the simulated water budget components (precipitation, runoff, storage, and evapotranspiration) with CRU observations and ERA5 reanalysis. The model underestimates the ERA5 precipitation (Fig. 2a) for the ocean and coastal Sierra Leone, Nigeria, and Liberia, while it overestimates precipitation for the mountains and highlands (Central Nigeria, Central Cameroon, and Guinea). The dry bias over the ocean is typical of simulations carried out using Era Interim initial and lateral boundary conditions (Tamoffo et al. 2019). A similar dry bias was found in Rossby Centre Regional Atmospheric Climate Model (RCA4) simulations, which used Era Interim initial and boundary conditions (Tamoffo et al. 2019). Other areas have low bias, approaching 0 mm·day^{-1}. Similar bias exists in the simulated precipitation with respect to CRU4.02 precipitation (Fig. 2b). The ERA5 evapotranspiration is overestimated by the model for the southern countries (south of 20°N), ocean, highlands, and mountains (Fig. 2c); bias is low for the northern land area (north of 20°N) of the simulation domain. Runoff is overestimated for the highlands and mountains with reference to ERA5 data, similar to the bias in simulated precipitation. However,

[1] https://cds.climate.copernicus.eu/cdsapp#!/home

the bias is higher in runoff than in precipitation. Very low bias exists in simulated runoff for the northern part (15-30°N) of the simulation domain (Fig. 2d). The water storage component is generally underestimated with low bias (–5 to 0 mm·day^{-1}) and isolated higher underestimation (–10 mm·day^{-1}) south of 15°N. Little or no bias in storage change exists north of 15°N (Fig. 2e). The CRU potential evapotranspiration is overestimated by RegCM4.7, largely in the northern area (north of 15°N) of the simulation domain, while the bias is reduced at the southern areas (south of 15°N, Fig. 2f). Bias in the mountains is probably due to the lack of gauging stations in these areas for generating observations and data for reanalysis (Chen et al. 2008). The biases in the RegCM4.7 simulations used in this study are due to the Era Interim initial and lateral boundary conditions used (Tamoffo et al. 2019), parameterizations, and the model's structural deficiencies. Bias correction was not applied to the simulation output in this study since the biases cancel out with the use of percentage change.

4.2. SIMULATED RESPONSES OF WATER BUDGET COMPONENTS TO DOUBLED CO_2

Figure 3 shows the percentage changes in the water budget components in response to CO_2 doubling (warming). The change in wind as a result of CO_2 doubling is also shown as a vector overlay on precipitation in Figure 3c. In response to CO_2 doubling under a warmer climate, general dryness (about 40%) and isolated wetness (20-100%) are simulated at north of 15°N. At the ocean between 0 and 18°N and 32 and 39°N, precipitation shows positive responses (60 to >100%) to CO_2 doubling under a warmer climate. Land area south of 15°N shows lower positive responses of 40 to >100%. Such findings are not unexpected, since the increase in atmospheric temperature allows for more moisture retention, and thus increased precipitation. Adeniyi et al. (2019) corroborate this finding with intensified and spatially extended precipitation increases for the ocean and most of the southern land areas between 5 and 10°N. However, in this study, more land areas south of 15°N show distinctive isolated dryness of about 40%. The simulated distinctive isolated dryness south of 15°N is probably due to more realistic simulation resulting from the 20 km × 20 km grid spacing used in this study compared to the 50 km × 50 km grid in Adeniyi et al. (2019). Precipitation over West Africa is mainly convective (Schumacher, Houze 2003), so different precipitation amounts are usually observed

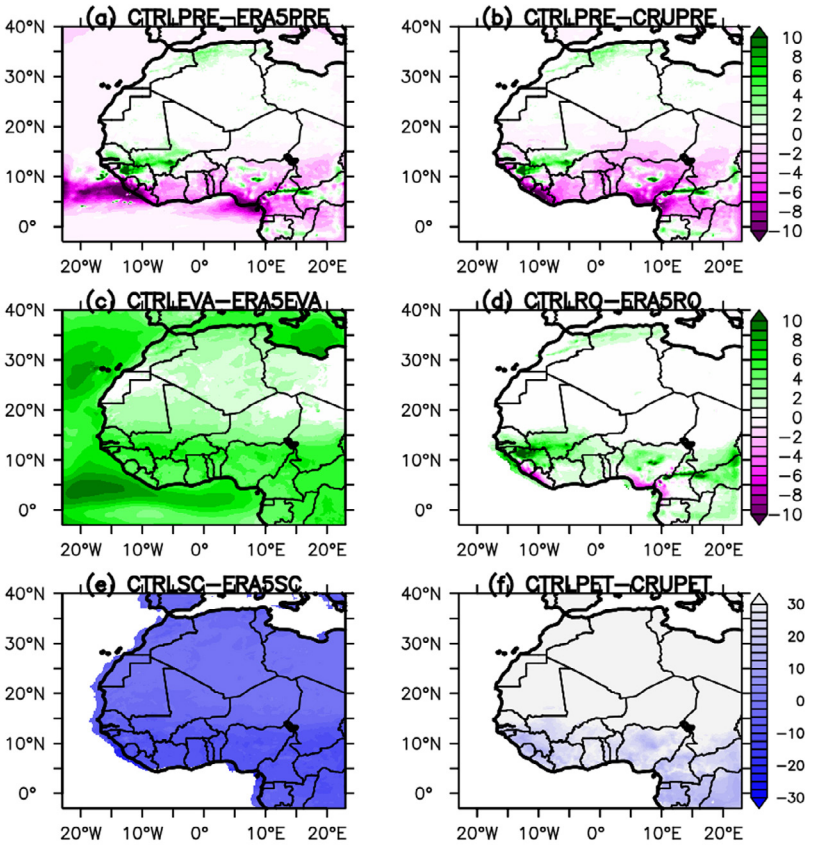

Fig. 2. Bias (mm·day^{-1}) in simulated components of the JJAS water budget over West Africa with respect to ERA 5 reanalysis and CRU time series. The panels are arranged as follows: (a) Control precipitation – ERA5 precipitation, (b) Control precipitation – CRU precipitation, (c) Control evapotranspiration – ERA5 evapotranspiration, (d) Control runoff – ERA5 runoff, (e) Control storage change – ERA5 storage change and, (f) Control potential evapotranspiration – CRU potential evapotranspiration.

over a range of a few kilometres, thus high-resolution simulation will capture more realistic values of precipitation. In addition, the increase in temperature from 1.5°C to 2°C in this study can result in intensified wetness or even dryness if evaporation exceeds precipitation. More distinct responses are simulated in this study as a result of the increase in atmospheric and ocean surface temperature when compared to the experiments in Adeniyi et al. (2019). In general, the ocean, highlands, and mountainous areas have more rainfall (Fig. 3c).

Responses of runoff (mostly ±60%) and storage terms to doubled CO_2 have similar spatial signals over land (Fig. 3a, d). However, the precipitation change signal is greater than those of runoff and storage (Fig. 3a, c, d). The southern land area (south of 15°N) has a higher runoff response than the storage response (Fig. 3a, d). Increases in precipitation and runoff in areas south of 15°N and along the coast tend to cause flooding (Blöschl et al. 2015). Evapotranspiration has a minimal (0 to ±20%) response to doubled CO_2 (Fig. 3). Burkina Faso and southern Mali, although adjacent, show opposite responses to CO_2 doubling (Fig. 3a, c, d). The underlying physical reasons for the opposite responses need further clarification. Wind vectors intensified from southerly and south-westerly directions at the ocean, while northerly, north-easterly, and north-westerly changes prevail to the north (Fig. 3c). With southerly and south-westerly intensification in the southern areas, precipitation is bound to increase, depending on the topography of the area, as a result of the prevailing moisture laden air-mass. Also, the intensification of northerly, north-westerly, and north-easterly winds to the north generally leads to dryness in the northern areas. Southern Mali is located at the leeward of the highland in far southern Mali. Southernmost Mali, at the windward of the highland, has increased precipitation, which could not reach the leeward side of the highland. However, the prevailing wind response and the orography favours the transportation of moisture to Burkina Faso, so the two

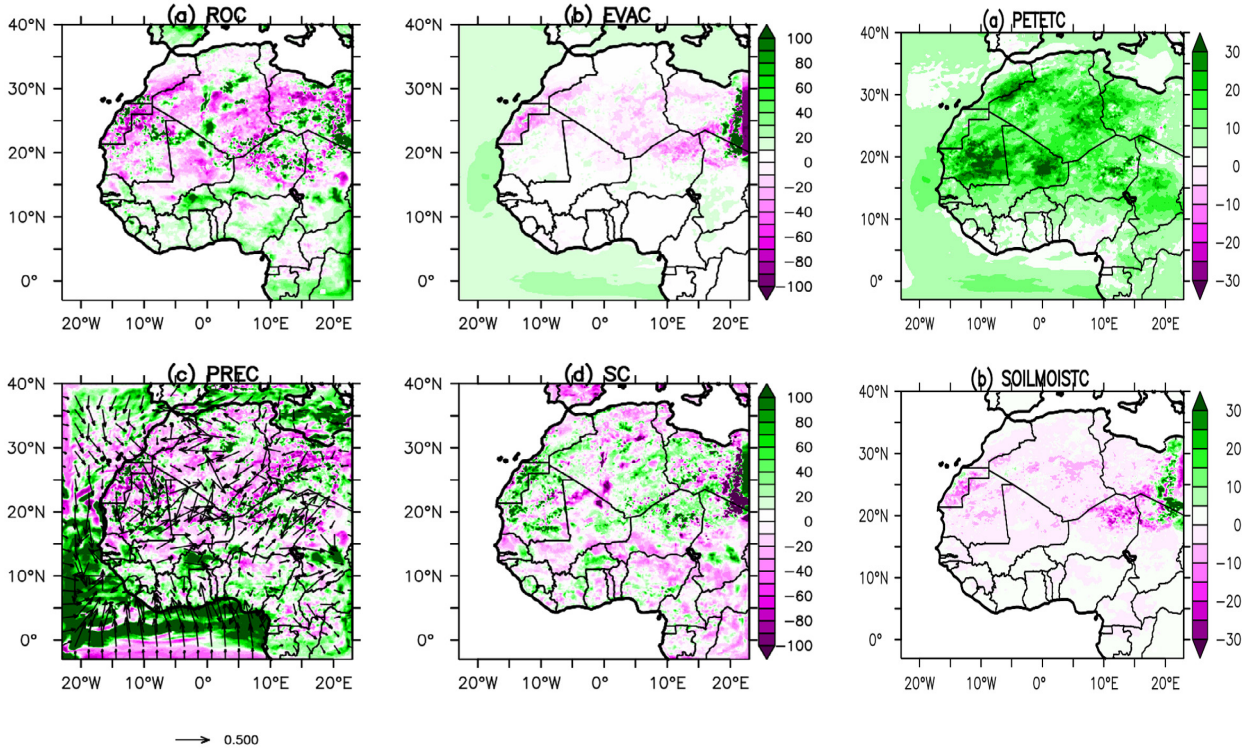

Fig. 3. Simulated JJAS percentage changes in (a) runoff, (b) evapotranspiration, (c) precipitation with change in wind vector overlay and (d) storage change over West Africa in response to doubled CO_2 concentration with 2°C warming of ocean and atmosphere. Simulated percentage changes in water budget components are shown in colour, while the change in wind vector is overlaid on percentage precipitation change.

Fig. 4. Simulated JJAS percentage changes in (a) required water and (b) soil moisture over West Africa in response to doubled CO_2 concentration under 2°C warming of ocean and atmosphere.

locations have opposite changes in response to doubled CO_2. The western side of Burkina Faso is to the windward of a highland where most of the available moisture in the cloud precipitates before getting to Niger (Fig. 3c), Adeniyi (2014).

Required water (potential evapotranspiration – evapotranspiration) increases (10-30%) in the north (>15°N) as a result of reduced evapotranspiration (1 to 20%; Figs. 3b, 4a). The greatest increase in required water is simulated at Mauritania and northeastern Mali, while isolated reduction (5-15%) is simulated at central and eastern Niger, northern Chad, central and northern Libya, eastern Nigeria, and southwestern Cameroon. There is little change in required water (<10%, Fig. 4a) at the south (<10°N) following insignificant change in evapotranspiration (<10%, Fig. 3b) in the area. Soil moisture increases slightly (<5%) with increased CO_2 in the countries south of 15°N as a result of increased precipitation and slight increases in the storage change, while soil moisture declines (5-15%) north of 15°N (Figs. 3, 4b) due decreased precipitation. However, increased soil moisture (15-30%) is simulated in the western Sahel, north-eastern Chad, and eastern Libya. This is corroborated by the reduction in required water (Fig. 4a, b) for these areas.

4.3. RESPONSES OF WATER BUDGET COMPONENTS TO DOUBLED CO_2 IN SOUTHERN MALI AND BURKINA FASO

The opposite responses for Burkina Faso and southern Mali are noteworthy – these are two adjacent locations (Figs. 1, 3). In order to examine these opposite responses, the percentage changes in monthly water budget components at both locations were extracted and compared.

Figure 5 shows the intra-annual variations in the response of the components of water budget to doubled CO_2 in southern Mali and Burkina Faso. The northern parts of the two countries are in the Sahel so the desert influence may affect their responses in the north. However, the latitudinal positions of southern Mali and Burkina Faso are also similar.

The simulated precipitation change in response to CO_2 doubling shows two peaks of increase, in June (70%) and September (290%), whereas it precipitation is reduced in other months, with the greatest reduction (–50%) in February in Burkina Faso. In southern Mali, precipitation declines throughout the year except in November when it increases by 60% (Fig. 5c). This finding is consistent with the report of Giannini et al. (2008) that global warming results in a dryer Sahel. Observed precipitation and water budget parameters usually have two peaks, one in June and another in September over Burkina Faso (Funk et al. 2012) and a greater percentage increase is expected during the peak period than during the dry season. The 50% reduction in precipitation during the dry season, especially in February, could be seen as a late onset of precipitation in Burkina Faso and possible flooding during summer as a result of increased precipitation. Evapotranspiration increases from January to November at both locations with percentage increases ranging from 2 to 10%; evapotranspiration declines in December (Fig. 5b) at both locations. Warming as a result of CO_2 doubling would lead to increased evaporation. Runoff shows a positive response to CO_2 doubling, with peaks in June (45%) and September (90%) and little or no change for other months in Burkina Faso. Runoff and precipitation increases would cause flooding in Burkina Faso. In southern Mali, runoff is reduced throughout the year with a maximum reduction of 20% in April (Fig. 5a). Stor-

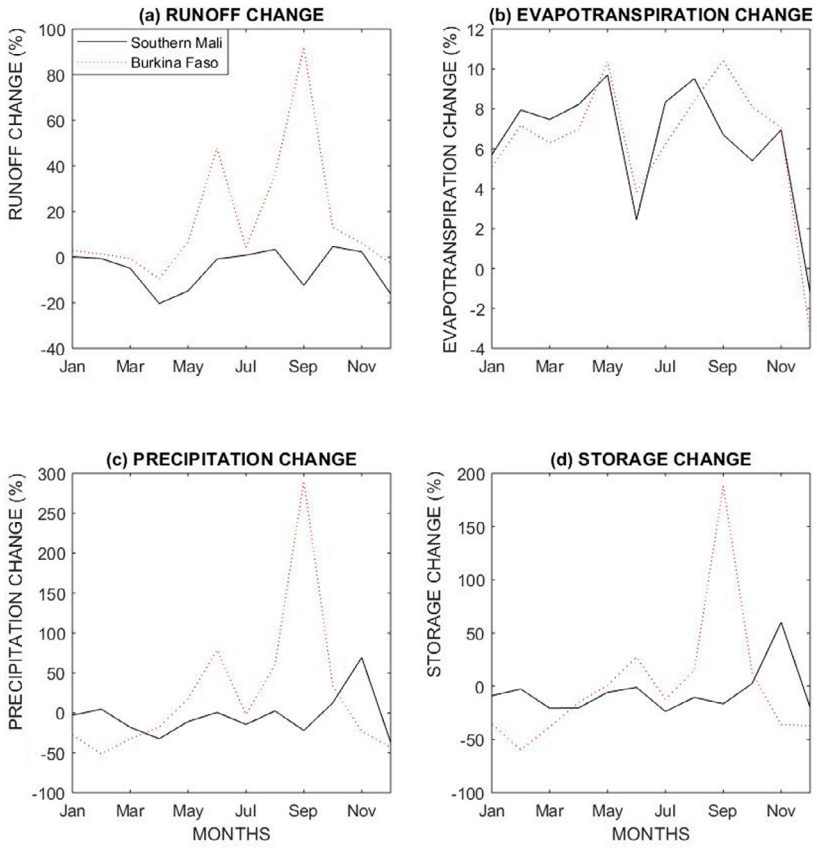

Fig. 5. Intra-annual variability in percentage (a) runoff change, (b) evapotranspiration change, (c) precipitation change and (d) storage change over West Africa in response to doubled CO_2 concentration under 2°C warming of ocean and atmosphere at southern Mali (latitude 12.5°N – 15°N, longitude 5.5°W – 10°W) with water deficit and Burkina Faso (longitude 0°W – 5°W, latitude 11.5°N – 14°N), which is exceptionally wet.

age change increases from June (25%) to October with maximum (185%) in September and declines in the remaining months in Burkina Faso (up to –60% in February). The increase in storage change will increase the water table level at Burkina Faso during summer. Storage change decreases throughout the year except in November, when it increases to about 60% in southern Mali (Fig. 5d); the result will be a dryer Mali with reduction in the water table level. Storage, precipitation, and runoff decrease in southern Mali, while they increase in Burkina Faso (Figs. 3, 5) as a result of doubled CO_2 and increase in atmospheric and oceanic surface temperature during summer (June-September), while evapotranspiration has a similar minimal response to doubled CO_2 at both locations (Fig. 5b).

5. CONCLUSION

The impact of increasing CO_2 concentration on spatial variations of precipitation and other water budget components over West Africa is not yet documented. In an attempt to document the impacts of CO_2 doubling on water budget components over West Africa, this paper simulates at high resolution (20 km × 20 km), the response of water budget components to CO_2 doubling, with 2°C warming of the atmosphere and ocean surface. The simulations were done using the latest version of the RegCM4.7.0 of the ICTP. As expected, precipitation increases over the ocean and some coastal areas, since the increase in the atmospheric temperature allows for more moisture retention. However, dryness prevails in some places, with more spatial coverage than reported by Adeniyi et al. (2019) with RegCM4.5 and 1.5°C warming of the atmosphere and ocean surface. The reduction in precipitation in some places is attributed to the increase in atmospheric and oceanic surface temperature and the relatively high resolution of the simulations, which allows for resolution of distinct responses. All the components of the water budget respond to CO_2 doubling similarly as precipitation (±60 to 100%) except evaporation, which has little response (±20%). The water budget components generally increase south of 15°N and decline north of 15°N. The results show spatial variations in response to doubled CO_2, depending on the topography of the area in relation to the windward or leeward location and the proximity to the ocean or water body. The areas with water surplus identified as a result of warming are Burkina Faso, eastern Senegal, Sierra Leone, the southwestern coast, and central Chad. Policy makers in these areas need to make proper adaptation plans against flooding that may result from increased precipitation and runoff. Areas with expected water deficits are extend northward from 15°N, so policy should be adaptable to increased water requirements and droughts as a result reduced precipitation, water storage, and soil moisture.

ACKNOWLEDGEMENTS

This research was carried out at the International Centre for Theoretical Physics (ICTP), Trieste. All the facilities used for the research were provided by the ICTP. The author is grateful for the release of ERA5 reanalysis data by the Copernicus Climate Change Service (https://cds.climate.copernicus.eu/cdsapp#!/home). The author also appreciates the Centre for Environmental Data Analysis for the release of Climate Research Unit time series data for use in this study.

REFERENCES

- Adeniyi M.O., 2014, Sensitivity of different convection schemes in RegCM4.0 for simulation of precipitation during the Septembers of 1989 and 1998 over West Africa, Theoretical and Applied Climatology, 115 (1-2), 305-322, DOI: 10.1007/s00704-013-0881-5
- Adeniyi M.O., 2017, Modeling the impact of changes in Atlantic sea surface temperature on the climate of West Africa, Meteorology and Atmospheric Physics, 129, 187-210, DOI: 10.1007/s00703-016-0473-x
- Adeniyi M.O., 2019a, On the influence of variations in solar irradiance on climate: a case study of West Africa, Earth Systems and Environment, 3,189-202, DOI: 10.1007/s41748-019-00103-2
- Adeniyi M.O., 2019b, Sensitivities of the Tiedtke and Kain-Fritsch Convection Schemes for RegCM4.5 over West Africa, Journal of Meteorology, Meteorology Hydrology and Water Management, 7 (2), 27-37, DOI: 10.26491/mhwm/103797
- Adeniyi M.O., Nymphas E.F., Oladiran E.O., 2019, Simulating the influence of greenhouse gases on the climate of West Africa, Pollution, 5 (2), 301-312, DOI: 10.22059/POLL.2018.266785.526

- Anyadike R.N.C., 1992, Hydrological regions of West Africa: a preliminary survey based on moisture regimes, Geografiska Annaler: Series A, Physical Geography, 74 (4), 375-382, DOI: 10.1080/04353676.1992.11880377
- Arnault J., Knoche R., Wei J., Kunstmann H., 2016, Evaporation tagging and atmospheric water budget analysis with WRF: a regional precipitation recycling study for West Africa, Water Resources Research, 52 (3), 1544-1567, DOI: 10.1002/2015WR017704
- Becker A., Inoue S., Fischer M., Schwegler B., 2011, Climate change impacts on international seaports: knowledge, perceptions and planning efforts among port administrators, Climatic Change, 110, 5-29, DOI: 10.1007/s10584-011-0043-7
- Blöschl G., Gaál L., Hall J., Kiss A., Komma J., Nester T., Parajka J., Perdigão R.A.P., Plavcová L., Rogger M., Salinas J.L., Viglione A., 2015, Increasing river floods: fiction or reality?, WIREs Water, 2 (4), 329-344, DOI: 10.1002/wat2.1079
- Buser C.M., Kunsch H.R., Luthi D., 2009, Bayesian multi-model projection of climate: bias assumptions and interannual variability, Climate Dynamics, 33, 849-868, DOI: 10.1007/s00382-009-0588-6
- Byeon S.J., 2014, Water balance assessment for stable water management in island region, Ph.D. dissertation, available online at https://tel.archives-ouvertes.fr/tel-01131202/document (data access 10.07.2020)
- Chen M., Shi W., Xie P., Silva V.B.S., Kousky V.E., Higgins R.W., Janowiak J.E., 2008, Assessing objective techniques for gauge-based analyses of global daily precipitation, Journal of Geophysical Research. Atmospheres, 113 (D4), DOI: 10.1029/2007JD009132
- Danielson J.J., 1996, Delineation of drainage basins from 1 km African digital elevation data, [in:] Proceedings of Pecora Thirteen, Human Interactions with the Environment – Perspectives from Space, Sioux Falls, South Dakota, August 20-22, 1996
- Dee D.P., Uppala S.M., Simmons A.J., Berrisford P., Poli P., Kobayashi S., Andrae U., Balmaseda M.A., Balsamo G., Bauer P., Bechtold P., Beljaars A.C.M., van de Berg L., Bidlot J., Bormann N., Delsol C., Dragani R., Fuentes M., Geer A.J., Haimberger L., Healy S.B., Hersbach H., Ho´lm E.V., Isaksen L., Kallberg P., Kohler M., Matricardi M., McNally A.P., Monge-Sanz B.M., Morcrette J.-J., Park B.-K., Peubey C., de Rosnay P., Tavolato C., Thepaut J.-N., d Vitart F., 2011, The ERA-Interim reanalysis: configuration and performance of the data assimilation system, Quarterly Journal of the Royal Meteorological Society, 137 (656), 553-597, DOI: 10.1002/qj.828
- Diallo I., Giorgi F., Sylla M.B., Mariotti L, Gaye A.T., 2014, Atmospheric water budget over the West African monsoon region in a regional climate model: the sensitivity of different lateral boundary conditions, Geophysical Research Abstracts, 16, DOI: 10.13140/2.1.3433.9528
- Dickinson R.E., Henderson-Sellers A., Kennedy P.J., 1993, Biosphere-Atmosphere Transfer Scheme (BATS) Version 1E as Coupled to the NCAR Community Climate Model, No. NCAR/TN-387+STR), University Corporation for Atmospheric Research, DOI: 10.5065/D67W6959
- Dorigo W.A., Wagner W., Albergel C., Albrecht F., Balsamo G., Brocca L., Chung D., Ertl M., Forkel M., Gruber A., Haas E., Hamer D.P., Hirschi M., Ikonen J., de Jeu R., Kidd R., Lahoz W., Liu Y.Y., Miralles D., Mistelbauer T., Nicolai-Shaw N., Parinussa R., Pratola C., Reimer C., van der Schalie R., Seneviratne S.I., Smolander T., Lecomte P., 2017, ESA CCI Soil Moisture for improved Earth system understanding: state-of-the art and future directions, Remote Sensing of Environment, 203, 185-215, DOI: 10.1016/j.rse.2017.07.001
- Friesen J., Andreini M., Andah W., Amisigo B., Van De Giesen N., 2005, Storage capacity and long-term water balance of the Volta Basin, [in:] Regional hydrological impacts of climatic change – Hydroclimatic variability, IAHS Publ. 296, 138-145
- Funk C., Rowland J., Adoum A., Eilerts G., White L., 2012, A climate trend analysis of Burkina Faso, Famine Early Warning Systems Network – Informing Climate Change Adaptation Series, Fact Sheet 2012-3084, available online at https://pubs.usgs.gov/fs/2012/3084/fs2012-3084.pdf (data access 10.07.2020)
- Giorgi F., Coppola E., Solmon F., Mariotti L., Sylla M.B., Bi X., Elguindi N., Diro G.T., Nair V., Giuliani G., Turuncoglu U.U., Cozzini S., Guttler I., O'Brien T.A., Tawfik A.B., Shalaby A., Zakey A.S., Steiner A.L., Storda F., Sloan L.C., Brankovic C., 2012, RegCM4: model description and preliminary tests over multiple CORDEX domains, Climate Research, 52, 7-29, DOI: 10.3354/cr01018
- Gruber A., Dorigo W.A., Crow W., Wagner W., 2017, Triple Collocation-based merging of satellite soil moisture retrievals, IEEE Transactions on Geoscience and Remote Sensing, 55 (12), 6780-6792, DOI: 10.1109/TGRS.2017.2734070
- Gruber A., Scanlon T., van der Schalie R., Wagner W., Dorigo W., 2019, Evolution of the ESA CCI Soil Moisture climate data records and their underlying merging methodology, Earth System Science Data, 11 (2), 717-739, DOI: 10.5194/essd-11-717-2019
- Harris I., Jones P.D., Osborn T.J., Lister D.H., 2014, Updated high resolution grids of monthly climatic observations – the CRU TS3.10 Dataset, International Journal of Climatology, 34 (3), 623-642, DOI: 10.1002/joc.3711
- Healy R.W., Winter T.C., LaBaugh J.W., Franke O.L., 2007, Water budgets: Foundations for effective water resources and environmental management, U.S. Geological Survey Circular, 1308, 90 pp.
- Holthuijzen W.A., 2011, Dry, hot, and brutal: climate change and desertification in the Sahel of Mali, Journal of Sustainable Development in Africa, 13 (7), 245-268
- Holtslag A.A.M., de Bruijn E.I.F., Pan H.-L., 1990, A high resolution air mass transformation model for short-range weather forecasting, Monthly Weather Review, 118 (8), 1561-1575, DOI: 10.1175/1520-0493(1990)118<1561:AHRAMT>2.0.CO;2
- Hostetler S.W., Bates G.T., Giorgi F., 1993, Interactive coupling of a lake thermal model with a regional climate model, Journal of Geophysical Research, 98 (D3), 5045-5057, DOI: 10.1029/92JD02843
- Jun M., Knutti R., Nychka D.W., 2008, Spatial analysis to quantify numerical model bias and dependence: how many climate models are there?, Journal of the American Statistical Association, 103 (483), 934-947, DOI: 10.2307/27640134
- Kain J.S., 2004, The Kain-Fritsch convective parameterization: an update, Journal of Applied Meteorology, and Climatology, 43 (1), 170-181, DOI: 10.1175/1520-0450(2004)043<0170:TKCPAU>2.0.CO;2
- Kain J.S., Fritsch J.M., 1990, A one-dimensional entraining/detraining plume model and its application in convective parameterization, Journal of the Atmospheric Sciences, 47 (23), 2784-2802, DOI: 10.1175/1520-0469(1990)047<2784:AODEPM>2.0.CO;2
- Kerkhoff C., Künsch H.R., Schär C., 2014, Assessment of bias assumptions for climate models, Journal of Climate, 27(17), 6799-6818, DOI: 10.1175/JCLI-D-13-00716.1
- Kiehl J.T., Hack J.J., Hurrell J.W., 1998, The energy budget of the NCAR Community Climate Model: CCM3, Journal of Climate, 11 (6), 1151-1178, DOI: 10.1175/1520-0442(1998)011<1151:TEBOTN>2.0.CO;2
- Ledger D.C., 1975, The water balance of an exceptionally wet catchment area in West Africa, Journal of Hydrology, 24 (3-4), 207-214, DOI: 10.1016/0022-1694(75)90081-5
- Liu M., Rajagopalan K., Chung S. H., Jiang X., Harrison J., Nergui V., Guenther A., Miller C., Reyes J., Tague C., Choate J., Salathé E.P., Stöckle C.O., Adam J.C., 2014, What is the importance of climate model bias when projecting the impacts of climate change on land surface processes?, Biogeosciences, 11, 2601-2622, DOI: 10.5194/bg-11-2601-2014
- Meigh J.R., Mckenzie A.A., Sene K.J., 1999, Grid-based approach to water scarcity estimates for Eastern and Southern Africa, Water Resources Management, 13 (2), 85-115, DOI: 10.1023/A:1008025703712

- Meynadier R., Bock O., Guichard F., Boone A., Roucou P., Redelsperger J.L., 2010, West African Monsoon water cycle: 1. A hybrid water budget data set, Journal of Geophysical Research, 115 (D19), DOI: 10.1029/2010JD013917
- Mikovits C., Rauch W., Kleidorfer M., 2014, Dynamics in urban development, population growth and their influences on urban water infrastructure, Procedia Engineering, 70, 1147-1156, DOI: 10.1016/j.proeng.2014.02.127
- Mikovits C., Tscheikner-Gratl F., Jasper-Tönnies A., Einfalt T., Huttenlau M., Schöpf M., Kinzel H., Rauch W., Kleidorfer M., 2017, Decision support for adaptation planning of urban drainage systems, Journal of Water Resources Planning and Management, 143 (12), DOI: 10.1061/(ASCE)WR.1943-5452.0000840
- North G.R., Schmandt J., Clarkson J., 1995, The impact of global warming on Texas: a report of the task force on climate change in Texas, Austin, University of Texas Press, First Edition, 242 pp.
- Pal J., Small E., Eltahir E., 2000, Simulation of regional scale water and energy budgets: representation of subgrid cloud and precipitation processes within RegCM, Journal of Geophysical Research. Atmospheres, 105 (D24), 29579-29594, DOI: 10.1029/2000JD900415
- Postel S.L., Daily G.C., Ehrlich P.R., 1996, Human appropriation of renewable fresh water, Science, 271 (5250), 785-788, DOI: 10.1126/science.271.5250.785
- Reynolds R.W., Rayner N.A., Smith T.M., Stokes D.C., Wang W., 2002, An improved in situ and satellite SST analysis for climate, Journal of Climate, 15 (13), 1609-1625, DOI: 10.1175/1520-0442(2002)015<1609:AIISAS>2.0.CO;2
- Schumacher C., Houze Jr. R.A., 2003, Stratiform rain in the tropics as seen by the TRMM precipitation radar, Journal of Climate, 16 (11), 1739-1756, DOI: 10.1175/1520-0442(2003)016<1739:SRITTA>2.0.CO;2
- Short M.D., Peirson W.L., Peters G.M., Cox R.J., 2012, Managing adaptation of urban water systems in a changing climate, Water Resources Management, 26, 1953-1981, DOI: 10.1007/s11269-012-0002-8
- Tamoffo A.T., Moufouma-Okia W., Dosio A., James R., Pokam W.M., Vondou D.A., Fotso-Nguemo T.C., Guenang G.M., Kamsu-Tamo P.H., Nikulin G., Longandjo G.-N., Lennard C.J., Bell J.-P., Takong R.R., Haensler A., Tchotchou L.A.D., Nouayou R., 2019, Process-oriented assessment of RCA4 regional climate model projections over the Congo Basin under 1.5°C and 2°C global warming levels: influence of regional moisture fluxes, Climate Dynamics, 53, 1911-1935, DOI: 10.1007/s00382-019-04751-y
- Tietdke M., 1996, An extension of cloud-radiation parameterization in the ECMWF model: the representation of subgrid-scale variations of optical depth, Monthly Weather Review, 124 (4), 745-750, DOI: 10.1175/1520-0493(1996)124<0745:AEOCRP>2.0.CO;2
- Van Beek L.P.H., Wada Y., Bierkens M.F.P., 2011, Global monthly water stress: 1. Water balance and water availability, Water Resources Research, 47 (7), DOI: 10.1029/2010WR009791
- Verdin K.L., Greenlee S.K., 1996, Development of continental scale digital elevation models and extraction of hydrographic features, [in:] Proceedings of the Third International Conference/Workshop on Integrating GIS and Environmental Modeling, National Center for Geographic Information and Analysis, Santa Barbara, CA
- Zeisl P., Mair M., Kastlunger U., Bach P.M., Rauch W., Sitzenfrei R., Kleidorfer M., 2018, Conceptual urban water balance model for water policy testing: an approach for large scale investigation, Sustainability, 10 (3), 716; DOI: 10.3390/su10030716
- Zeng X., Zhao M., Dickinson R.E., 1998, Intercomparison of bulk aerodynamic algorithms for the computation of sea surface fluxes using TOGA COARE and TAO data, Journal of Climatology, 11 (10), 2628-2644, DOI: 10.1175/1520-0442(1998)011<2628:IOBAAF>2.0.CO;2
- Zhuang Q., Melillo J.M., Mcguire A.D., Kicklighter D.W., Prinn R.G., Steudler P.A., Felzer B.S., Hu S., 2007, Net emissions of CH4 and CO2 in Alaska: implications for the region's greenhouse gas budget, Ecological Applications, 17 (1), 203-212, DOI: 10.1890/1051-0761(2007)017[0203:NEOCAC]2.0.CO;2

Meteorology Hydrology and Water Management
Volume 8 | Issue 2

Bioclimatic zoning of the territory of Ukraine based on human thermal state assessment

Liudmyla Malytska
Ukrainian Hydrometeorological Institute, Prospekt Nauky 37, 03028 Kyiv, Ukraine, e-mail: m_alitsk_a@i.ua

Stanislav Moskalenko
Taras Shevchenko National University of Kyiv, Volodymyrska Street 60, 01033 Kyiv, Ukraine

DOI: 10.26491/mhwm/125755

ABSTRACT. This research focuses on objective assessment of bioclimatic conditions through analyses of biometeorological indices based on Harrington's desirability function. Evaluation criteria for the Harrington desirability function during winter are: Bodman's winter severity index (*S*), equivalent-efficient temperatures (*EETA*), index of wind cooling (K_0), and wind chill temperature (*WC*). These metrics were integrated into one complex, generalized desirability index for winter (*DW*). For the summer period, equivalent-efficient temperatures of Missenard (*EET*) index, radiation equivalent-effective temperature (*PEET*) and Heat Index (*HI*), were combined to form a desirability index for summer (*DS*). Zoning of the territory by e integrating the indices (*DW/DS*) portrays the seasonal and spatial differentiation of bioclimatic conditions over Ukraine. These differences were used to highlight the most favorable and unfavorable regions (zones) for humans and, accordingly, the level of bioclimatic resources for each region. In winter across Ukraine, four zones with different levels of weather comfort were identified, with only three zones in summer. For both seasons meteorological conditions are mostly comfortable based on human thermal state. Zone 3, with satisfactory bioclimatic resources and comfortable weather, is the largest of all zones in both winter and summer, making up 49.61% and 61.0% Ukraine's territory, respectively. Average values of climatic characteristics were calculated for the specified zones for both seasons (1981-2010).

KEYWORDS: Bioclimatic conditions, Harrington Desirability function, biometeorological indices, human thermal state.

SUBMITTED: 16 April 2019 | **REVISED:** 19 July 2020 | **ACCEPTED:** 27 July 2020

1. INTRODUCTION AND BACKGROUND

Meteorological conditions affect the human thermal state. To assess this effect, scientists use indicators that describe certain aspects of influence: thermal load, thermal stress, wind cooling, and others. These indicators are known as biometeorological indices (Epstein, Moran 2006). Throughout the twentieth century and into the twenty-first century there has been an active development of these indices (Epstein, Moran 2006). However, the question of the impact of weather and climate on the state of human health remains open, and scientists of various countries investigate it (Kalkstein, Davis 1989; Kalkstein 2001; Mohan et al. 2014; Frohlich, Matzarakis 2015), indicating a considerable interest in this topic. Their works describe the mechanisms of how climate influences humans, especially, morbidity and mortality, the problems of acclimatization, as well as the possibility of applying natural bioclimatic resources for the prevention and treatment of diseases of various organs and their systems, etc. Matthies et al. (2011) noted a significant increase in deaths during heatwaves.

An important task of modern bioclimatology is to evaluate the properties of the climate in terms of favorable or unfavorable conditions for human life based on bioclimatic resources[1] (Jendritzky et al. 2007). The assessment of such resources requires the development of a universal index that would allow taking into account the accumulation of negative effects of the meteorological condition on human thermal comfort. Work toward the development of such an index has been underway since 2005 as a part of the project COST Action 730. The working title of the index is "Universal Thermal Climate Index" (*UTCI*), currently still under development. Frohlich and Matzarakis (2015) conducted a comparative analysis of *UTCI*, *PET* (physiologically equivalent temperature) and *PT* (perceived temperature). They showed the indices' applicability and reliability in hot and windy conditions by analyzing their distribution and sensitivity under the given conditions based on the modification of a real data set. Scientists have concluded that none of the tested indices meets all requirements for a universal index, but they can be used to solve various applied problems of biometeorology. The indices should therefore be improved to be valid for several kinds of climates (Frohlich, Matzarakis 2015).

Table 1. Description of the level of bioclimatic resources of the human thermal state through the function of Harrington's desirability index (compiled by the authors based on Harrington 1965).

Hdf value	The degree of weather comfort	Level of resource
0.81-1.00	extremely comfortable	excellent
0.64-0.80	very comfortable	good
0.38-0.63	comfortable	satisfactory
0.21-0.37	uncomfortable	unsatisfactory
0.00-0.20	extremely uncomfortable	unacceptable

In Ukraine, the assessment of bioclimatic resources is a priority area of research in applied meteorology (Strategy of Sustainable Development "Ukraine – 2020", 2015). Complex studies of the thermal comfort regime, its features in the summer and winter periods, and the assessment of the effects of climate change on human health are highlighted in works of Stepanenko et al. (2011, 2015). However, it should be noted that maps for generalizing these characteristics into a single-scale bioclimatic resource are not presented.

The aim of this article is to study the spatial distribution of bioclimatic conditions through analyses of biometeorological indices by seasons (winter and summer), based on the Harrington Desirability function in Ukraine (1981-2010).

2. DATA AND METHODS

2.1. DATASET

The research was conducted for the period of 1981-2010 using daily data for temperature, wind speed, and humidity from the 187 meteorological stations across the Ukraine. Data were provided by the Central Geophysical Observatory (www.cgo.kiev.ua).

For spatial distribution (mapping) we used an open source geographic information system (QGIS modification 3.4.3 Madeira). Interpolation of data was carried out using the inverse distance weighted method (IDW interpolation).

2.2. METHODS

To comprehensively assess bioclimatic resources and develop a universal index, it is necessary to combine the bioclimatic indices that characterize various aspects of the influence of the meteorological conditions on the human thermal state. As a rule, multiple bioclimatic indices are used for this purpose. They use different scales that complicate comparison and generalization. Harrington's desirability function allows not only normalization of certain factors, but also integration of them into a one index that determines the most favorable or unfavorable conditions following established criteria (Harrington 1965).

The Harrington desirability function (*Hdf*) takes values from 0 to 1 (Table 1). Value 0 is the worst value of the index, reflecting extremely uncomfortable weather conditions, with the greatest thermal load on humans and an unacceptable level of bioclimatic resources. Value 1 reflects extremely comfortable conditions with the least thermal load and an excellent level of bioclimatic resources.

Since heat exchange between the human body and the environment differs in warm and cold periods with different meteorological conditions, it is advisable to make assessments separately for each period, according to the Harrington desirability function (*DW* for the winter and *DS* for the summer). The average values of climatic characteristics for 1981-2010 were calculated for selected zones.

2.3. CALCULATION OF *DW*

In the winter period it is advisable to account for the severity of the season, human heat loss due to cooling through the combined action of wind and low temperatures, thermal sensation, and heat transfer of the human body for certain values of wind speed, temperature, and air humidity, etc. For this purpose, we used the following biometeorological indices: the Bodman winter severity index (*S*), equivalent-efficient temperatures of Missenard (*EET*), and Eisenstadt (*EETA*), index of wind cooling (K_0) by Siple and Passel, wind chill temperature (*WC*) (Siple, Passel 1945; OFCM 2003; Kobysheva 2008).

For each observation station, for all selected bioclimatic indices we calculated their average long-term values for the winter ($\overline{x}$) 1981-2010. The next step was to choose maximum permissible limits (x_0, x_1) for the "satisfactory" zone. Then partial func-

[1] In general, «climatic resources» are a supply of matter, various types of energy, and information about the atmosphere and the topsoil that can be used to solve specific problems aimed at improving human living standards and creating material goods (Kobysheva 2008). The climatic properties favorable for human life create bioclimatic resources.

tions of desirability – $d(z)$ were established. Based on these functions, we calculated the generalized desirability index *DW*, reflecting the level of bioclimatic resources of the human thermal state in the winter period that correspond to a certain degree of weather comfort:

$$\begin{aligned} DW &= (dS * dK_0 * dEET * dEETA * dWC)^{\frac{1}{5}} \\ dS &= \exp(-\exp(-(x_0 - S)/(x_0 - x_1))) \\ dK_0 &= \exp(-\exp(-(x_0 - K_0)/(x_0 - x_1))) \\ dEET &= \exp(-\exp(-(x_0 - EET)/(x_0 - x_1))) \\ dEETA &= \exp(-\exp(-(x_0 - EETA)/(x_0 - x_1))) \\ dWC &= \exp(-\exp(-(x_0 - WC)/(x_0 - x_1))) \end{aligned} \quad (1)$$

where: *DW* – generalized desirability index in winter; *dS*, dK_0, *dEET*, *dEETA*, *dWC* – the partial feedback of Harrington desirability functions of the Bodman winter severity index (*S*), index of wind cooling (K_0), equivalent-efficient temperatures of Missenard (*EET*), and Eisenstadt (*EETA*), wind chill temperature (*WC*); x_0, x_1 – minimum and maximum allowable values of the characteristic in the "satisfactory" zone.

The limits of the "satisfactory" zone (x_0, x_1) were established in accordance with the scales of heat perception and heat loss of bioclimatic indices (Table 2). The interval $[x_0 \ldots x_1]$ is conventionally accepted as a range within which the weather is comfortable and on the Harrington scale of desirability corresponds to the critical points $d(x_0) = 0.37$ and $d(x_1) = 0.64$.

2.4. CALCULATION OF *DS*

To evaluate the human thermal state in summer and assess the level of bioclimatic resources we used the equivalent-efficient temperatures of Missenard (*EET*), radiation equivalent-effective temperature (*PEET*) and Heat Index (*HI*) (Kobysheva et al. 2008; Mohan et al. 2014). The limits of the "satisfactory" zone are presented in Table 3. Partial feedback of desirability functions and generalized desirability index in summer were calculated according to the formulas:

$$\begin{aligned} DS &= (dEET * dPEET * dHI)^{\frac{1}{3}} \\ dEET &= \exp(-\exp(-(x_0 - EET)/(x_0 - x_1))) \\ dPEET &= \exp(-\exp(-(x_0 - PEET)/(x_0 - x_1))) \\ dHI &= \exp(-\exp(-(x_0 - HI)/(x_0 - x_1))) \end{aligned} \quad (2)$$

where: *DS* – generalized desirability index in summer; *dEET*, *dEET*, *dHI* – the partial feedback of Harrington desirability functions of equivalent-efficient temperatures of Missenard (*EET*), radiation equivalent-effective temperature (*PEET*) and Heat Index (*HI*); x_0, x_1 – minimum and maximum allowable values of the characteristic in the "satisfactory" zone.

Table 2. The limits of the "satisfactory" zone according to bioclimatic indices (winter period) (compiled by the authors based on Kobysheva et al. 2008).

Bioclimatic index	Limits of "satisfactory" zone	
	x_0	x_1
Bodman's winter severity index *S*, unit	3	2
index of wind cooling K_0 kcal/(h.m²)	1000	799
equivalent-efficient temperatures of Missenard, *EET*, °C	–12	–6
equivalent-efficient temperatures of Eisenstadt, *EETA*, °C	–17	–11
wind chill temperature *WC*, °C	–27	–10

Table 3. The limits of the "satisfactory" zone by bioclimatic indices (summer period).

Bioclimatic index	Limits of "satisfactory" zone	
	x_0	x_1
equivalent-efficient temperatures of Missenard *EET*, °C	18	12
radiation equivalent-effective temperature *PEET*, °C	21	17
Heat Index (*HI*), °F	90	80

3. RESULTS

3.1. ASSESSMENT OF BIOCLIMATIC RESOURCES OF THE HUMAN THERMAL STATE IN WINTER (DECEMBER, JANUARY, FEBRUARY)

The analysis of the generalized desirability index in winter (*DW*) and its partial feedbacks showed that in Ukraine winter meteorological conditions are mostly comfortable for the human thermal state. Partial feedbacks of *Hdf* for the five selected bioclimatic indices are presented in Figure 1. They illustrate the relationship between the quantitative values of the dimensionless scale that match psychological perception of a person on one side and values of bioclimatic indices on the other. Values of desirability are on the ordinate axis, with the values of the characteristics under study along the abscissa. The x-axis also illustrates the range of the values of bioclimatic indices in Ukraine.

The values of indices that lie beyond the limit of 0.63 on the scale of desirability correspond to very comfortable environment conditions for a person, and values of 0.37 and below match uncomfortable weather conditions, when the body's thermoregulation system is in a state of stress (Table 1).

The zoning of the Ukraine territory according to the integrated index of *DW* has identified four zones with different levels of bioclimatic resources and comfort of weather conditions.

Based on *DW* values during winter, extreme weather discomfort and the lowest level of bioclimatic resources occur in the mountainous regions of the Carpathians, the eastern (Donetsk ridge area, Fig. 2) and northeastern regions of the country (Zone 1 on Figure 3). This zone occupies an area of 43,824 km², or 7.26% of the territory of Ukraine.

The values of the generalized function *DW* in this zone are in the interval [0.0-0.2]. This suggests that most of the bioclimatic indices lie outside the comfort requirement. This territory is characterized by a persistent cold, there is a high risk of overcooling, the duration of being safely outdoors (without the risk of frostbite of open areas of the body) is from 10 to 30 minutes. It was established that across Zone 1, winter is moderately severe, the average seasonal temperature is –3.4°C, the mean minimum is –6.0°C, and the mean maximum is –0.7°C (Table 4). There are 60 winter days with an average temperature equal or less 0°C per day and 33 days with a temperature below –10°C. The absolute maximum duration of the period with such temperature may be longer than a month (36 days). In general, there are 3 days per season with temperatures below –20°C, although in single years there can be significantly more days below –20°C, and the absolute maximum duration of a period with a very low temperature can extend to 8 days. In the long-term, there are six days per season with daily temperature variability >6°C. This zone experiences the highest wind speeds, with a long-term average value per season of 4.4 m·s^{-1}. Zone 1 also has the highest frequency of days with wind speed ≥7 m·s^{-1} (11 days) and the smallest frequency of calm (0-1 m·s^{-1}) and light wind (1-4 m·s^{-1}) conditions: 4 and 39 days, respectively. High wind speeds cause the most rapid losses of heat by the human body due to wind cooling, i.e. –983 kcal/(h·m²). The region is also characterized by the highest relative humidity in winter (77%), the lowest values of the *EET* and *EETA* (–17.4°C and –28.9°C, respectively) and the lowest values of cold stress by *WC* (–20.6°C).

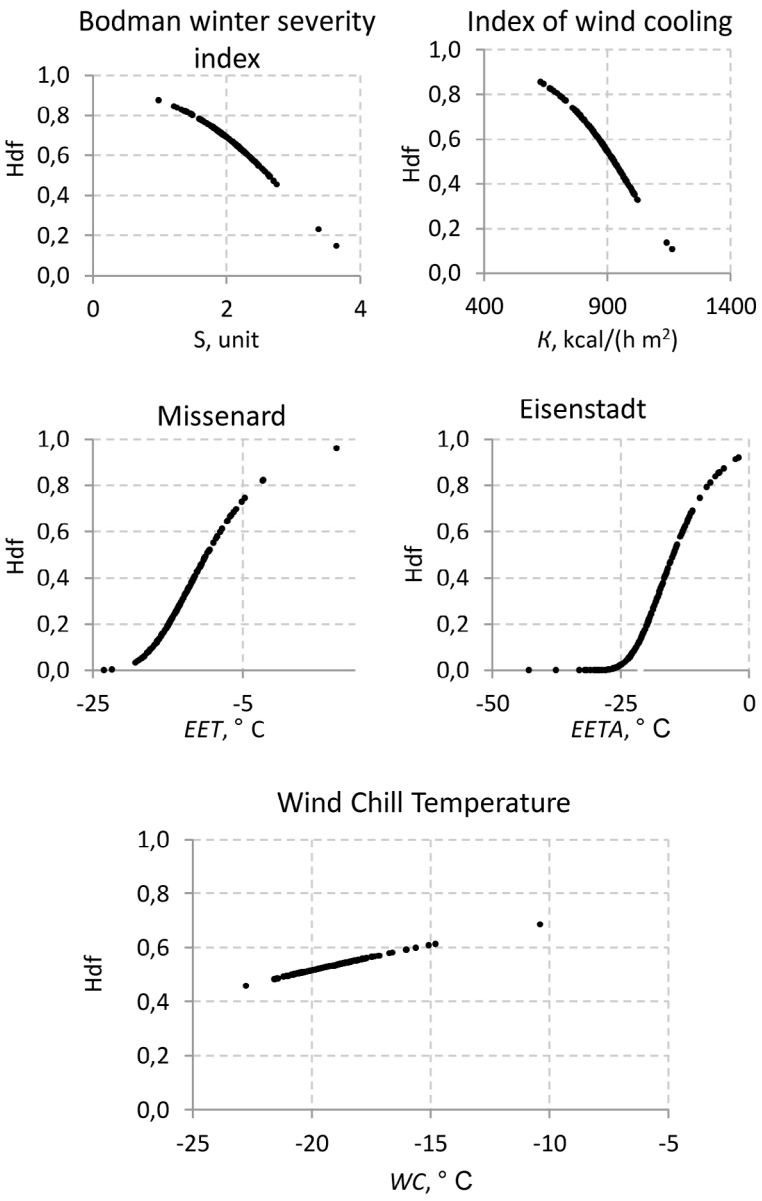

Fig. 1. Harrington partial functions (*Hdf*) of desirability for bioclimatic indices (average long--term values for the winter of 1981-2010).

Fig. 2. Physical-geographical map of Ukraine.

It was found that significant levels of discomfort and unsatisfactory bioclimatic resources for the human thermal state are located in Livoberezhno-Dnieper-Pryazovsky Krai, the Carpathian Mountains, the eastern slopes of the Podolsk Hills, and the coastal areas of the Black Sea and Azov Sea (Zone 2 on Fig. 3). The total area of Zone 2 is 252,196 km^2, or 41.78% of the territory of Ukraine. In these regions there is a moderately severe winter with an average temperature of –2.7°C. The average minimum temperature is –5.4°C and the maximum temperature is above zero, reaching up to +0.2°C. In general, according to average values, there are 56 winter days, but the number of days with low temperatures remains high – up to 30 days with a temperature below –10°C and 3 days with a temperature below –20°C. However, in anomalously cold years these durations can be longer, the period with frost can reach 34 days, and conditions with temperature below –20°C can last up to 7 days. In Zone 2, there are 6 days with daily temperature variability >6°C. The average values of *EET* and *EETA* correspond to the categories "cold" and "very cold" (–14.7°C and –22.6°C respectively). High average wind speeds (3.5 m·s^{-1}) cause significant heat losses due to wind cooling. For Zone 2, the index of wind cooling (K_0) is equal to 910 kcal/(h·m^2), while the wind chill temperature (*WC*) is –19.8°C. Recreational activities in this area in the winter season are limited by weather conditions and require additional resources for development.

The southern regions of Odessa, the western districts of the Transcarpathian region, and the southern coast of Crimea have the most comfortable weather conditions in winter, as evidenced by the high values of *DW* (Zone 4 in Fig. 3). Zone 4 occupies a small territory, a total area of 8,150 km^2, representing only 1.35% of Ukraine. This zone, with favorable bioclimatic resources for the human thermal state and very comfortable weather, has the highest air temperatures: the seasonal average temperature is 0.5°C, the average of the maximum 4°C, and only the minimum temperatures remain below zero (–2.4°C). In Zone 4 counts of frosty days ($T_{min} \le -10$°C) and days with strong frost ($T_{min} \le -20$°C) are 200% lower than in the rest of Ukraine: 17 and 1 day, respectively. For this zone, low wind speeds are typical, average value 2 m·s^{-1}. Days with calm conditions or light winds are prevalent. The region also has the lowest relative humidity in winter (68.8%), the highest values of the *EET* and *EETA* (–6.8°C and –8.6°C, respectively) and the lowest values

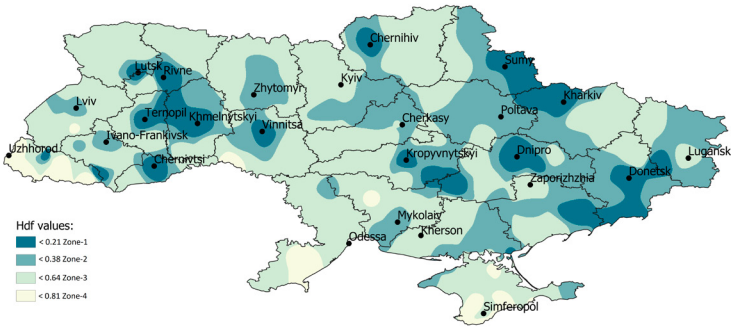

Fig. 3. Spatial distribution of *DW* values (1981-2010) across Ukraine.

Table 4. Climatic characteristics of zones with different levels of bioclimatic resources for the human thermal state during the winter period (1981-2010) in Ukraine.

Characteristics	Zones with different levels of bioclimatic resources			
	1*	2*	3*	4*
average temperature, °C	–3.4	–2.7	–2.3	0.5
mean minimum temperature, °C	–6.0	–5.4	–5.2	–2.4
mean maximum temperature, °C	–0.7	0.2	0.8	4.0
number of days with $T_{av} \leq 0$°C, days	60	56	53	37
number of days with $T_{min} \leq -10$°C, days	33	30	29	17
number of days with $T_{min} \leq -20$°C, days	3	3	3	1
number of days with daily temperature variability >6°C, days	6	6	6	5
absolute maximum duration of the period with $T_{min} \leq -10$°C, days	36	34	31	19
absolute maximum duration of the period with $T_{min} \leq -20$°C, days	8	7	7	3
average wind speed, m·s^{-1}	4.4	3.5	2.7	2.0
number of days with wind ≥7 m·s^{-1}, days	11	5	3	2
number of days with wind 0-1 m·s^{-1}, days	4	5	13	23
number of days with wind 1-4 m·s^{-1}, days	39	54	61	56
average relative humidity, %	76.8	75.1	73.7	68.8
Bodman's winter severity index *S*, unit	2.5	2.1	1.9	1.5
index of wind cooling K_0 kcal/(h.m^2)	983	910	844	723
equivalent-efficient temperatures of Missenard *EET*, °C	–17.4	–14.7	–12.3	–6.8
equivalent-efficient temperatures of Eisenstadt *EETA*, °C	–28.9	–22.6	–17.4	–8.6
wind chill temperature *WC*, °C	–20.6	–19.8	–19.2	–17.1

*1 – unacceptable level, extreme uncomfortable weather; *2 – unsatisfactory level, uncomfortable weather; *3 – satisfactory level, comfortable weather; *4 – good level, very comfortable weather.

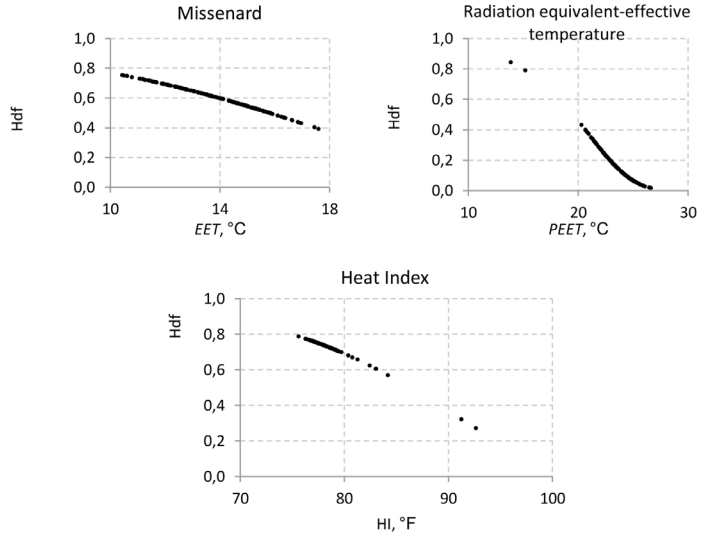

Fig. 4. Harrington partial functions of desirability for bioclimatic indices (average long-term values for the summer of 1981-2010).

of *WC* (–17.1°C). According to the indexes of Bodman (*S*) and wind cooling (K_0), the winters in this zone are not very severe, the category of thermal sensation is "cool" with a slight heat loss of 723 kcal/(h·m^2).

The rest of Ukraine (Zone 3 in Fig. 3) during the winter has a satisfactory level of bioclimatic resources for the human thermal state and comfortable weather conditions. This area occupies the largest area – 299,460 km^2, 49.61% of Ukraine. This zone has non-severe winters with an average temperature of –2.3°C, minimum temperature of –5.2°C, and maximum of 0.8°C (Table 4). The average number of winter days in this region is 53; there are 29 days with temperature ≤ –10°C , and only 3 days per season with temperature ≤ –20°C. However, in anomalously cold years weather conditions with frost may persist in this territory for a month (31 days). Moderate winds of 2.7 m·s^{-1} are typical for this zone, which also has the largest number of days with light winds (63 days per season). The average humidity in the winter is 73.7%. Due to the cooling effect of wind and humidity, average values of *EET* and *EETA* at 10°C and 15°C are lower than the average air temperature. They equal –12.3°C and –17.4°C, respectively, corresponding to the category of thermal sensation "chilly". The loss of heat by the human body due to wind cooling is 844 kcal/(h·m^2).

3.2. ASSESSMENT OF BIOCLIMATIC RESOURCES OF THE HUMAN THERMAL STATE IN SUMMER (JUNE, JULY, AUGUST)

Analysis of the generalized desirability index *DS* and its partial feedback showed that in Ukraine summer meteorological conditions are mostly comfortable for humans, and thermal load is moderate. Partial functions of the Harrington desirability function for the three selected bioclimatic indices are presented in Figure 4.

Zoning of Ukraine according to the integrated index of *DS* has identified only three zones with different levels of bioclimatic resources and comfort of weather conditions (Fig. 5). For selected zones the average values of climatic characteristics were calculated for 1981-2010 (Table 5).

It was found that in summer a considerable level of thermal load and, accordingly, unsatisfactory level of bioclimatic resources for the human thermal state is observed in the southern and the south-eastern regions of Ukraine (Zone 2 in Fig. 5). Zone 2 covers an area of 235,294 km^2, 38.98% of Ukraine.

In this area, the values of bioclimatic indices are 10-20% higher than the maximum comfort limit. There is overheating of the human body, fatigue, and heat exhaustion during prolonged exposure to the outdoors and physical activity. In this zone, the average summer temperature is 21.4°C, the average of the maximum 27.2°C, and the minimum 15.9°C. The average number of summer days is 86. Every year 65 days of high temperatures are recorded and the maximum duration of the hot period in some years can be up to 40 days. The load on the body's thermoregulation system is intensified when high air temperatures are maintained not only during the day but also at night. In Zone 2, the average number of tropical nights is 11 (Table 5). During the summer, 4 days with stuffiness are recorded. This region is characterized by the lowest relative humidity (45.5%), the smallest number of days with comfortable air humidity for humans (within 40-60%) – only 42 days per season, and the highest values of wind speed (2.3 m·s^{-1}). Due to the cooling effect of the wind, the value of *EET* for the comfort zone is 15.3°C, but the value of *PEET* exceeds the maximum comfort zone limit at 3.7°C (Table 5).

This study revealed that in the summer in Ukraine only individual stations have a complex of meteorological conditions that form unsatisfactory levels of bioclimatic resources for the human thermal state; the overall category of thermal sensation is "moderately cool." Most stations are within the comfortable range with tolerable heat loads.

The most uncomfortable area is the southern coast of the Crimean Peninsula, where the level of bioclimatic resources is unacceptable (*DS* ≤ 0.20); weather conditions are classified as extremely uncomfortable with moderate thermal load (Zone 1 in Fig. 4). Its area is 78.48 km^2 (0.013% of the territory of Ukraine). The highest values of average temperature (22.7°C), minimum temperature (18.6°C), and maximum temperature (27.1°C) are typical for this area. The records showed 90 summer days, 69 hot days, and 31 tropical nights. However, the absolute maximum duration of the hot period is 35 days, fewer than in Zone 2. Zone 1 also has the highest relative humidity (52.7%), the most days with stuffiness – an average of 5 days per season – and the lowest wind speeds (1.6 m·s^{-1}). Such a complex of weather conditions enhances the thermal load on the human body. The value of *EET* is close to the upper limit of comfort, i.e. 17.5°C, and the *PEET* exceeds it by 5.5°C.

For the rest of Ukraine, 61% of the country (368,212 km^2), the values of *DS* vary from 0.37 to 0.65, indicating satisfactory levels of bioclimatic resources. Zone 3 is characterized by comfortable weather conditions for humans, with moderate thermal load. The average air temperature is 18.5°C. The mean maximum reaches 24.4°C, and the mean minimum is 13.2°C. There are 76 summer days, with the fewest hot days (42 days per season). This area has the shortest duration of the hot period, only 15 days, half of that in an area with unsatisfactory heat levels and uncomfortable weather (Zone 2). For Zone 3, days with stuffiness or tropical nights are infrequent, averaging only 2 days per season. The region also has the lowest values of *EET* and *PEET* (12.6°C and 22.4°C, respectively). Bioclimatic resources in this zone are favorable for the development of resort recreational activities in summer.

Fig. 5. Spatial distribution of *DS* values (1981-2010) across Ukraine.

Table 5. Climatic characteristics of zones with different levels of bioclimatic resources for the human thermal state during the summer period (1981-2010) in Ukraine.

Characteristics	Zones with different levels of bioclimatic resources		
	1*	2*	3*
average temperature, °C	22.7	21.4	18.5
mean minimum temperature, °C	18.6	15.9	24.4
mean maximum temperature, °C	27.1	27.2	13.2
number of summer days with $T_{av} \geq 15$°C, days	90	86	76
number of hot days with $T_{max} \geq 25$°C, days	69	65	42
number of tropical nights with $T_{min} \geq 20$°C, days	31	11	2
absolute maximum duration of the period with $T_{max} \geq 25$°C, days	35	40	15
average relative humidity, %	52.7	45.5	50.7
number of days with relative humidity within 40-60%, days	53	42	49
number of days with stuffiness, days	5	4	2
average wind speed, m·s^{-1}	1.6	2.3	2.2
equivalent-efficient temperatures of Missenard *EET*, °C	17.5	15.3	12.6
radiation equivalent-effective temperature (*PEET*), °C	26.5	24.7	22.4
Heat Index (*HI*), °F	76.9	77.1	78.8

*1 – unacceptable level, extremely uncomfortable weather; *2 – unsatisfactory level, uncomfortable weather; *3 – satisfactory level, comfortable weather.

4. CONCLUSIONS

It is established that, depending on what factors or their complex is being considered, the same regions of Ukraine can be both comfortable and uncomfortable for humans. We have presented a method for integrated assessment of the seasonal level of comfort of climatic conditions and the degree of endowment with bioclimatic resources. The method employs comprehensive indicators that account for various aspects of the influence of meteorological conditions on the human thermal state, separately for the winter (*DW*) and summer (*DS*), using Harrington's desirability function. Based on these indicators, we have specified quantitative criteria, and boundaries of zones with different comfort levels and degree of endowment with bioclimatic resources in Ukraine. The locations of regions with comfortable and uncomfortable conditions, and their total area was determined.

Four zones were identified for the winter across Ukraine. In Zone 1, with unacceptably cold and extremely uncomfortable weather, there is the greatest influence of meteorological conditions on human health, heat load on the human body, and bodily heat loss.

Zone 1 comprises the north-eastern regions of the country, the highlands of the Carpathians, and the Donetsk ridge, 7.26% of the total area of Ukraine. Zone 2, with unsatisfactory levels of indicators and uncomfortable weather makes up 41.78% of Ukraine. Zone 3, with satisfactory bioclimatic resources and comfortable weather, is the largest of all zones (49.61% of Ukraine). Thus, winter meteorological conditions in Ukraine are mostly comfortable for the human thermal state. Zone 4, with good values of indicators and very comfortable weather, is only 1.35% of the territory: the southern region of Odessa, the western district of the Transcarpathian region, and the southern coast of Crimea.

In summer across Ukraine only 3 zones were identified. Zone 4, with good levels of indicators and very comfortable weather, was not highlighted by the *DS* integrated index. Zone 1, with unacceptable levels of indicators and extremely uncomfortable weather occupies a small territory (0.013% of Ukraine) on the southern coast of the Crimean Peninsula that has extreme thermal stress. Zone 2, with unsatisfactory levels of indicators and uncomfortable weather makes up 38.98% of Ukraine. Zone 3, with the satisfactory levels of bioclimatic resources and comfortable weather, as in winter, is also the largest of all zones. Across 61% of the territory of Ukraine in summer, meteorological conditions are comfortable for the human thermal state.

The main scientific findings of the study can be used to assess climate risks in the fields of tourism, recreation, medicine, balneology, and urban development. They should have importance in the development of strategies, programs, and measures to adapt to climate change. The results contribute to the expansion of scientific knowledge about the variability of weather and climatic comfort in the various regions of Ukraine and the state of bioclimatic resources of the country in the current climatic period.

REFERENCES

- Epstein Y., Moran D.S., 2006, Thermal comfort and the heat stress indices, Industrial Health, 44 (3), 388-398, DOI: 10.2486/indhealth.44.388
- Fröhlich D., Matzarakis A., 2015, A quantitative sensitivity analysis on the behaviour of common thermal indices under hot and windy conditions in Doha, Qatar, Theoretical and Applied Climatology, 124, 179-187, DOI: 10.1007/s00704-015-1410-5
- Harrington E.C., 1965, The desirability function, Industrial Quality Control, 21, 494-498
- Jendritzky G., Havenith G., Weihs P., Batchvarova E., DeDear R., 2007, The Universal Thermal Climate Index UTCI. Goal and state of COST Action 730, [in:] Bioclimatology and natural hazards, K. Strelcova, J. Skvarenina, M. Blazenec (eds.), International Scientific Conference, Polana nad Detvou, Slovakia, September 17-20
- Kalkstein L.S., 2001, Biometeorology – looking at the links between weather, climate and health, WMO Bulletin, 2, 136-142
- Kalkstein L.S., Davis R.S., 1989, Weather and human mortality: an evaluation of demographic and interregional responses in the United States, Annals of Association of American Geographers, 79 (1), 44-64, DOI: 10.1111/j.1467-8306.1989.tb00249.x
- Kobysheva N.V., Stadnik V.V., Kljueva M.V., 2008, Manual of specialized climatological services for Economy, (in Russian), SPb, 336 pp.
- Matthies F., Bickler G., Marin N.C, Hales S. (eds.), 2011, Action plans for protecting public health from the effects of heat waves, (in Russian), available online at http://www.euro.who.int/__data/assets/pdf_file/0003/147873/E91347R.pdf (data access 09.08.2020)
- Mohan M., Gupta A., Bhati S., 2014, A modified approach to analyze thermal comfort classification, Atmospheric and Climate Sciences, 4 (1), 7-19, DOI: 10.4236/acs.2014.41002
- OFCM, 2003, Report on wind chill temperature and extreme heat indices: evaluation and improvement projects, FCM-R19-2003, 75 pp., available online at https://www.hsdl.org/?view&did=22050 (data access 09.08.2020)
- Siple P.A., Passel C.F., 1945, Measurements of dry atmospheric cooling in subfreezing temperatures, Proceedings of the American Philosophical Society, 89 (1), 177-199
- Stepanenko S.M., Pol'ovyy A.M. (eds.), 2011, The assessment of impact of climate change on the Ukraine industry, (in Ukrainian), Odessa: Ecology Publ., 696 pp.
- Stepanenko S.M., Pol'ovyy A.M. (eds.), 2015, Climate change and its impact on sectors of the Ukraine economy, (in Ukrainian), Odessa: TES Publ., 520 pp.
- Strategy of sustainable development "Ukraine – 2020", 2015, (in Ukrainian), available online at https://zakon.rada.gov.ua/laws/show/5/2015 (data access 09.08.2020)

Photo by Alina Fedorchenko on Unsplash

Meteorology Hydrology and Water Management
Volume 8 | Issue 2

Trends in monthly, seasonal, and annual fluctuations in flood peaks for the upper Dniester River

Serhii Melnyk
Odessa National Polytechnic University, Shevchenko av. 1, 65044 Odessa, Ukraine, e-mail: melnik.s.v@opu.ua

Nataliia Loboda
Odessa State Environmental University, Lvivska Street 15, 65016 Odessa, Ukraine, e-mail: natalie.loboda@gmail.com

DOI: 10.26491/mhwm/126705

ABSTRACT. The importance of the Dniester River in the socio-economic life of Moldova and Ukraine necessitates research into the main trends in the river's runoff characteristics and dynamics, especially now, when climate change is significantly altering the water regime of rivers. This paper presents a solution for the problems of identifying the main trends in daily maximum river discharge by seasons and months for various calculation intervals. Two calculation intervals (1981-1998; 1999-2015) with different climatic conditions are considered. Each interval corresponds to one complete cycle of river water discharge. Climatic conditions as a result of global warming are changing differently in the mountains and on the plain, therefore, the identification of trends was performed separately for the alpine and lowland parts of the Dniester River annual runoff formation zone. The search for statistically significant trends was carried out by means of the Mann-Kendall test. The analysis of the frequency of maximum discharges (peak over threshold; POT3) was performed for selected rivers in the studied area. The earlier period (1981-1998) showed statistically significant positive trends for both alpine and lowland rivers of the Upper Dniester. The later period (1999-2015) differed, exhibiting exclusively negative significant trends in daily peaks both by months and by seasons. This result indicates a persistent tendency toward decreasing maximum water runoff for all rivers of the Upper Dniester catchment. There were no statistically significant trends in the frequency of floods.

KEYWORDS: Mann-Kendall test, Dniester, peak over threshold, daily runoff maxima, trends in the changes in maximum.

SUBMITTED: 2 March 2020 | **REVISED:** 14 July 2020 | **ACCEPTED:** 24 August 2020

1. INTRODUCTION

Climate change necessitates sustainable development strategies for countries with economies in transition (Corobov 2011). Socio-economic challenges in the Dniester River basin are associated with an uneven distribution of runoff along the length of the river. The river basin is divided into a runoff formation zone and a runoff management zone. The formation zone covers about 1/3 of the total catchment area and belongs to the region of excess and sufficient water content. This zone is called the Upper Dniester. A major part of the water runoff in this zone enters the main river from the Carpathian right-bank mountain tributaries, and the smaller part from the left-bank, lowland Podolsk tributaries.

The topical task of hydrology in the upper part of the Dniester River catchment area is flood protection during spring floods and high-water periods. In the middle and lower parts the main task is the search for ways to control the current shortage of water resources. The solution to these problems was achieved through long-term regulation of the runoff by the Dniester and Dubossary reservoirs. The Dniester reservoir is designed to provide hydropower and has a negative impact on the aquatic ecosystem of the middle and lower parts of the Dniester River basin. The hydrological regime and the hydro-ecological status of the Middle and Lower Dniester are completely dependent on the dates and volumes of releases from the Dniester reservoir which do not always meet environmental requirements. Climate changes in the early 21st century exacerbated the uneven distribution of runoff along the length of the river. The dependence of the water content of the entire river on the volume of water in the formation zone has increased. To solve the environmental problems of the Dniester, the Environment and Security Initiative (ENVSEC 2015) suggested a project on "Promotion of transboundary cooperation and integrated water resources management in the Dniester River basin" at the request of the governments of the Republics of Moldova and Ukraine. According to Libert (2019), international organizations such as OSCE, the UNECE, and the ENVSEC are currently taking measures to adapt the Dniester basin to climate change. Further strategies for the use of water resources of the Dniester River will depend on forecast data on the changes in runoff volumes in the formation zone.

This paper is aimed at a search for the prevailing trends in dynamics of the maximum water runoff characteristics of the upper Dniester in the late 20th and early 21st century, whence significant climate changes have occurred. Perspectives for changes in maximum flow determine the strategy of river water resources management in the future. Positive trends will require expansion of flood and landslide protection, whereas negative trends will require the use of long-period storage reservoirs for saving and redistributing water resources within the river basin. The area of study includes the alpine (Ukrainian Carpathians) and lowland (Podolia) tributaries of the Dniester River located in the runoff formation zone. The subject of study is trends in maximum runoff by months and seasons. The main research method is the non-parametric Mann-Kendall test for monotonic trends over time.

An analysis of research papers on relationships between climate change and the runoff of mountain watersheds leads to conflicting conclusions (Sayemuzzaman, Manoj 2014; Pluntke et al. 2016; Piniewski et al. 2017; Szwejkowski et al. 2017; Mangini et al. 2018; Kohnová et al. 2019). The fact is that the main climatic factors involved in the formation of river runoff are air temperature and precipitation. The first factor is characterized by some inertia, and the second one is variable both in time and in space. In the mountains, as a rule, the determining factor in runoff formation is precipitation, the spatiotemporal distribution of which depends on the geographic location of the study area, its distance from the sea (ocean), the orientation of the mountain slopes with respect to the direction of the main moisture transfer by air currents, and the type of mountainous terrain and location of mountain ranges.

International organizations (ENVSEC, UNEP, UNECE, OSCE etc.) place high emphasis on long-term forecasts of changes in river runoff characteristics in various regions of the Earth in accordance with climate scenarios. According to the research under the international project "Climate Change and Security in Eastern Europe, Central Asia and Southern Caucasus", with the component of "Climate Change and Security in the Dniester River Basin" (ENVSEC/UNECE/OSCE 2015), the Dniester River runoff formation zone will experience an increase in the average long-term air temperature of +1°C during 2021-2050 compared to 1981-2010, and the annual precipitation will increase 1-2%. No changes in the average long-term runoff in the mountainous part of the Dniester are expected, and in the plains within the study area, the runoff may decrease from 0 to 10%. The same paper indicates the possibility of a significant increase in the intensity of floods during the warm period (by 30-40%). The report by the transboundary (Ukraine-Moldova) project "Reducing vulnerability to extreme floods and climate change in the Dniester river basin" (ENVSEC 2013), being implemented under the Environment and Security Initiative (ENVSEC), mentioned that considerable changes in maximum discharges in the mountainous part are not expected for the period 2021-2050. In Podolia (the plains), flood reduction by 15-16% is possible (the A1B scenario, the REMO, ECHAM5 model). According to forecasts, the intra-annual distribution of the runoff of Carpathian rivers may change as follows: runoff during the cold season will increase, runoff during spring floods will decrease, with peaks shifting to earlier dates, and the frequency of floods will increase. Substantial changes in the maximum runoff in Podolia are not expected. A comprehensive paper by authors from several countries (Blöschl et al. 2019), examined the changes in the maximum runoff of European rivers under global warming (1960-2010). It was observed that in Eastern Europe there was a decrease in floods and the snow melt shifted to earlier dates. These tendencies are assumed to persist in the future.

Various conditions for the formation of the upper Dniester maximum runoff make it necessary to further analyze the dynamics of its changes and identify the main trends.

2. THE STUDY AREA

The Dniester River is transboundary and belongs to the Black Sea basin. The river catchment stretches from the northwest to the southeast. The total length of the river is 1,350 km. The catchment area is 72,300 sq. km, 72.1% of which belongs to Ukraine, 26.8% to Moldova, and 0.4% to Poland (Fig. 1). The average long-term annual runoff of the Dniester river is 10 km^3. According to Sukhodolov et al. (2009), the river water is used by various consumers (drinking and municipal water supply, agriculture, and industry).

The area of river runoff formation is located at the Ukrainian Carpathian Mountains (at altitudes of 300-1100 m). The area of intensive consumption is located in the middle and lower reaches of the river (Forest-Steppe and Steppe geographical zones). The intensity of water consumption increases with the transition from the Forest-Steppe geographical zone to the Steppe. The river is fed from snow and rain sources, and during the low water period from groundwater. Sources of Dniester River runoff

Fig. 1. The studied part of the Dniester River basin.

in the formation zone differ: rain predominates in the mountains, and snow on the plain. The response of water resources to climate change since the late 20th century is also different for lowland and alpine rivers. In lowland rivers, the increased air temperatures in the cold season and their transition from negative to positive reduces the depth of frost penetration into the soil, and thus, the accumulated water reserves in the snow cover before snowmelt begins. More frequent winter thaws contribute to the formation of winter floods and melt water filtration into subterranean aquifers, which is facilitated by the presence of karst, easily eroded rocks, in the basins of the left-bank tributaries. As a result, the maximum discharges during spring floods decrease, and the runoff during the low-water period increases; there is a shift to earlier dates of snowmelt and spring flood onset.

In the mountains, the distribution of climatic factors and runoff depends on altitude. The response of the temperature regime to changes in the climate system is slower compared to the plain. The main source feeding alpine rivers is rain floods, which form almost every month. The maximum runoff values during rain floods can significantly exceed the maximum values during spring floods. Thus, the role of precipitation changes in the formation of alpine river runoff is fundamental in comparison with the changes in air temperature.

3. METHODOLOGY AND DATA

3.1. FACTOR ANALYSIS

Factor analysis was applied to zoning according to similarities in fluctuations of maximum runoff within the upper part of the Dniester River basin. Districts were identified by means of graphs, on the axes of which factor loads were marked. The closer the points are located on the graph, the closer the relationship between the series of observations. Sets of closely spaced points form a district with synchronous runoff fluctuations. The location of centers of the sets at an angle close to 90 degrees indicates non-synchronism. Non-synchronism of fluctuations in the studied parameter is the result of differences in the runoff formation conditions in the territory under study.

The general principles of factor analysis and their use in mathematical software packages are widely described in the literature, e.g., Pituch and Stevens (2016). We applied the standard module "Factor analysis" of the Statistica program, using catchment areas (Catchments) as variables, and observation years as cases. The factor extraction method was principal components, and the factor rotation method was Varimax normalized.

3.2. DIFFERENCE CUMULATIVE (RESIDUAL MASS) CURVE

To assess the spatiotemporal fluctuations in the maximum runoff and to identify the phases of high and low water content, we used the graph of the difference cumulative curve. These graphs are often used to determine long-term cycles in runoff fluctuations (Zabolotnia et al. 2019). The ordinates for this curve $f(t)$ are accumulation over time for the sum of deviations of the relative values of discharges from one:

$$f(t) = \Sigma_{t=1}^{T}(k(t) - 1) \quad (1)$$

where: T is the number of observation years, $k(t) = Q(t)/Q_{aver.}$ is the modular coefficient; $Q(t)$ is the maximum daily discharge for a year, $Q_{aver.}$ is the average value of the maximum daily discharges for the entire observation period, and the average value of the modular coefficient for a long-term period is one: $k_{aver.} = 1$.

The period for which the integral curve section has a slope upward with respect to the horizontal line corresponds to the positive phase of the runoff fluctuations. The period for which the integral curve section has a slope downward with respect to the horizontal line corresponds to the negative phase.

3.3. MANN-KENDALL TEST

The main research method for revealing statistically significant trends was the Mann-Kendall test, which is widely used in hydrology (Yue, Pilon 2004; Khan et al. 2015). The Mann-Kendall test uses nonparametric criteria for testing the significance of a trend. Statistics S has the following form:

$$S = \Sigma_{i=1}^{n-1}\Sigma_{j=i+1}^{n} sgn(x_j - x_i) \quad (2)$$

where n is the number of observations.

$$sgn(x) = \begin{cases} 1 & if\ x > 0 \\ 0 & if\ x = 0 \\ -1 & if\ x < 0 \end{cases} \quad (3)$$

For $n \geq 40$, the statistics S will be asymptotic, subject to the normal distribution law, in which the average value is zero, and the variance is calculated by the following equation:

$$Var\{S\} = \frac{1}{18}[n(n-1)(2n+5) - \Sigma_t t(t-1)(2t+5)] \quad (4)$$

where t is the size of this related group; $\sum_t$ is the sum of all related groups in the data sample.

Table 1. List of selected catchment areas along the Dniester River Basin within Ukraine.

No.	River (water gauge)	Catchment area [km²]	No.	River (water gauge)	Catchment area [km²]
1	Dniester (Strilky site)	384	27	Bystrytsia Solotvynska (Ivano-Frankivsk site)	777
2	Dniester (Sambir site)	850	28	Strvyazh (Luky site)	910
3	Dniester (Zhuravne site)	9.910	29	Vereshchytsia (Komarne site)	812
4	Dniester (Halych site)	14.700	30	Shchyrets (Shchyrech site)	307
5	Dniester (Zalishchyky site)	24.600	31	Svirzh (Bukachivtsi site)	465
6	Dniester (Mohyliv-Podilskyi site)	43.000	32	Gnyla Lypa (Bilshivtsi site)	848
7	Bystrytsia (Ozymyna site)	206	33	Zolota Lypa (Berezhany site)	690
8	Tysmenytsia (Drohobych site)	250	34	Zolota Lypa (Zadariv site)	1.390
9	Stryi (Matkiv site)	106	35	Koropets (Pidhaitsi site)	227
10	Stryi (Zavadivka site)	740	36	Koropets (Koropets site)	476
11	Stryi (Verkhnie Syniovydne site)	2.400	37	Strypa (Kaplytsi site)	411
12	Opir (Skole site)	733	38	Strypa (Buchach site)	1.270
13	Slavska (Slavske site)	77	39	Seret (Velyka Berezovytsia s.)	939
14	Golovchanka (Tukhlia site)	130	40	Seret (Chortkiv site)	3.170
15	Orava (Sviatoslav site)	204	41	Nichlava (Strelkivtsi site)	584
16	Svicha (Myslivka site)	201	42	Zbruch (Volochysk site)	712
17	Svicha (Zarichne site)	1.280	43	Zbruch (Zavallia site)	3.240
18	Luzhanka (Hoshiv site)	146	44	Zhvanchyk (Kuhaivtsi site)	229
19	Sukel (Tysiv site)	138	45	Zhvanchyk (Lastivtsi site)	703
20	Limnytsia (Osmoloda site)	203	46	Smotrych (Kupyn site)	799
21	Limnytsia (Perevozets site)	1.490	47	Smotrych (Tsybulivka site)	1.790
22	Chechva (Spas site)	269	48	Muksha (Mala Slobidka site)	302
23	Lukva (Bodnariv site)	185	49	Ushytsia (Zinkiv site)	525
24	Bystrytsia-Nadvornianska (Pasichna site)	482	50	Ushytsia (Kryvchany site)	1.370
25	Vorona (Tysmenytsia site)	657	51	Kalius (Nova Ushytsia site)	259
26	Bystrytsia Solotvynska (Guta site)	112	52	Markivka (Pidlisivska site)	615

The standardized verification statistic Z is calculated by the equation:

$$Z = \begin{cases} if\ S > 0, \frac{S-1}{\sqrt{Var(S)}} \\ if\ S = 0, \quad 0 \\ if\ S < 0, \frac{S+1}{\sqrt{Var(S)}} \end{cases} \quad (5)$$

The statistic Z follows the standard normal distribution law with a mean of zero value and a unit variance (Yue, Pilon 2004).

The values p of the statistic Z is determined from the tables of a two-sided function of the normal integral distribution.

In many papers (Pujol et al. 2007; Svensson et al. 2009; Melnyk, Loboda 2018) the concept of "trend index" (Ti) is used for assessment of a trend. In Kundzewicz et al. (2005) use of Ti is explained that: "the value of the Mann-Kendall test statistic is hard to interpret; therefore, the results are stated using the trend index (Ti), a measure directly related to the computed significance level (p value), α, or to the confidence level $(1-\alpha)$." It is calculated as $Ti = (1-\alpha)\cdot 100\%$ for a positive trend and $Ti = -(1-\alpha)\cdot 100\%$ for a negative one. For two-tailed tests, Ti ranges from –100% to +100%.

Negative values of Ti indicate a tendency to decrease, and positive values indicate a tendency to increase in the studied parameter.

3.4. PEAK-OVER-THRESHOLD (POT)

To determine the trends of extreme hydrological phenomena frequency, the method for calculation of changes in the frequency of discharges exceeding the threshold value, peak-over-threshold (POT), was chosen. For each river, discharges which were exceeded on average 3 times year over the observation period, were taken as a threshold value (POT3). This method has been widely used in hydrological studies, e.g., by Svensson et al. (2009), Mangini et al. (2018).

3.5. INITIAL DATA

Observational data on daily maximum water discharges for 1981-2015 for 22 catchment areas in the mountainous part of the Dniester River basin (6 stations of which are located on the main river) and 24 catchment areas in the plains at the left bank are used in the paper (Table 1). To build the series of initial data on runoff in each month of the current year, the maximum daily water discharge was selected. The calculation period was chosen based on research into the patterns of fluctuations in the annual runoff of the Dniester River at the Zalishchyky site (1949-2015). This site is the last hydrological site (of all hydrological stations located upstream), in which runoff fluctuations retain a natural (undisturbed by regulation) pattern. The Dnistrovske reservoir is situated below the Dniester River Zalishchyky site.

4. RESULTS

At the first stage of factor analysis, the variance is calculated and explained by each successive factor. In our case, the first factor accounts for 36% of the total variance, and the second one 25%. Subsequent factors account for 6% or less. Therefore, the data matrix was analyzed with 2 factors. The results are given in Figure 2, where two sets of points are marked out. The first set includes lowland rivers (left-bank tributaries of the Dniester River), and the second set alpine ones (right-bank tributaries of the Dniester River). Marking-out of the two districts allows us to conclude that there are differences in fluctuations in the maximum runoff between left-bank and right-bank tributaries. The physical interpretation of the results is that the maximum runoff of alpine rivers is formed as the combined result of snow melt and rainfall, whereas the maximum runoff of lowland rivers is formed mainly during spring floods owing to snow melt.

A similar approach based on the analysis of correlations between the series of maximum runoff values was used in the paper by Viglione et al. (2010).

Fluctuations in the mainstem river runoff are determined by the patterns of fluctuations in the runoff of alpine tributaries, since a major part of the runoff is formed in the mountains. That is why the stations located on the main river are assigned to the mountainous region.

Fluctuations in runoff are cyclical. An analysis of the patterns of these fluctuations based on difference integral curves was performed for both annual and maximum runoff over the entire observation

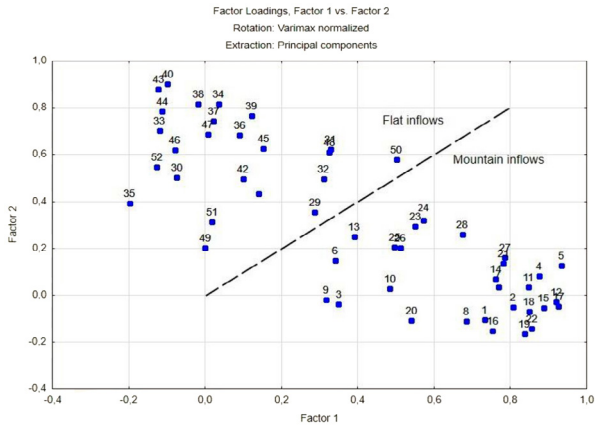

Fig. 2. Plot of factor loadings. Numbers correspond to the catchments specified in Table 1.

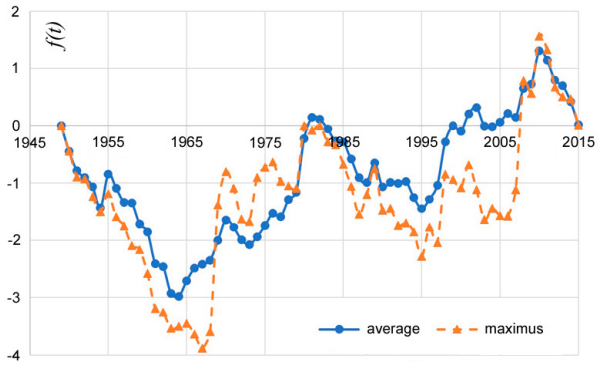

Fig. 3. The residual mass curves of annual and maximum runoff, Dniester – Zalishchyky site). If the curve goes up, then a positive phase of flow fluctuations is noted, if down, negative.

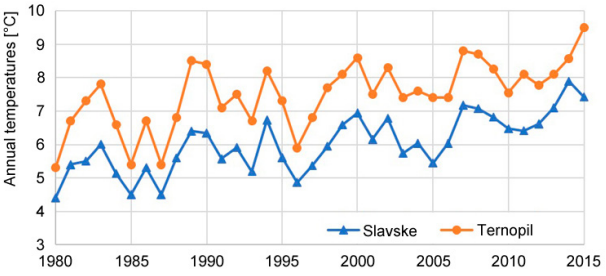

Fig. 4. Fluctuations of annual temperatures at meteorological stations Ternopil (left-bank area, altitude of 300 m) and Slavske (the Ukrainian Carpathians, the altitude of 600 m).

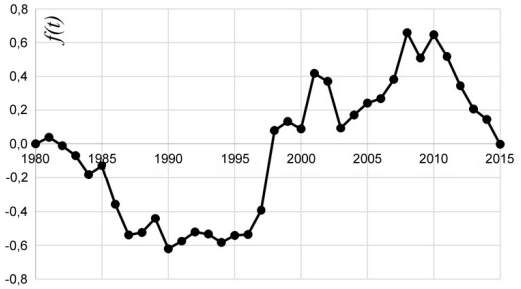

Fig. 5. The residual mass curves of annual precipitation for the period of 1980-2015, Slavske meteorological station.

period (1949-2015). Based on the difference integral curves, three complete cycles of river discharge were identified: 1949-1980, 1981-1998, and 1999-2015 (Fig. 3). The last two cycles (1981-2015) relate to the period of increased air temperatures (Fig. 4). In the fluctuations in annual precipitation during this period (Fig. 5), two cycles, 1981-1998 and 1999-2015, are also distinguished; in what follows, they are considered as calculation intervals.

The values of the trend index $|Ti|$ were defined for each month, season, and year. The presence of trends was indicated by the sign of the index (Ti), with selection of the predominant sign and calculation of the absolute and relative frequency of the event.

The presence of statistically significant trends was identified when the condition ($|Ti| > 0.9$) was met. The relative frequency of an event or an empirical probability was estimated as the ratio of the number of cases when the studied event was observed to the total number of events considered. As an example, the trend indices for specific sites are given in Table 2.

Assessment of the empirical probability of tendencies and statistically significant trends in the fluctuations of the daily runoff maxima by months showed that they occurred most often in the calculation interval of 1981-1998 (March, October, November, and December) and were not found in the period of 1999-2015. For the alpine tributaries (Table 3), in contrast to the lowland tributaries (Table 4), the frequency of positive indices $Ti > 0$ in 1981-1998 was also observed in the summer months (May and July), owing to formation of rain floods in the mountains. For the lowland tributaries in the summer months there is a low water season and rain floods are rarely formed. Therefore, positive tendencies and trends were not identified.

The increase in air temperatures in the late 20th and the early 21st century (Table 5) is of great importance in formation of positive maximum runoff trends in the cold period months (December-March). A significant increase in air temperatures in March with their transition from negative to positive values (March for the calculation interval of 1981-1999) was one of the reasons for occurrence of a large number of cases with positive temperatures ($Ti > 0$) and ($Ti > 0.9$).

The absence of positive tendencies and trends in the second calculation period (1999-2015) results from a decrease in the amount of precipitation compared to the previous period of 1981-1998. which is clearly seen in Figure 6.

During the study of the patterns of fluctuations in maximum runoff by season positive tendencies were observed for the autumn and winter seasons for both lowland and alpine rivers in the period of 1981-1998 (Table 6, Table 7). Statistically significant positive trends were identified only in the maximum runoff of alpine tributaries that is associated with a greater amount of rainfall in the mountains compared to the plain areas. In the period of 1999-2015, all identified tendencies and trends are negative.

According to several research papers, e.g., European Academies' Science Advisory Council (EurekAlert! 2018), a significant increase in the frequency of extreme hydrological events was observed during 1980-2016. To test the hypothesis of an increase in the frequency of floods in the studied area, a selective analysis was conducted

Table 2. Monthly trend indices (*Ti*) for 1999-2015 for specific sites (statistically significant values are shown in bold).

River (water gauge)	I	II	III	IV	V	VI	VII	VIII	IX	X	XI	XII
Dniester (Sambir)	**–0.92**	–0.80	–0.67	**–0.90**	0.59	–0.30	–0.71	–0.80	–0.77	–0.77	–0.64	0.00
Dniester (Zalishchyky)	–0.46	**–0.91**	**–0.94**	–0.75	0.30	0.58	–0.77	–0.77	–0.66	–0.69	–0.59	–0.18
Svicha (Zarichne)	0.67	0.17	**–0.95**	–0.24	0.63	–0.02	–0.14	–0.17	–0.45	–0.29	–0.40	0.50
Bystrytsia Solotvynska (Ivano-Frankivsk)	–0.50	–0.50	**–0.91**	**–0.91**	0.06	–0.30	**–0.91**	–0.67	**–0.93**	–0.12	–0.83	–0.21
Zolota Lypa (Zadariv)	**–0.94**	**–0.97**	**–0.98**	–0.79	–0.50	–0.87	**–0.91**	–0.80	**–0.97**	**–0.92**	**–0.98**	**–0.96**
Smotrych (Kupyn)	**–0.97**	**–0.99**	**–0.99**	–0.80	**–0.94**	–0.87	**–0.98**	**–0.99**	**–0.98**	**–0.98**	-0.80	-0.87

Table 3. Relative frequency of appearance [%] of tendencies and trends in fluctuations in the daily maxima for alpine tributaries of the Dniester River by months.

Months	I	II	III	IV	V	VI	VII	VIII	IX	X	XI	XII
Calculation interval	1981-1998											
Sign and relative frequency of a tendency appearance [%]	–60	–65	+95	–100	+80	–60	+85	–80	–55	+100	+90	+100
Sign and relative frequency of a statistically significant trend appearance [%]	0	–5	+60	–60	+25	–5	+5	–10	–15	+10	+30	+40
Calculation interval	1999-2015											
Sign and relative frequency of a tendency appearance [%]	–70	–90	–100	–100	+70	–70	–90	–90	–100	–85	–85	–50
Sign and relative frequency of a statistically significant trend appearance [%]	–10	–15	–55	–40	0	0	–30	–30	–50	–30	–20	0

Table 4. Relative frequency of appearance [%] of tendencies and trends in fluctuations in the daily maxima for left-bank (lowland) tributaries of the Dniester River (Ukraine) by months.

Months	I	II	III	IV	V	VI	VII	VIII	IX	X	XI	XII
Calculation interval	1981-1998											
Sign and relative frequency of a tendency appearance [%]	–86	–80	+68	–100	–80	–89	–70	–70	–70	+75	+75	+70
Sign and relative frequency of a statistically significant trend appearance [%]	–28	–14	+4	–76	–11	–15	–15	–12	–12	+12	+12	+9
Calculation interval	1999-2015											
Sign and relative frequency of a tendency appearance [%]	–86	–90	–90	–86	–55	–50	–86	–86	–68	–65	–55	–68
Sign and relative frequency of a statistically significant trend appearance [%]	–32	–38	–38	–32	–12	–8	–25	–35	–35	–35	–32	–42

of the change in frequency of discharges that were exceeded 3 times a year on average during the observation period (i.e. a peak-over-threshold analysis, or POT3).

For calculation of the *Ti* index, 6 sites with an observation period of 1992-2015 were selected. Of the 6 studied sites, 2 sites are located on the right-bank tributaries, 2 on the left-bank tributaries and 2 on the mainstem river, but upstream from the Dniester reservoir (Zalishchyky site). The results obtained (by the chosen method) allow us to conclude that there are no statistically significant trends in the frequency of floods (Fig. 7).

5. DISCUSSION

This article can be viewed as a continuation of the discussion on the presence of maximum flow trends for rivers of the European continent, proposed by a number of authors: Pujol et al. (2007), Kundzewicz et al. (2013), Mangini et al. (2018), and Kohnová et al. (2019).

On the maps of hydro-climatic regions in Europe based on a bio-geographical classification provided by the EEA, which is cited in a number of papers, e.g., Walter Mangini et al. (2018), the study area is located in two districts: alpine and continental. This is in good agreement with the results of our factor analysis. It is significant that the water regime of the main

Table 5. Average monthly air temperatures [°C] for various calculation periods (Ternopil weather station).

Months	Calculation period 1949-1980	Calculation period 1981-1998	Calculation period 1999-2015
I	–5.9	–3.90	–3.72
II	–4.5	–3.4	–2.93
III	–0.47	0.83	1.90
IV	7.25	7.38	8.9
V	12.9	13.7	14.5
VI	16.5	16.3	17.3
VII	17.7	17.7	19.6
VIII	17.1	17.3	18.7
IX	12.9	12.8	13.5
X	7.44	7.5	8.0
XI	2.22	1.28	3.33
XII	–2.67	–2.64	–2.02

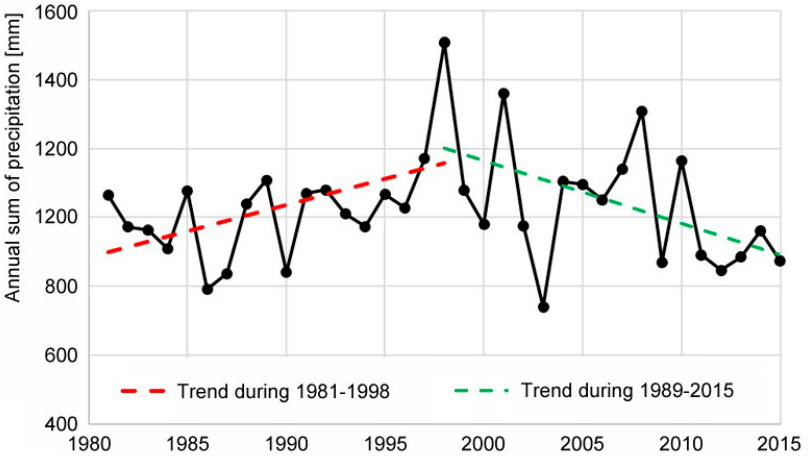

Fig. 6. Fluctuations of annual of precipitation on meteorological station Slavske.

Table 6. Relative frequency of appearance [%] of tendencies and trends in the daily maxima for alpine tributaries of the Dniester River by season.

Seasons	Winter	Spring	Summer	Autumn	Year
Calculation interval	1981-1998				
Sign and relative frequency of a tendency appearance [%]	+96	–50	–86	+90	–55
Sign and relative frequency of a statistically significant trend appearance [%]	+50	0	–8	+22	0
Calculation interval	1999-2015				
Sign and relative frequency of a tendency appearance [%]	–95	–100	–90	–87	–75
Sign and relative frequency of a statistically significant trend appearance [%]	–15	–25	–18	–22	–15

Table 7. Relative frequency of appearance [%] of tendencies and trends in the daily maxima for left-bank (lowland) tributaries of the Dniester River by season.

Seasons	Winter	Spring	Summer	Autumn	Year
Calculation interval	1981-1998				
Sign and relative frequency of a tendency appearance [%]	+72	–72	–100	+55	+65
Sign and relative frequency of a statistically significant trend appearance [%]	0	–3	–82	+3	0
Calculation interval	1999-2015				
Sign and relative frequency of a tendency appearance [%]	–72	–92	–80	–80	–90
Sign and relative frequency of a statistically significant trend appearance [%]	–38	–38	–12	–27	–46

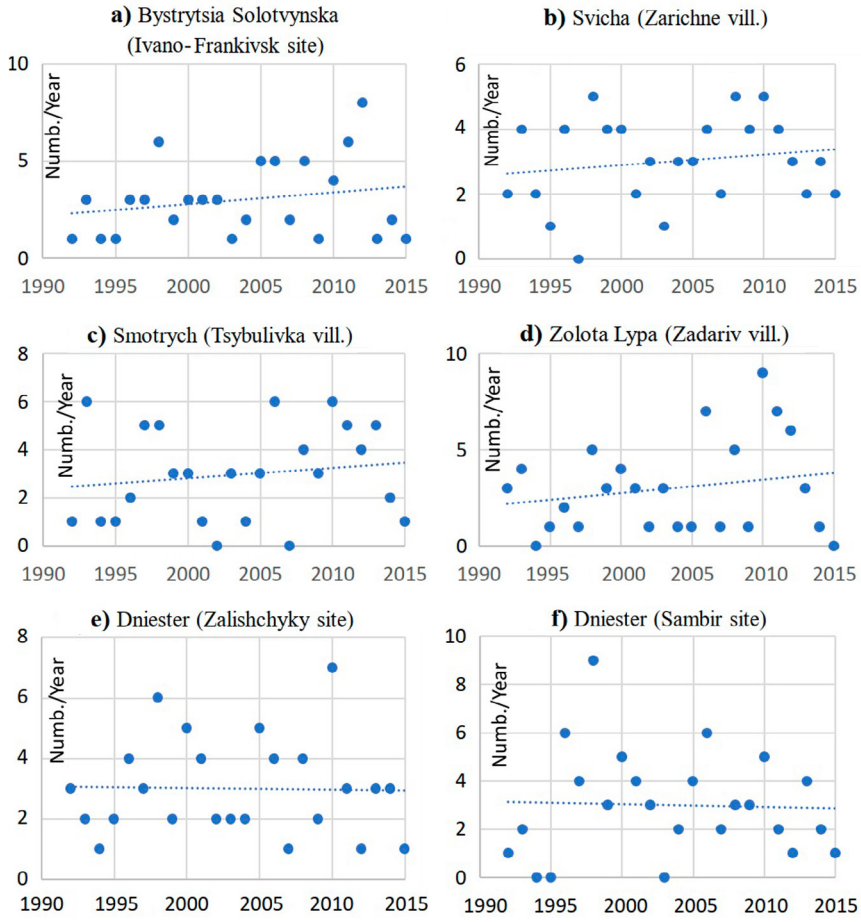

Fig. 7. Linear trends in the annual maxima of daily mean runoff frequency POT3; Slopes of trend lines: (a) *Ti* = 0.56, (b) *Ti* = 0.57, (c) *Ti* = 0.51, (d) *Ti* = 0.30, (e) *Ti* = –0.22, (f) *Ti* = –0.30.

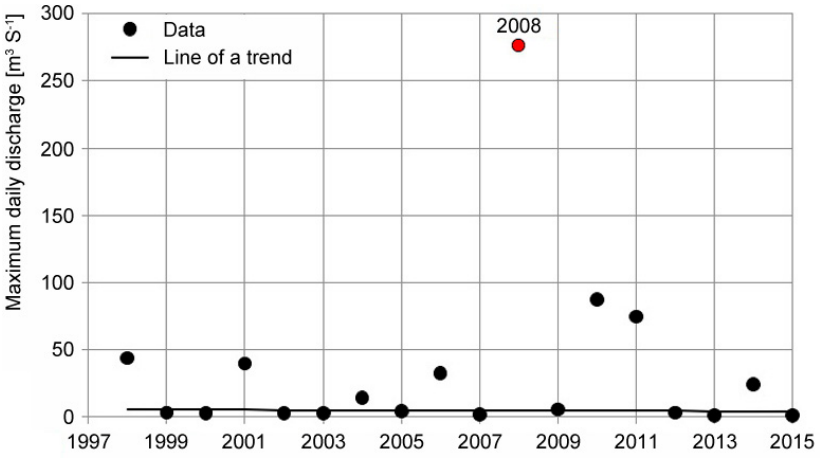

Fig. 8. The maximum daily discharge for July on the river Bystrytsia (Ozymyna site), *Ti* = –0.18; Linear trend obtained from data on the maximum daily discharge constructed by the Mann-Kendall method.

river (the Dniester) is determined mainly by the water content of the alpine district.

The autumn increase in maximum runoff we identified in the late 20th century was also observed in other regions of Europe, e.g., France (Pujol et al. 2007).

For the south-western part of Poland and eastern Saxony a similar increase, especially in the mountainous part, is accounted for by increased precipitation at altitudes of 350-650 m (Pluntke et al. 2016).

The increased maximum runoff in March for the study period is explained by warming, the transition of the average air temperature in the river basin from below to above zero degrees (Table 4). This phenomenon causes intensive snow melting, which increases the maximum runoff. Such changes have been found in basins throughout eastern Europe (Blöschl et al. 2019).

In the Upper Dniester basin, no change in the frequency of floods (POT freq) was identified. In this matter, the results in this paper coincide with the trend analysis through 2000 worldwide by Svensson et al. (2009) and through 2005 in Europe by Mangini et al. (2018).

Negative trends observed in the maximum runoff of the Upper Dniester (1999-2015) confirm conclusions about decreases in runoff maxima for eastern Europe, obtained by analysis of data through 2010 (Hall et al. 2014; Blöschl et al. 2019).

Although the Mann-Kendall test can detect the presence of monotonic trends oscillations, even if significant, are not detected (Fig. 8). For the latter purpose, confidence intervals can be used.

During catastrophic rain floods with a low probability of occurrence (1-2%), large areas may be flooded. Such rainfall floods were observed on the Dniester River in summer in 2008 and 2020.

6. CONCLUSION

I. Factor analysis of fluctuations in the maximum runoff of the rivers of the Upper Dniester basin has made it possible to distinguish two regions: mountain and plain. These regions are characterized by different origins of the maximum runoff in the mountains and on the plain.

In the mountains, runoff maxima are observed mainly during rain floods, and on the plains mainly during spring floods. Therefore, the search for trends in runoff maxima by months and seasons by means of the Mann-Kendall test (Ti) has been performed separately for lowland and alpine rivers.

II. The tendencies have been identified by the number of cases when $Ti > 0$ or $Ti < 0$, and the statistically significant trends by the number of cases when $Ti > 0.9$ or $Ti < -0.9$.

III. The tendencies observed are the same in both mountain and lowland areas, since they are due to precipitation. The influence of the air temperature changes is not yet significant.

IV. The research has shown that the late 20th century period (1981-1998) was characterized by the presence of statistically significant positive trends in the winter and autumn seasons, revealed in fluctuations in the maximum runoff. A steady tendency towards an increase in the daily maxima has been identified for March, October, and November.

V. The early 21st century (1999-2015) was distinguished from the previous calculation period (1981-1998) by the presence of exclusively negative tendencies and statistically significant trends for both months and seasons, i.e. there has been a steady tendency to decreased maximum water runoff for all the rivers of the Upper Dniester basin.

VI. Statistically significant trends in changes in the frequency of extreme events (floods) have were not found.

VII. The results show that the ongoing climate change in the Upper Dniester basin may cause both an increase and a decrease in the maximum river runoff. The major role in trends in the maximum runoff is played by precipitation. The role of thaws in the cold season may increase, especially in the lowlands, where most of the annual runoff is formed by snow melt.

VIII. The possibility of catastrophic rain floods and the predominance of the role of precipitation in the formation of the Upper Dniester runoff allow us to conclude that in order to adapt to climate change in the 21st century, it is necessary to regulate the river runoff through reservoirs and build structures to protect against floods and landslides.

IX. The results reported here comport with the conclusions of other authors about the existing trends in the maximum river flow in mountainous regions.

REFERENCES

- Blöschl G., Hall J., Viglione A., Perdigão R.A.P., Parajka J., Merz B., Lun D., Arheimer B., Aronica G.T., Bilibashi A., Boháč M., Bonacci O., Borga M., Čanjevac I., Castellarin A., Chirico G.B., Claps P., Frolova N., Ganora D., Gorbachova L., Gül A., Hannaford J., Harrigan S., Kireeva M., Kiss A., Kjeldsen T.R., Kohnová S., Koskela J.J., Ledvinka O., Macdonald N., Mavrova-Guirguinova M., Mediero L., Merz R., Molnar P., Montanari A., Murphy C., Osuch M., Ovcharuk V., Radevski I., Salinas J.L., Sauquet E., Šraj M., Szolgay J., Volpi E., Wilson D., Zaimi K., Živković M., 2019, Changing climate both increases and decreases European river floods, Nature, 573, 108-111, DOI: 10.1038/s41586-019-1495-6
- Corobov R., 2011, Climate change adaptation policies in the framework of sustainable environmental management: An emphasis on countries in transition, Eko-TIRAS, 664 pp.
- ENVSEC, 2013, Integrated vulnerability analysis of the Dniester basin, (in Ukrainian), Kiev, 188 pp., available online at https://dniester-commission.com/wp-content/uploads/2018/12/4_Vulnerability-Report.pdf (24.08.2020)

- ENVSEC/UNECE/OSCE, 2015, Strategical Framework for Adaptation to Climate Change in the Dniester River Basin, The Environment and Security Initiative, 72 pp., available online at http://www.unece.org/fileadmin/DAM/env/water/meetings/NPD_meetings/Publications/2015/Strategic_Framework_for_Adaptation_to_Climate_Change_in_the_Dniester_River_Basin/Dniester_English_web.pdf (data access 24.08.2020)
- EurekAlert!, 2018, New data confirm increased frequency of extreme weather events, available online at https://www.eurekalert.org/pub_releases/2018-03/eas-ndc031918.php (data access 24.08.2020)
- Hall J., Arheimer B., Borga M., Brázdil R., Claps P., Kiss A., Kjeldsen T.R., Kriaučiūnienė J., Kundzewicz Z.W., Lang M., Llasat M.C., Macdoland N., McIntyre N., Mediero L., Merz B., Merz R., Molnar P., Montanari A., Neuhold C., Parajka J., Perdigão R.A.P., Plavcová L., Rogger M., Salinas J.L., Sauquet E., Schär C., Szolgay J., Viglione A., Blöschl G., 2014, Understanding flood regime changes in Europe: a state-of-the-art assessment, Hydrology and Earth System Sciences, 18 (7), 2735-2772, DOI: 10.5194/hess-18-2735-2014.
- Khan A., Chatterjee S., Bisai D., 2015, On the long-term variability of temperature trends and changes in surface air temperature in Kolkata Weather Observatory, West Bengal, India, Meteorology Hydrology and Water Management, 3 (2), 9-16, DOI: 10.26491/mhwm/59336
- Kohnová S., Rončák P., Hlavčová K., Szolgay J., Rutkowska A., 2019, Future impacts of land use and climate change on extreme runoff values in selected catchments of Slovakia, Meteorology Hydrology and Water Management, 7 (1), 47-55, DOI: 10.26491/mhwm/97254
- Kundzewicz Z.W., Graczyk D., Maurer T., Pińskwar I., Radziejewski M., Svensson C., Szwed M., 2005, Trend detection in river flow series: 1. Annual maximum flow, Hydrological Sciences Journal, 50 (5), 796-810, DOI: 10.1623/hysj.2005.50.5.797
- Kundzewicz Z.W., Pińskwar I.,Brakenridge G.R., 2013, Large floods in Europe, 1985-2009, Hydrological Sciences Journal, 58 (1), 1-7, DOI: 10.1080/02626667.2012.745082
- Libert B., 2019, Joint and coordinated monitoring of transboundary rivers. flameworks. opportunities and bottlenecks – the example of the Dniester River, Proceedings of the International Conference "Hydropower impact on River Ecosystem Functioning", Eco-TIRAS, 212-216
- Mangini W., Viglione A., Hall J., Hundecha Y., Ceola S., Montanari A., Rogger M., Salinas J.L., Borzì I., Parajka J., 2018, Detection of trends in magnitude and frequency of flood peaks across Europe, Hydrological Sciences Journal, 63 (4), 493-512, DOI: 10.1080/02626667.2018.1444766
- Melnyk S., Loboda N., 2018, Maximum flow of rivers of the Ukrainian Carpathians (in the Upper Dniester) in the climate change conditions, Journal of Fundamental and Applied Science, 10 (3), 357-375, DOI: 10.4314/jfas.v10i3.24
- Piniewski M., Szcześniak M., Kundzewicz Z.W., Mezghani A., Hov O., 2017, Changes in low and high flows in the Vistula and the Odra basins: model projections in the European scale context, Hydrological Processes, 31 (12), 2210-2225, DOI: 10.1002/hyp.11176
- Pituch K., Stevens J., 2016, Applied multivariate statistics for the social sciences: analyses with SAS and IBM's SPSS, Routledge, New York, London, 793 pp.
- Pluntke T., Schwarzak S., Kuhn K., Lünich K., Adynkiewicz-Piragas M., Otop I., Miszuk B., 2016, Climate analysis as a basis for a sustainable water management at the Lusatian Neisse, Meteorology Hydrology and Water Management, 4 (1), 3-11, DOI: 10.26491/mhwm/61735
- Pujol N., Neppel L., Sabatier R., 2007, Regional tests for trend detection in maximum precipitation series in the French Mediterranean region, Hydrological Sciences Journal, 52 (5), 952-973, DOI: 10.1623/hysj.52.5.956
- Sayemuzzaman M., Jha Manoj K., 2014, Seasonal and annual precipitation time series trend analysis in North Carolina, United States, Atmospheric Research, 137, 183-194, DOI: 10.1016/J.ATMOSRES.2013.10.012
- Sukhodolov A., Arnaut N.A., Kudersky L.A., Loboda N.S., Bekh V.V., Skakalsky B.G., Katolikov V.M., Usatti M.A., 2009, Western steppic Rivers, [in:] Rivers of Europe, K. Tockner, C.T. Robinson, U. Uehlinger (eds.), Academic Press, 497-524, DOI: 10.1016/B978-0-12-369449-2.00013-8
- Svensson C., Kundzewicz Z., Maurer T., 2009, Trend detection in river flow series: 2. Flood and low-flow index series, Hydrological Sciences Journal, 50 (5), 811-824, DOI: 10.1623/hysj.2005.50.5.811
- Szwejkowski Z., Dragańska E., Cymes I., Timofte C.M., Suchecki S., Craciun I., 2017, Rainfall and water conditions in the region of the upper glacial in Europe, Meteorology Hydrology and Water Management, 5 (1), 15-28, DOI: 10.26491/mhwm/65538
- Viglione A., Chirico G.B., Komma J., Woods R., Borga M., Blöschl G., 2010, Quantifying space-time dynamics of flood event types, Journal of Hydrology, 394 (1-2), 213-229, DOI: 10.1016/j.jhydrol.2010.05.041
- Yue S., Pilon P., 2004, A comparison of the power of the t test. Mann-Kendall and bootstrap tests for trend detection, Hydrological Sciences Journal, 49 (1), 21-37, DOI: 10.1623/hysj.49.1.21.53996
- Zabolotnia T., Gorbachova L., Khrystiuk B., 2019, Estimation of the long-term cyclical fluctuations of snow-rain floods in the Danube basin within Ukraine, Meteorology Hydrology and Water Management, 7 (2), 3-12, DOI: 10.26491/mhwm/99752

Photo by Roman Lupan on Unsplash

Meteorology Hydrology and Water Management
Volume 8 | Issue 2

Temperature and ice regimes of waterbodies under the impacts of global warming and a hydropower plant

Viktor Ivanovych Vyshnevskyi
National Aviation University, Liubomyra Huzara 1, 03058 Kyiv, Ukraine, e-mail: vishnev.v@gmail.com

DOI: 10.26491/mhwm/127538

ABSTRACT. Based on the results of regular monitoring and remote sensing data the patterns of water temperature and ice regime of the Dnipro River within Kyiv, as affected by global warming and a hydropower plant, were identified. The characteristic features of this stretch of the river are increasing water temperature, and the decreasing thickness and duration of ice cover. The largest water temperature increase is in summer, with a somewhat smaller increase in autumn. The increase of water temperature in spring is much less than the increase in air temperature. In summer, the gradient of water temperature increase is a little bit less than that of air temperature. In autumn, the gradient of water temperature increase is larger than the gradient of air temperature increase. From April to August the lowest water temperature is usually observed near the Kyivska hydropower plant (HPP), which is located upstream. During this period the water temperature downstream from HPP increases. The uneven daily operation of HPP causes the alternation of areas with different temperature along the Dnipro River. In the cold season the water temperature in the Dnipro River is usually higher than in other nearby urban water bodies. Freezing of the water area usually starts from the small and shallow lakes and ponds. The main branch of the Dnipro River freezes last. On the whole, the sequence of ice melting on the waterbodies is the reverse of the freezing process. The longest ice cover duration in spring is observed in the bays with small water exchange, mainly located at a large distance from Kyivska HPP.

KEYWORDS: Water temperature, ice cover, Dnipro, Kyivska HPP, reservoir, remote sensing data.

SUBMITTED: 23 August 2019 | **REVISED:** 31 July 2020 | **ACCEPTED:** 15 September 2020

1. INTRODUCTION

Water temperature and ice cover duration are important parameters that impact the ecological state of waterbodies. But regular monitoring of water temperature and ice cover at the hydrological station provides insufficient data. These data can be used to characterize only local conditions of a limited number of waterbodies. The conditions of unmonitored waterbodies remain unknown; likewise for water areas located far from the hydrological stations. Under these conditions, remote sensing data provide additional information on water temperature and ice cover. Nevertheless, these data have some disadvantages. The persistent cloud cover (most prevalent in cold seasons) is an obstacle to getting a sufficient number of high-quality satellite images.

The number of publications devoted to water temperature and ice regimes of rivers, lakes, and reservoirs, is large. Nowadays, changes caused by global warming, are the most popular issue. Considering the long-term observations, many authors (Austin, Colman 2007; Adrian et al. 2009; Strutynska, Grebin 2010; Litvinov, Zakonnova 2012; Filatov et al. 2014; Woolway et al. 2017; Czernecki, Ptak 2018; Ptak et al. 2020) state that there is an increasing trend in water temperature. This increase depends on the specific region and the period of observation. Studies of the water temperature of Lake Śniardwy (Northern Poland), carried out during 1972-2019, have shown a positive trend of mean water temperature of 0.44°C per decade, with the maximum increase in April of 0.77°C per decade (Ptak et al. 2020). In that study, the trend of water temperature rise was greater than the increase of air temperature. Similar results, with a positive trend in all months were obtained for 20 Central European Lakes from 1961 to 2010 (Woolway et al. 2017). The more intensive trend of temperature rise (0.89°C/decade in July) was determined for the Rybińsk Reservoir on the Upper Volga River during the period from 1976 to 2008 (Litvinov, Zakonnova 2012). The trend for Lake Superior (North America) during 1979 to 2006 was even greater – the water temperature increase in July, August, and September reached 1.1°C per decade (Austin, Colman 2007).

One more point of the study in this area is the impact of reservoirs, especially the uneven operational regime of hydropower plants on tailwater temperatures. Relevant research (Meilutyte-Barauskiene et al. 2005) showed decreasing tailwater temperature in July, increasing temperature in October.

There are many studies of surface water temperature, based on remote sensing data. Studies by Barsi et al. (2014) and Sharaf et al. (2019) prove a strong correlation between measured and calculated data obtained from the Landsat 8 satellite, and found that thermal Band 10 gives more reliable results than Band 11.

A study based on remote sensing data by Pareeth et al. (2017), showed increasing water temperature in Perialpine lakes. The warming trend of mean water temperature was 0.17°C/decade, and 0.32°C/decade during summer.

Interesting results were obtained by Lieberherr and Wunderle (2018), based on remote sensing data of 26 lakes, located in different zones of Europe. It was revealed that the trends of mean water temperature are increasing from south to north and from west to east. There are seasonal variations: at lower latitudes winter trends and some spring trends are dominant, but farther north, first the spring and then the summer trends dominate.

Global warming affects the ice regime as well. The freezing of waterbodies starts later, while the ice break-up starts earlier than in the previous decades. A study (Ptak et al. 2020) found that over the past fifty years the ice cover duration has been decreasing at a rate of 8.7 days per decade. A trend toward reduced maximum ice cover thickness was determined as well.

A study of ice cover on the Dnipro Reservoirs was reported by Vyshnevskyi (2011). Based on regular monitoring data, decreases in ice cover thickness and duration were observed. Some results of studies of water temperature and ice cover of the Dnipro Reservoirs, based on remote sensing data, have been reported by Vyshnevskyi and Shevchuk (2018, 2020).

Important questions for additional study are (1) the interdependence between the dates of freezing and ice break-up, and (2) the dependence of the ice thickness on hydrometeorological conditions (Brown, Duguay 2010; Efremova et al. 2010; Kalinin 2008).

Despite the large number of research works in this field, the peculiarities of water temperature and ice cover of waterbodies under the impacts of upstream hydropower plants, have not been studied. The primary concern is for waterbodies connected with the main river channel. Some of them are shallow, and some very deep. Thus, the main objective of this research is to specify the corresponding features of waterbodies connected with the main river channel under the impacts of an upstream hydropower plant. Another important task is the evaluation of changes caused by global warming.

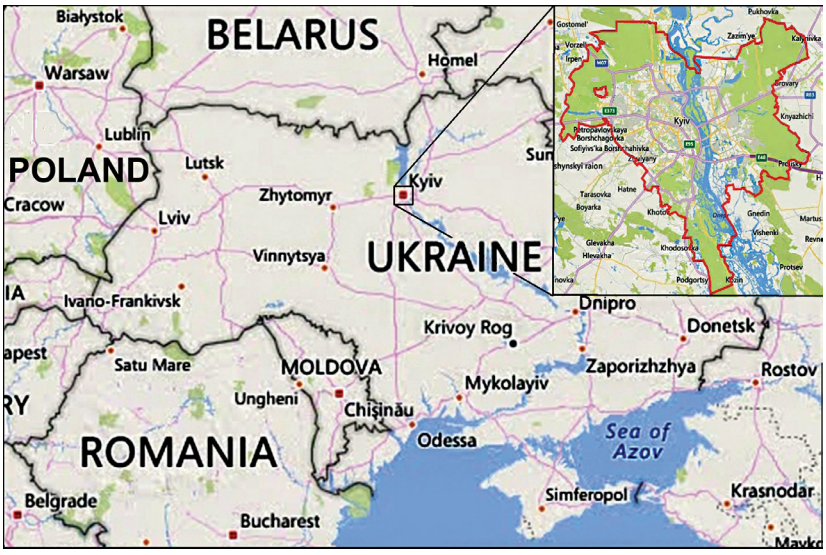

Fig. 1. The location of Kyiv and its administrative boundaries.

2. THE STUDY AREA

The study area covers the territory of Kyiv, where besides the Dnipro River, there are many lakes and ponds (Fig. 1).

An important factor that significantly affects the thermal and ice regimes of the Dnipro River, including its secondary branches and bays, is the vicinity of the Kyivske Reservoir and Kyivska HPP. The distance between the HPP and the urban territory is only a few kilometers.

The water from the Kyivske Reservoir is withdrawn from a depth greater than 10 m. The temperature of this water mass differs from the temperature of the surface layer. An important factor is the uneven operation of the HPP. The daily amplitude of water level near the HPP is usually 0.5-0.8 m, whereas in the central part of the city near the hydrological station it is 1.5-2.0 times less. As a rule, in winter there are two flushes per day, morning and evening, and in summer only one evening flush. In the latter case the highest

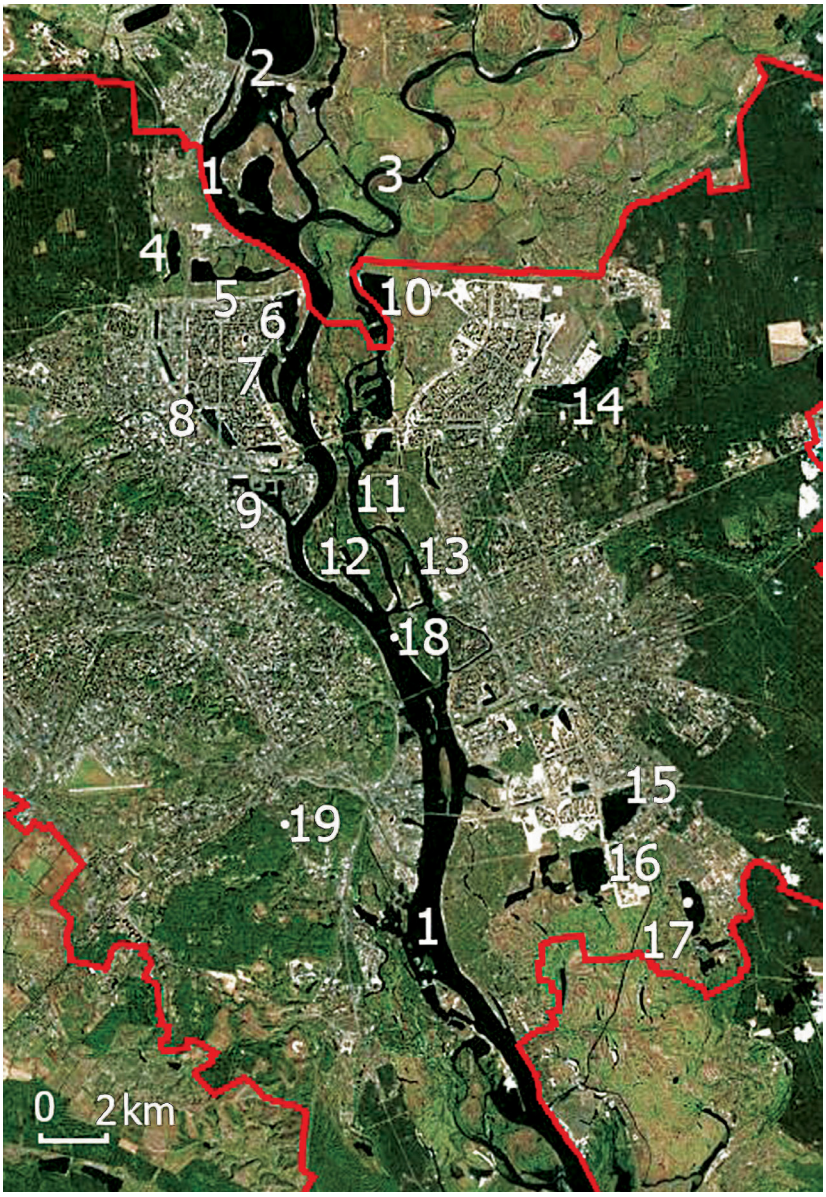

Fig. 2. The location of main water bodies and stations of data collection: 1 – Dnipro River, 2 – Kyivska HPP, 3 – Desna River, 4 – Lake Redchyne, 5 – Verbliud Bay, 6 – Sobache Hyrlo Bay, 7 – Obolon Bay, 8 – Lakes Opechen, 9 – Harbor, 10 – Domania Bay, 11 – Desenka Strait, 12 – Matviyivska Bay, 13 – Rusanivska Strait, 14 – Lake Almazne, 15 – Lake Vyrlytsa, 16 – Lake Tiagle, 17 – Lake Zaplavne, 18 – hydrological station, 19 – meteorological station.

water level near the hydrological station is observed after the end of the evening flush at about 23:00-24:00.

The section of the Dnipro River within the territory of Kyiv also includes the Kanivske Reservoir, which was constructed in the mid-1970s. As a result, the water level in the Dnipro River within the urban area increased in summer by 1.5-2.0 m, while water velocity in the river decreased.

The Dnipro River within the urban area is divided into two or even three branches, of which the right one is the largest. The mean width of this main river branch is 400-600 m, and typical depth is 7-10 m. The maximum depth in narrow places and in some bays, from where the sand was extracted for construction needs, can exceed 15 m. Such bays are: Verbliud, Sobache Hyrlo, Obolon, Domania, etc. Among them Domania Bay is the deepest (>25 m).

The largest lakes are located in the left-bank territory of the city, which was once the floodplain of the Dnipro River. Most of these lakes were artificially created by sand extraction for construction needs. The length of the largest lakes and ponds exceeds 1 km; depths reach 15-20 m. The largest lakes are: Redchyne in the right-bank part of the city, Almazne, Vyrlytsa, Tiagle and Zaplavne in the left-bank part of the urban area (Fig. 2).

3. METHODOLOGY AND DATA

The main source of data for this research was the regular monitoring and remote sensing programs.

The hydrological station that supplied data is located on the left bank of the main branch of the Dnipro River not far from the city center. This measurement site is rather shallow, and the bank is oriented to the west-southwest. Regular observations at this station are carried out twice daily, at 8 AM and 8 PM local time.

In addition, data from the meteorological station, located 6 km to southwest of the hydrological station, were collected and analyzed. Mainly, these data were the mean monthly air temperature. In some cases, the daily data were also analyzed.

The study of the spatial and temporal features of water temperature and ice regime of the Dnipro River and other waterbodies was mainly based on remote sensing data. Relevant satellite images cover all the territory of Kyiv, which makes it possible to analyze the data of both water temperature and ice cover.

The main source of data for determining water surface temperature were images taken by Landsat 8 satellite, which was launched in February 2013. The revisit time of this satellite is 16 days. The satellite imagery of the territory of Kyiv is carried out at about noon. The spatial resolution of most of the spectral bands is 30 m, whereas the spatial resolution of the thermal bands (B10 and B11) is 100 m.

The water surface temperature was determined based on the B10 data, using ArcMap 10. The calculations were carried out with the use of an equation recommended by NASA:

$$t = (1321.08/(\mathrm{Ln}((774.89/((\text{“LC80990232013252LGN00\_B10.TIF”} * 0.0003342) + 0.1)) + 1))) - 273.15.$$

This approach is rather common (Sharaf et al. 2019). The reliability of the calculated and measured values was proved based on studies of Kyiv water bodies (Vyshnevskyi, Shevchuk 2018). Other studies have also shown the validity of the results, based on the use of B10 (Barsi et al. 2014).

Dozens of satellite images were downloaded and analyzed. Colored images, which show the spatial distribution of water temperature, were created for visualization of temperature features. Territory not belonging to the water area, was specified based on Landsat 8 images and calculation of the Normalized Difference Pond Index. *NDPI* = (B6 – B3)/(B6 + B3). Images were then classified into 32 classes. Those with values less than zero were treated as transparence, others were ordered as grey.

The study of ice cover was carried out mainly based on satellite images taken by Sentinel-2.

In fact, there are two Sentinel-2 satellites, launched in 2015 and 2017. Quite high spatial resolution (10 m) and relatively small revisit time (2-3 days) are the advantages of these data. However, these satellite images do not support water temperature determination. These satellite images were taken from the website of US Geological Survey (www.glovis.usgs.gov).

4. RESULTS AND DISCUSSION

4.1. WATER TEMPERATURE

Water temperature at the hydrological station in Kyiv has been measured for more than 100 years. This period can be divided into two parts – before and after creation of the Kanivske Reservoir, to which the water area of Kyiv now belongs. The analysis of water temperature, therefore, has been conducted only for the later period, i.e. since 1977. During 1977-2019 the highest water temperature was usually observed in July. The mean July water temperature is 22.1°C. The highest mean monthly temperature (25.8°C) was observed in 2010 and the lowest (19.3°C) was observed twice, in 1985 and 1993. The highest measured temperature (29.1°C) within the standard time (at 8 PM) was registered on 10 August 2015. A slightly higher temperature (29.4°C) was measured in the daytime on 23 June 2019, during the period of a heat wave that covered a large part of Europe (Fig. 3).

In general, the water temperature at 8 PM is higher than at 8 AM. To some extent this can be explained by the location of the hydrological station on the bank, which slopes to the west-southwest. In summer at 8 PM the water temperature is usually 1-2°C higher than at 8 AM. In the daytime the temperature can be 1-2°C higher than at 8 PM. In the cold season daily fluctuations are rather small.

During the observation period 1977 to 2019 water temperature has tended to increase. In this period, the mean water temperature increase from May to September has been 0.72°C/decade, while the increase of air temperature is 0.75°C/decade. The increase of temperature for April to October has been somewhat less: 0.69°C/decade for water and 0.70°C decade for air (Fig. 4).

This result differs somewhat from that obtained by Ptak et al. (2020) for a Polish lake. The main reason is the difference between lake and river conditions. Greater rates of water exchange in rivers slows the increase of water temperature compared with lakes. Another important factor is the large reservoir on the Dnipro River.

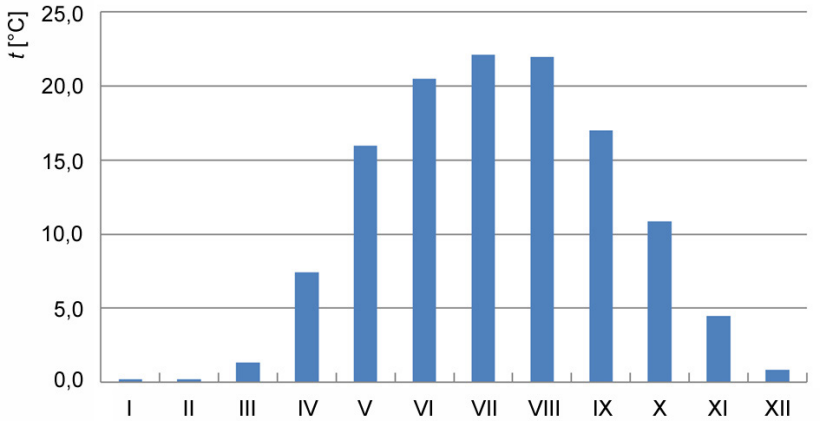

Fig. 3. Mean monthly water temperature in the Dnipro River at Kyiv hydrological station during 1977-2019.

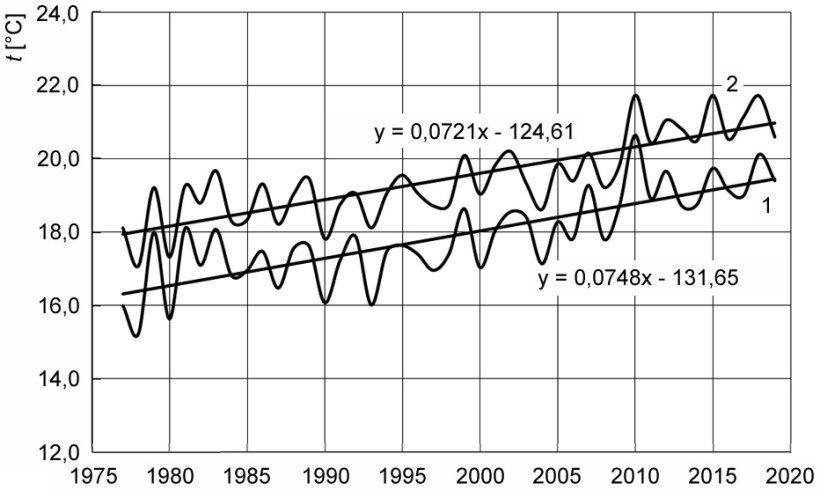

Fig. 4. The changes in air temperature (1) at Kyiv meteorological station and water temperature (2) in the Dnipro River at Kyiv hydrological station during May-September.

Table 1. The changes of air and water temperature and correlation between them in the period 1977-2019.

Months	The changes of air temperature	The changes of water temperature	Correlation between air and water temperature
III	y = 0.0457x + 0.80	y = 0.0307x + 0.51	0.20
IV	y = 0.0886x + 7.48	y = 0.0690x + 5.89	0.72
V	y = 0.0496x + 14.6	y = 0.0609x + 14.6	0.84
VI	y = 0.0757x + 17.3	y = 0.0749x + 18.8	0.91
VII	y = 0.0950x + 18.4	y = 0.0756x + 20.4	0.94
VIII	y = 0.0880x + 17.9	y = 0.0797x + 20.2	0.92
IX	y = 0.0658x + 13.0	y = 0.0692x + 15.4	0.90
X	y = 0.0248x + 7.83	y = 0.0510x + 9.70	0.64
XI	y = 0.0570x + 1.03	y = 0.0753x + 2.80	0.81

The largest increase of water temperature is observed in August – about 0.80°C/decade. This increase is somewhat less in other summer months and in September. A much smaller increase is observed in March (Table 1).

The largest standard deviations of water temperature are from April to June and in December. The increases of mean monthly water temperatures in all months from March to November are significant at $p = 0.05$.

Variation of gradients during separate months is less when data are generalized over seasons. In this case the changes of air and water temperature are more natural. The increase in water temperature in spring is much less than the increase in air temperature. The corresponding values are

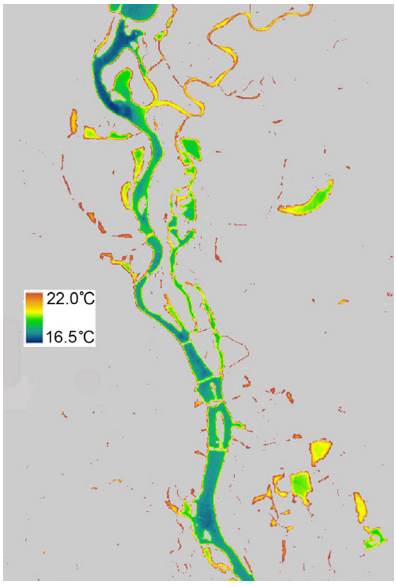

Fig. 5. The surface water temperature in water bodies in Kyiv on 19 May 2019.

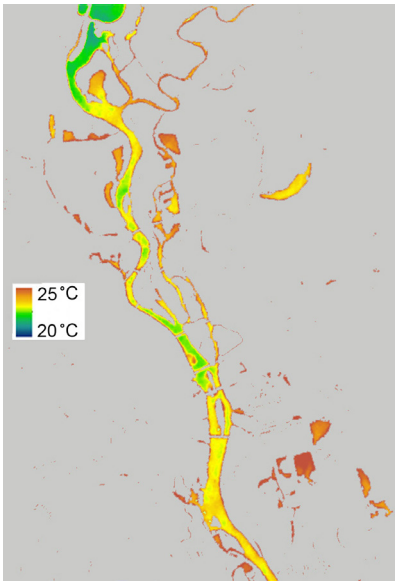

Fig. 6. The surface water temperature in water bodies in Kyiv on 29 July 2016.

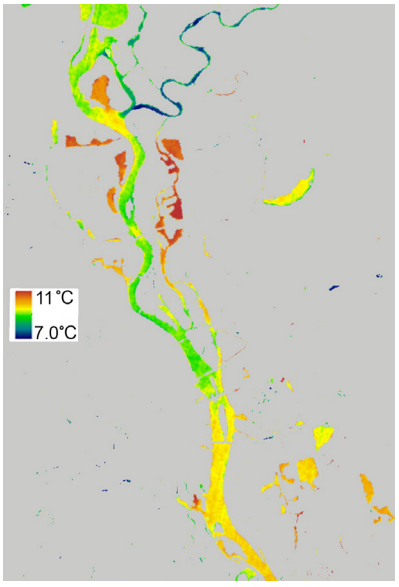

Fig. 7. The surface water temperature in water bodies in Kyiv on 15 October 2015.

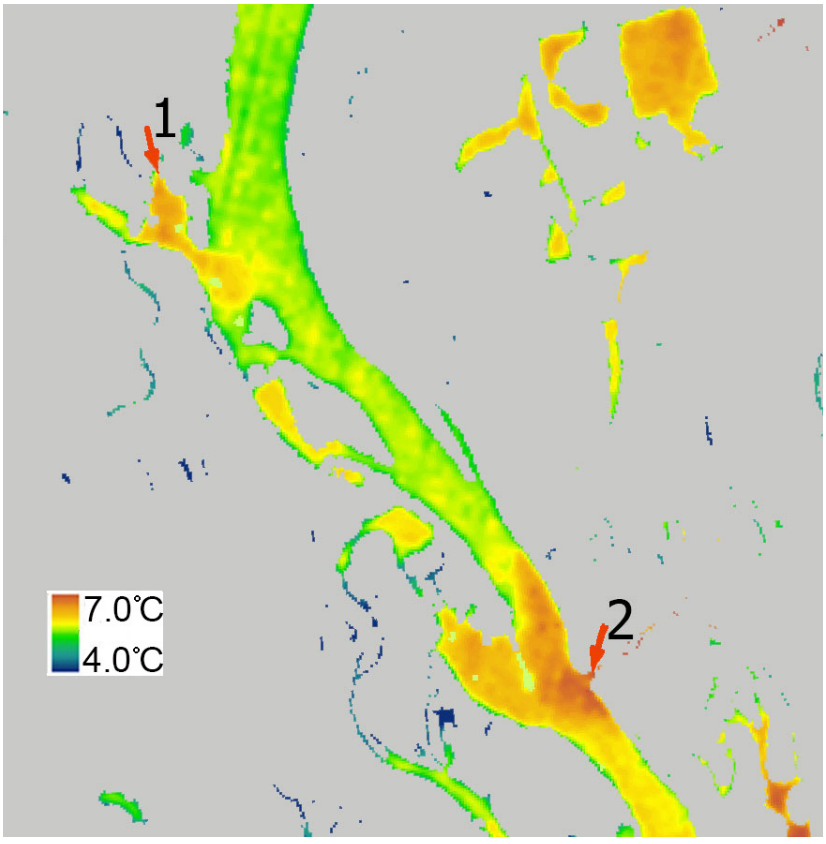

Fig. 8. The impact of Kyivska TPP-5 (1) and Bortnitska Station of Aeration (2) on water temperature in the Dnipro River on 31 October 2015.

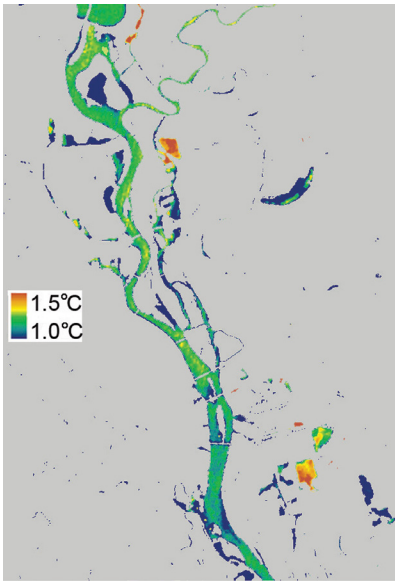

Fig. 9. The surface water temperature in water bodies in Kyiv on 8 January 2018.

0.38°C and 0.74°C/decade. In summer, the gradient of water temperature increase is slightly less (0.77°C/decade) than that of air temperature (0.86°C/decade). But in autumn the gradient of water temperature increase is larger (0.65°C/decade) than the gradient of air temperature increase (0.49°C/decade).

The correlation between water and air temperature during the year is not constant. The strongest correlations are observed in July (r = 0.94) and in August (r = 0.92). In our view, the strength of these correlations can be explained by low and relatively stable water runoff during this period of year. In spring, when air temperature increases earlier than water temperature, the correlation is rather weak. During this time, there is rather large variability in water runoff. In autumn, most notably in October, the decrease in air temperature is more rapid than the decrease in water temperature. In our view, these correlations for the winter are biased because water temperature has a lower limit of 0°C, in contrast to the lack of a practical lower limit on air temperature.

The increase in maximum temperature (about 1.0°C/decade) over the period 1977 to 2019 was more significant than changes in monthly average values. In recent years, the maximum water temperature has been approximately 27°C, which

is about 4°C higher than it was at the beginning of the observations.

In fact, with the help of regular monitoring data it is possible to characterize water temperature at only one measurement point – on the Dnipro River at the hydrological station. The changes of water temperature along the length of the river, as well as in its branches and bays, remain unknown. The same can be said about the water temperature in the lakes and ponds. Satellite image processing provides much more additional information.

The temperature regime of waterbodies varies throughout the year. From January to April water temperature is rather low. The lowest temperature in the first half of spring is observed in the main branch of the Dnipro River, which is heavily influenced by Kyivske Reservoir, located upstream. At this time, the water temperature in the Desna River, bays, and lakes is higher than it is in the main branch of the Dnipro River. The greatest differences in water temperature in the zone near Kyivska HPP and the lakes are observed in the second part of May, reaching as much as 5°C. Thus, on the bases of the obtained satellite data, it was specified that the water temperature on 19 May 2019 near HPP was 16.8°C, and 17.6°C at the hydrological station. At the same time the water temperature reached 21°C in small lakes. This fact verifies our finding of earlier increase in air temperature compared with water temperature, especially in the river (Fig. 5).

These results to some extent correlate with those obtained for the course of river downstream from the lake by Nowak et al. (2020). In our case the impact of the reservoir is larger as the result of its large volume and the discharge of water from the bottom layer.

The uneven operation of Kyivska HPP during the day causes the alternation of different temperature zones along the length of the Dnipro River. The water from the Desna River alternates with the water from the Kyivske Reservoir.

The water heating in the bays and lakes depends on their depths. The deep waterbodies (Verbliud Bay, Sobache Hyrlo Bay, Obolon Bay, Domania Bay, Almazne Lake, Tiagle Lake) warm much slower than the shallow ones.

As a rule, the highest water temperature is observed in the second part of July. In this time the water temperature in lakes is higher than it is in bays, while the temperature in bays is higher than in the Dnipro River. One of the main reasons for these distinctions is the difference in the water exchange. Another important feature of water temperature in summer is that it is higher near the banks than in the central reaches of waterbodies (Fig. 6).

During the summer, the surface water temperature along the length of the Dnipro River increases. On the section from Kyivska HPP to the southern boundaries of Kyiv the difference can reach 2°C. Thus, on 29 July 2016 downstream from the HPP the water temperature was 21.1°C, while downstream from the Southern Bridge it was 22.9°C, and in Lake Tiagle it reached 25.1°C.

With the onset of autumn, the spatial differences in water temperature change; the water in the Desna River becomes colder than in the Dnipro River. Simultaneously, the temperature in the deep bays and lakes is higher than in the Dnipro River. The highest temperature in autumn is usually observed in deep bays. One can assume that groundwater discharge takes place in these bays. At this time, the water temperature in deep Domania Bay is much higher than in the mainstem river. Almost the same temperature is observed in other deep bays: Verbliud, Sobache Hyrlo, Obolon etc. (Fig. 7).

In the cold season the impact of industrial enterprises becomes noticeable. First of all, this concerns Kyivska TPP-5, which operates on the right bank of the Dnipro River in the southern part of the city. The daily water volume, used in technological process, is about 800,000 cubic meters. The impact of Bortnitska Station of Aeration, which purifies the city wastewater, is also seen in the satellite images. The water discharge of this water treatment station is 700,000-750,000 cubic meters per day. The temperature of the treated wastewater, discharged into the Dnipro River, is higher than it is under natural conditions. As a result, the water temperature in this part of the river is higher than it is nearby (Fig. 8).

As can be seen in Figure 8, the warm water of Bortnitska Station of Aeration was not moving downstream in the Dnipro River because of a very low water discharge resulting from the weekend stoppage of Kyivska HPP operation.

In winter, the number of high-quality satellite images is limited due to the great cloudiness, which generally becomes less in the second part of winter. But at this time most of the water area is covered by ice. On 8 January 2018 only one high-quality satellite image of Kyiv water area was found without ice cover. It can be seen that at this time spatial differences in the temperature were not large. In contrast to summer, water temperature in winter gradually decreases downstream from Kyivska HPP. We can assume that the discharge of groundwater into Domania Bay causes relatively high water temperature there (Fig. 9).

The water temperature at the hydrological station on 8 January 2018, calculated on the base of satellite image, was 0.5°C. In Domania Bay it reached 1.6°C. Almost the same temperature was observed in the southern part of Lake Tiagle. One can assume that there is some underground wastewater flow from Bortnitska Station of Aeration to the lake. This intrusion intensifies biochemical processes and causes additional water heating. Indeed, the ecological state of this lake is unsatisfactory. The relevant research shows low water clarity, high chemical oxygen demand, high pH and high concentrations of inorganic phosphorus. In August 2020, chemical oxygen demand was 45 mg/dm^3. In summer, especially in August, major algal blooms are observed in this lake. This phenomenon effects the water temperature and vice versa.

4.2. ICE REGIME

Ice cover on the waterbodies of Kyiv is observed in all years, including during warm winters. Even under these conditions, there are certain periods when the air temperature drops below 0°C. The mean monthly temperature at the meteorological station in Kyiv during a standard observation period from 1961 to 1990 was the following: December – minus 2.3°C, January – minus 5.6°C, February – minus 4.2°C.

During the period 1991 to 2020 mean monthly air temperature was higher: December – minus 1.9°C, January – minus 3.2°C, February – minus 2.3°C. The coldest winter during this period was in 1995-1996, while the warmest one was in 2019-2020. Moreover, the winter of 2019-2020 was the warmest throughout all the observation period, which started in 1881. All winter months of 2019-2020 had positive temperatures. The coldest month was January of 1996, when the mean air temperature in Kyiv dropped to –9.8°C (Fig. 10).

The regular observation of ice regime on the Dnipro River has been carried out for more than 100 years. The largest ice cover duration (151 days) was recorded in the coldest winter of the 20th century in 1941-1942. The largest ice cover thickness (77 cm) was measured in February of 1963.

After the construction of Kyivske and Kanivske Reservoirs, the hydrological regime of the Dnipro River within Kyiv changed substantially. The global warming affected this regime as well. As a result, currently ice cover formation starts later than at the beginning of observations. Accordingly, the ice cover duration became shorter. The thickness of ice decreased as well. During past decades the longest duration of ice cover (87 days) was observed in the cold winter of 1984-

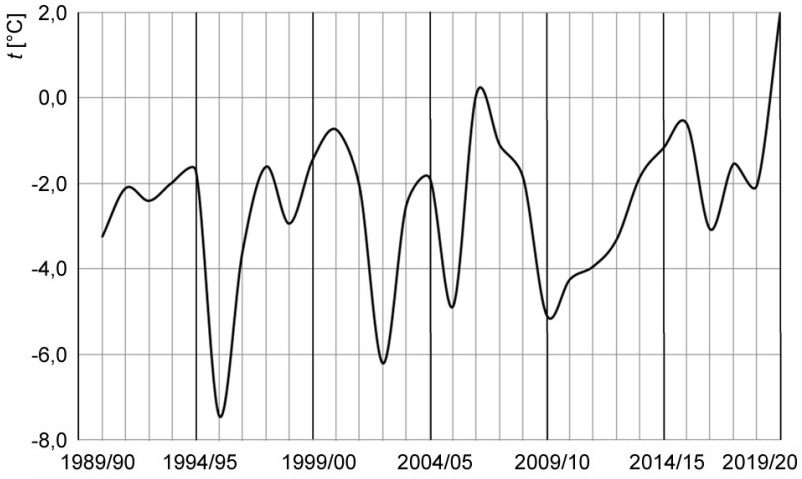

Fig. 10. The fluctuations of winter temperature (December-February) in Kyiv during 1991-2020.

Fig. 12. Ice cover on the water bodies of Kyiv on 16 January 2017.

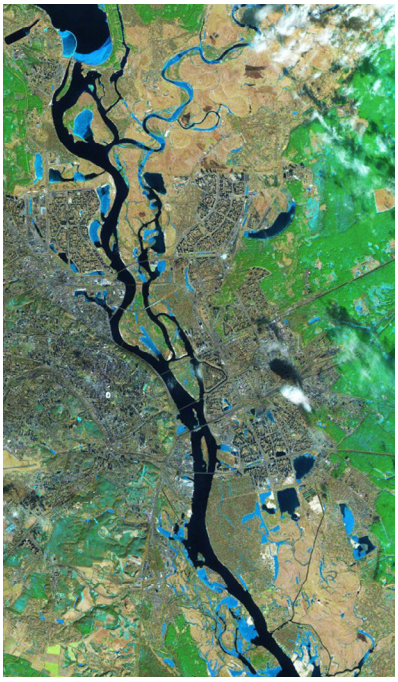

Fig. 13. Ice cover on the water bodies of Kyiv on 25 February 2019.

Fig. 11. Ice cover on the water bodies of Kyiv on 7 December 2016.

1985. The largest ice cover thickness (42 cm) was recorded in January 1977. In many cases, particularly over the past three decades, it has become difficult to measure the thickness of ice, it is so thin.

All the above information about the ice cover on the Dnipro River is based on the regular monitoring data. Obviously, these data are insufficient for a proper study of the plot of the Dnipro River within urban territory. In this case the use of remote sensing data is necessary.

Similar to water temperature, the ice regime of the Dnipro River and its bays is heavily influenced by Kyivska HPP. Due to the discharge of water from the deep layer of the reservoir, the temperature near the HPP in the beginning of winter became warmer than in waterbodies under natural conditions. Ice formation starts in small and shallow lakes followed by the bays, located in the southern part of Kyiv, where the water exchange is rather small. Then ice is formed in the large bays in the northern part of the city. The next stage is the formation of ice on the secondary branches of the Dnipro River. The main branch of the Dnipro River freezes last. One of the places of early ice formation is in front of the main bridge of Podilsko-Voskresenskyi bridgework crossing, which is being constructed now. This is partly due to the accumulation of ice carried by the Desna River. The next place with an early ice formation is located downstream in the secondary branch of the Dnipro River between Small and Great Islands and the right bank of the river. The third place of ice formation is located downstream from the Southern Bridge in the zone of significant increase of water area and relatively small water level fluctuation, caused by Kyivska HPP (Fig. 11).

In some cases, the freezing of large and deep lakes, as well as the bays, is observed after the freezing of the main branch of the Dnipro River.

In January, most waterbodies in the territory of Kyiv are covered with ice, except for the main Dnipro branch near Kyivska HPP. In warm conditions there is no ice along the length of river up to the southern boundaries of Kyiv (Fig. 12).

In late February and in March, the ice begins to melt on the main branch of the Dnipro River. Gradually this process extends to the secondary branches. After that, there is a clearing of the ice float between the river branches. The longest ice cover duration on the Dnipro River is observed in the bays in the southern part of the city. All of these dynamics are driven essentially by the uneven daily discharge from Kyivska HPP (Fig. 13).

5. CONCLUSIONS

The use of regular monitoring and remote sensing data provided the capability to characterize the features of water temperature

and ice cover of waterbodies as they are affected by global warming and the HPP, located upstream. In recent decades water temperatures of the Dnipro River near Kyiv have tended to increase, in the warm season about 0.7°C/decade. The operation of Kyivska HPP, located upstream, has an essential impact on the thermal and ice regime of the Dnipro River. In the warm season the water temperature near HPP is lower than that of areas far from it. The uneven operation of the HPP causes uneven water temperatures along the river and the alternation of water areas of higher and lower temperature. In the warm season the water temperature in the lakes is higher than in the river bays, while in the river bays it is higher than in the river. In winter, the situation is quite different – the water temperature in the Dnipro River is higher than in the lakes.

The substantial heat storage in the large and deep bays and lakes causes less fluctuations of water temperature than in smaller and shallower water bodies. As a result, the water temperature in the warm season in deep water bodies is colder than in shallower ones. In the cold season it is vice versa. The possible discharge of groundwater may be the reason of relatively high temperature in the deepest bays and lakes in the cold season. The city's industrial enterprises also affect the water temperature in the river during the cold season.

On the whole, the ice cover on the Dnipro River within the territory of Kyiv is unstable, mainly due to the operation of Kyivska HPP and changeable climate conditions. The process of waterbodies freezing starts on small and shallow lakes and ponds. Then ice covers the river bays and secondary river branches. The main branch of the river freezes last. The sequence of ice break-up on the waterbodies is opposite. The disappearance of ice begins with the main branch of the river. Gradually, this process extends to the secondary river branches. Then the ice disappears from the straits, connecting the bays and river branches. The longest ice cover duration in spring is observed in bays with low rates of water exchange.

REFERENCES

- Adrian R., O'Reilly C.M., Zagarese H., Baines S.B., Hessen D.O., Keller W., Livingstone D.M., Sommaruga R., Straile D., Van Donk E., Weyhenmeyer G.A., Winder M., 2009, Lakes as sentinels of climate change, Limnology and Oceanography, 54 (6), 2283-2297, DOI: 10.4319/lo.2009.54.6_part_2.2283
- Austin J.A., Colman S.M., 2007, Lake Superior summer water temperatures are increasing more rapidly than regional water temperature: A positive ice-albedo feed-back, Geophysical Research Letters,. 34 (6), DOI: 10.1029/2006GL029021
- Barsi J.A., Schott J.R., Hook S.J., Raqueno N.G., Markham B.L., Radociński R.G., 2014, Landsat-8 Thermal Infrared Sensor (TIRS) vicarious radiometric calibration, Remote Sensing, 6 (11), 11607-11626, DOI: 10.3390/rs61111607
- Brown L.C., Duguay C.R., 2010, The response and role of ice cover in lake-climate interactions, Progress in Physical Geography: Earth and Environment, 34 (5), 671-704, DOI: 10.1177/0309133310375653
- Czernecki B., Ptak M., 2018, The impact of global warming on lake surface water temperature in Poland – the application of empirical-statistical downscaling, 1971-2100, Journal of Limnology, 77 (2), 340-348, DOI: 10.4081/jlimnol.2018.1707
- Efremova T.V., Zdorovennova G.E., Palshyn N.I., 2010, Ice regime of the Karelian lakes, (in Russian), Proceedings of Karelian Scientific Centre, 31-40
- Filatov N.N., Rukhovets L.A., Nazarova L.E., Georgiev A.P., Ephraim T.V., Pal'shin N.I., 2014, Climate change impacts on the ecosystem of north of European Russia, (in Russian), Proceedings of the Russian State Hydrometeorological University. A Theoretical Research Journal, 34, 49-55
- Kalinin V.G., 2008, Ice regime of rivers and reservoirs of the Upper Kama River, (in Russian), 252 pp.
- Klavins M., Briede A., Rodinov V., 2009, Long term changes in ice and discharge regime of rivers in the Baltic region in relation to climatic variability, Climatic Change, 95 (3-4), 485-498, DOI: 10.1007/s10584-009-9567-5
- Korhonen J., 2006, Long-term changes in lake ice cover in Finland, Nordic Hydrology, 37 (4-5), 347-363, DOI: 10.2166/nh.2006.019
- Lieberherr G., Wunderle S., 2018, Lake surface water temperature derived from 35 years of AVHRR sensor data for European Lakes, Remote Sensing, 10 (7), 990, DOI: 10.3390/rs10070990
- Litvinov A.S., Zakonnova A.V., 2012, Thermal regime in the Rybinsk Reservoir under global warming, Russian Meteorology and Hydrology, 37, 640-644, DOI: 10.3103/S1068373912090087
- Magnuson J.J., Robertson D.M., Benson B.J., Wynne R.H., Livingstone D.M., Arai T., Assel R.A., Barry R.G., Card V., Kuusisto E., Granin N.G., Prowse T.D., Steward K.M., Vyglinski V.S., 2000, Historical trends in lake and river ice cover in the Northern Hemisphere, Science, 289 (5485), 1743-1746, DOI: 10.1126/science.289.5485.1743
- Marszelewski W., Skowron R., 2006, Ice cover as an indicator of winter air temperature changes: case study of the Polish Lowland lakes, Hydrological Sciences Journal, 51 (2), 335–349, DOI: 10.1623/hysj.51.2.336
- Meilutyte-Barauskiene D., Kovalenkoviene M., Sarauskiene D., 2005, The impact of runoff regulation on the thermal regime of the Nemunas, Environmental Research, Engineering and Management, 4 (34), 43-50
- Nowak B.M., Ptak M., Stanek P., 2020, Influence of a lake on river water thermal regime: a case study of Lake Sławianowskie and the Kocunia River (Pomeranian Lakeland, Northern Poland), Meteorology Hydrology and Water Management, 8 (1), 78-83, DOI: 10.26491/mhwm/115222
- Pareeth S., Bresciani M., Buzzi F., Leoni B., Lepori F., Ludovisi A., Morabito G., Adrian R., Neteler M., Salmaso N., 2017, Warming trends of perialpine lakes from homogenised time series of historical satellite and in-situ data, Science of the Total Environment, 578, 417-426, DOI: 10.1016/j.scitotenv.2016.10.199
- Ptak M., Sojka M., Nowak, B., 2019, Changes in ice regime of Jagodne Lake (North-Eastern Poland), Acta Scientiarium Polonorum. Serie Formatio Circumiectus, 18 (1), 89-100, DOI: 10.15576/ASP.FC/2019.18.1.89
- Ptak M., Sojka M., Nowak B., 2020, Effect of climate warming on a change in thermal and ice conditions in the largest lake in Poland – Lake Śniardwy, Journal of Hydrology and Hydromechanics, 68 (3), 260-270, DOI: 10.2478/johh-2020-0024
- Rachmatullina E.R., Grebin V.V., 2011, Researching long-term dynamic of ice cover thickness of the Pivdennyi Bug River basin, (in Ukrainian), Hydrology, Hydrochemistry and Hydroecology, 3 (24), 93-98
- Sharaf N., Fadel A., Bresciani M., Giardino C., Lemaire B.J., Slim K., Faour G., Vincon-Leite B., 2019, Lake surface temperature retrieval from Landsat-8 and retrospective analysis in Karaoun Reservoir, Lebanon, Journal of Applied Remote Sensing, 13 (4), DOI: 10.1117/1.JRS.13.044505
- Stonevicius E., Stankunavicius G., Kilkus G., 2008, Ice regime dynamics in the Nemunas River, Lithuania, Climate Research, 36 (1), 17-28, DOI: 10.3354/cr00707
- Strutynska V.M., Grebin V.V., 2010, Thermal and ice regime of the Dnipro River basin rivers from the second half of the XX century, (in Ukrainian), Nika-Tsentr, Kyiv, 196 pp.
- Vyshnevskyi V.I., 2011, The Dnipro River, (in Ukrainian), Interpres LTD, Kyiv, 384 pp.
- Vyshnevskyi V.I., Shevchuk S.A., 2018, Use of remote sensing data in the study of water objects of Ukraine, (in Ukrainian), Interpres LTD, Kyiv, 116 pp.
- Vyshnevskyi V.I., Shevchuk S.A., 2020, Use of remote sensing data to study ice cover in the Dnipro Reservoirs, Journal of Geology, Geography and Geoecology, 29 (1), 206-216, DOI: 10.15421/112019
- Woolway R.I., Dokulil M.T., Marszelewski W., Schmid M., Bouffard D., Merchant C.J., 2017, Warming of Central European lakes and their response to the 1980s climatic regime shift, Climate Change, 142, 505-520, DOI: 10.1007/s10584-017-1966-4

Meteorology Hydrology and Water Management
Volume 8 | Issue 2

Flood frequency analysis for an ungauged Himalayan river basin using different methods: a case study of Modi Khola, Parbat, Nepal

Bibek Acharya
Tribhuvan University, Department of Civil Engineering, Pulchowk Campus, 44600 Lalitpur, Nepal, e-mail: acharya.bibek76@gmail.com

Bisesh Joshi
University of Memphis, Department of Civil Engineering, 104 Engineering Science Building, Memphis, TN 38152, USA

DOI: 10.26491/mhwm/131092

ABSTRACT. Predicting flood discharges in the rivers of an ungauged basin is tedious because essential hydrological data is lacking. In mountainous countries like Nepal, the design of hydraulic structures in these steeply sloped rivers is of prime importance for flood control, as well as for electricity generation where hydraulic head is gained over short, steep reaches. This study illustrates a variety of approaches that can be used to perform flood frequency analysis of typical ungauged mountainous rivers, where discharge data are available from hydrologically similar catchments. The various methods are evaluated by comparing the goodness of fit of an array of hydrologic distribution functions. From each probability density function or regional empirical method, we predict the multi-year return periods for floods, information that is generally required to design the hydraulic structures. The analysis was done based on the annual maxima, peaks above threshold, and widely used regional empirical methods. This analysis was accomplished using the discharge data of Nayapul station near Jhapre Bagar collected from the Department of Hydrology and Meteorology, Government of Nepal, Kathmandu. The analysis and results of this study paved the way for the hydraulic design of water systems in the ungauged study region and demonstrated how the information acquired can be used for water resource management in catchments with similar hydrologic features.

KEYWORDS: Return periods, ungauged basin, design flood, hydrologic data, probability distribution functions, annual maximum discharge, peaks above threshold.

SUBMITTED: 26 June 2020 | **REVISED:** 24 November 2020 | **ACCEPTED:** 2 December 2020

1. INTRODUCTION

The design and construction of water systems, as well as water resource management, requires in-depth knowledge of different flood events for different return periods (Tao et al. 2002). The faulty design of engineering structures will have a serious economic impact due to structural damage. Over-designing or under-designing of a hydraulic structure may result in the waste of natural resources or may compromise the structural safety (Reich 1961, 1963). Developing such designs becomes more challenging because of the impact of greenhouse gases, which are changing the hydrological cycle, precipitation patterns, and temperature regimes. Increasing temperatures are altering the physical characteristics of catchments by melting snow and glaciers (Singh et al. 2018). Researchers are thus challenged to devote more effort to analyzing discharges in the water sources for planning and management.

Adequate discharge data are required for the study, analysis, and quantification of various parameters, including design flood. Hydrological stations are not established in all rivers due to economic and geographical limitations, and hence hydrological analysis in such areas is complicated. The availability of discharge data in Nepal is limited. Rivers that descend from hilly areas of Nepal carry large amounts of sediments, so for the ungauged rivers, the design of hydraulic structures such as weirs, canals, sluice gates, and dams become more complex (Sapkota et al. 2016). Therefore, the main objective of this study is to estimate flood discharges at specific place in ungauged river basins for various return periods, compare estimates and determine the best fit.

The discharge used for the design of a hydraulic structure is called the "design flood". Designing hydraulic structures for the maximum possible flood for a catchment is very costly. Engineering structures, whose failure may lead to huge loss of lives and properties, are generally designed for floods of large return periods (Izinyon et al. 2011). Design flood estimation is essential for the design of hydraulic structures, flood management and insurance studies, development, and planning (Rahman et al. 2013).

Hydrologic events have random probability distributions for which statistical analysis can be performed, but precise predictions might not be achieved. Flood frequency analysis is used to estimate design floods for sites along a river that uses observed flow discharge data to calculate statistical information, which is utilized to construct frequency distributions. There is no specific rule for the length of data required for the frequency analysis. Parameter estimation techniques in flood frequency analysis include the graphical method, frequency factor method, method of moments, and method of probability-weighted moments and L-moments (Ojha et al. 2008). Flood frequency estimation is a challenging task for a researcher and has been associated with confusion and controversies (Bobee et al. 1993). Flood frequency analysis helps to predict future flows of different magnitudes and provides reliable predictions in regions of similar climatic conditions. A wide range of research has been conducted to predict the suitable probability distribution functions for annual maximum flood events. Some of the commonly used probability distribution functions include general extreme value, log-normal, normal, Gumbel, Weibull 3P and log Pearson methods. For analysis of the short-term annual maximum discharge, there is no strict rule for using a particular distribution function (Alam et al. 2016).

The bed slope is steep in the mountainous rivers where water flows rapidly, and it is necessary to predict floods for various return periods to design hydraulic structures. Hydropower generation is most common in these rivers. Therefore, designing hydraulic structures like levees, guide walls, dams, intakes, weirs, and barrages need estimates of 10, 20, 50, 100, 200 etc. years return period floods to reduce the risk. Return period flood predictions differ based on the hydrologic distributions selected.

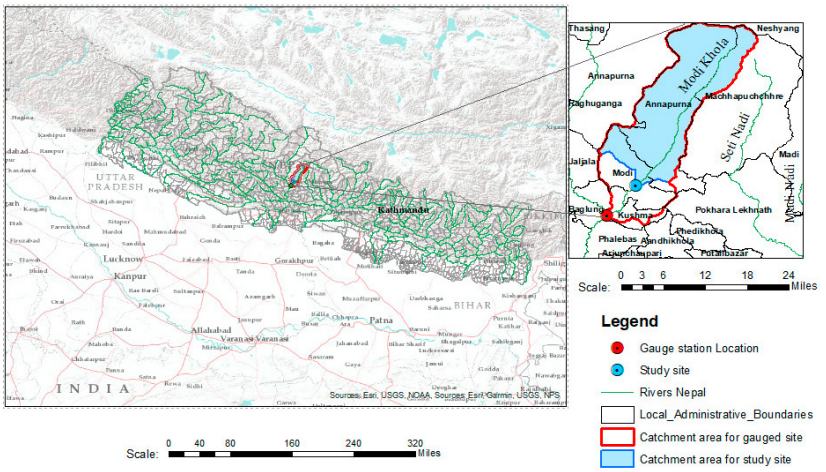

Fig. 1. Location of study basin.

2. STUDY AREA

Modi Khola is a major tributary of the Kali Gandaki River, which originates from the Annapurna Conservation area of Nepal. The study basin (Fig. 1) has an area of 510 square kilometers. The location selected for study is at 28.273 N and 83.744 E, in the Parbat district. Climate varies from warm temperate to alpine (Rijal 2007), and most of the precipitation occurs during monsoon season (June, July, August, and September). Quartzite, phyllitic slate, schist, and gneiss were found during a site visit. The sediment yield in the river is high because of the steep gradient, erosion of riverbanks, and fragile geological conditions in the upper part of the river basin. Modi Khola carries sediments ranging from sand to huge boulders during the monsoon, eroded from the banks and transported into it by its tributaries. Many hydropower projects are in operation or under construction; there are also new projects proposed for this river.

3. METHODOLOGY

3.1. DATA COLLECTION

Daily discharge data used in this study are collected from the Department of Hydrology and Meteorology, Government of Nepal, from 1976 to 2010, except data from 1980 to 1987 were not available. The flow data available were point discharge data measured once a day at Nayapul near Jhapre Bagar.

3.2. ANALYSIS

The oldest and most common technique to estimate the daily flow of an ungauged catchment with the use of a reference catchment is the drainage area ratio method (Archfield, Vogel 2010; Gianfagna et al. 2015). Our study catchment is part of a gauged catchment therefore we used the drainage area ratio method for the nested watersheds.

$$Q_1/A_1 = Q_2/A_2 \quad (1)$$

where Q_1 and A_1 are discharge and area for the gauged catchment, and Q_2 and A_2 are discharge and area for the ungauged catchment.

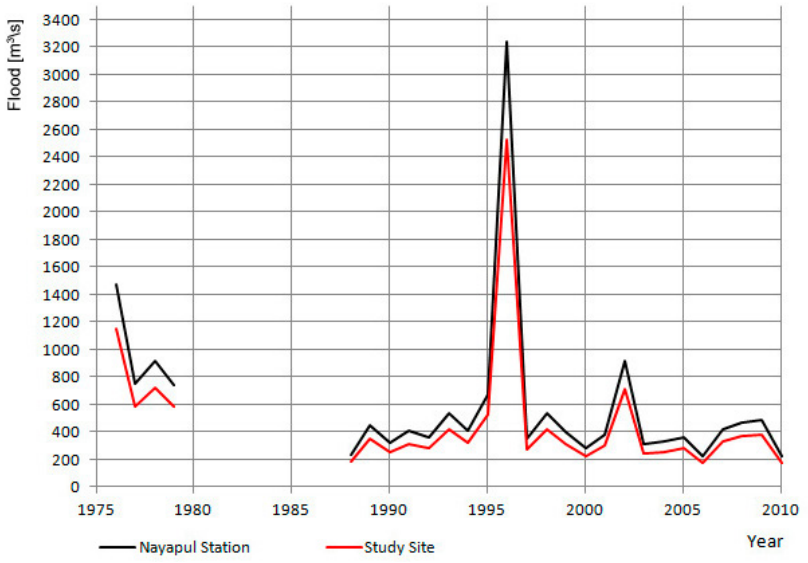

Fig. 2. Transfer of flow data from Nayapul (Gauged Station) to study basin.

Table 1. Values of standard variates based on return periods.

Return Period (T) in years	Standard Variate (S)
2	0
5	0.842
10	1.282
20	1.645
50	2.054
100	2.326
200	2.576

Annual maximum discharge data were obtained from the dataset for each year by selecting the largest daily flood from that particular year. For hydrological analysis, these data were transferred to the selected outlet point of the study basin by the drainage area ratio method; the data are plotted in Figure 2.

For flood frequency analysis using peaks above threshold, identifying such large floods from years of daily data is difficult. We simplified this job by taking the largest flood in a monthly interval from the chunk of daily discharge data. This data series cutoff value was set equal to the smallest discharge from the annual maxima series at Nayapul Station. The selected 61 discharge data points were then transferred to the study basin using the drainage area ratio method. For partial flood frequency analysis, we calculated the average return interval (*ARI*) from these selected floods. The average number of occurrences of peak flood events (k) is equal to 61events divided by 27 years, i.e. 2.26 events per year. After adjusting *ARI* to k times *ARI*, the flood values were predicted based on the adjusted *ARI* values from various distribution functions.

To select the best fit probability distribution, first of all, alternative probability distribution models need to be analyzed. Continuous probability distributions used in the hydrology sector, including generalized extreme value, Gumbel maximum, log Pearson type III, log Normal (3P), normal, and Weibull 3P were fitted to the processed flood data. The regional empirical methods Hydest and Modified Hydest were used for predicting discharges for different return periods.

3.3. THEORETICAL DESCRIPTION

3.3.1. WECS/DHM METHOD (HYDEST METHOD)

The WECS/DHM method was developed by the Water and Energy Commission Secretariat, Department of Hydrology and Meteorology (WECS/DHM) of Nepal. This method is generally used to determine the hydrological features of an ungauged basin for the pre-feasibility study of hydro-electric projects in Nepal. For this purpose, the whole country is considered as a single hydrological region, and the method is suitable for any basin with area ≥100 km². Hydest is available in the form of an Excel file, which requires input for total catchment area, area of catchment below 5,000 m elevation, area of catchment below 3,000 m elevation, and monsoon wetness index.

Instantaneous peak flood discharges for return periods of 2 and 100 years are:

$$Q_2 = 1.8767 \times (A_{below\,3000\mathrm{m}} + 1)^{0.8783} \quad (2)$$

$$Q_{100} = 14.630 \times (A_{below\,3000\mathrm{m}} + 1)^{0.7342} \quad (3)$$

Peak flood discharge for different return periods:

$$Q_T = e^{(\ln Q_2 + S\sigma)} \quad (4)$$

$$\sigma = \ln (Q_{100}/Q_2)/2.326 \quad (5)$$

where: Q_2 – two-year instantaneous flood in m³/s; Q_{100} – 100-year instantaneous flood in m³/s; Q_T – T-year instantaneous flood in m³/s; $A_{below\ 3000m}$ – basin area below 3000 m elevation in km²; σ is a parameter; S is a standard normal variate whose value depends on return periods (Table 1).

3.3.2. MODIFIED HYDEST

This method is the updated version of WECS/DHM method in which one more parameter, basin average elevation, is also taken into consideration.

For 2- and 100-year return periods, flood discharges are given by:

$$Q_2 = 2.29(A_{area\ below\,3000\mathrm{m}})^{0.86} \quad (6)$$

$$Q_{100} = 20.7(A_{area\ below\,3000\mathrm{m}})^{0.72} \quad (7)$$

Peak flood discharge for other return periods (T):

$$Q_T = e^{\ln Q_2 + S\sigma} \quad (8)$$

$$\sigma = \ln(Q_{100}/Q_2)/2.32 \quad (9)$$

The relationship between T and S is shown in Table 1; where: Q_2 – two-year instantaneous flood in m³/s; Q_{100} – 100-year instantaneous flood in m³/s; Q_T – T year instantaneous flood in m³/s; $A_{below\ 3000m}$ – basin area below 3000 m elevation in km²; σ is a parameter; S is a standard normal variate whose value depends on return periods.

3.3.3. GOODNESS OF FIT TESTS

The goodness of fit technique is a method of examining how a sample of data aligns with a given distribution as its population (Wickramaarachchi 2016). The data were fitted in the EasyFit software (https://easyfit.soft32.com/) to check fits for distributions common in hydrology, and then floods for selected return periods were predicted.

4. RESULTS AND DISCUSSIONS

The discharge data were obtained for 27 years, and maximum annual discharge data were calculated from maximum daily discharge values.

Table 2. Floods [m³/s] of different return periods using different methods for annual maxima (GEV = generalized extreme value, LP 3 = log Pearson, Type III, LN = log Normal, 3P = Three Parameter.

		Annual Maxima					
Return period T (years)	Exceedance Probability (p) = 1/T	GEV	LP 3	LN (3P)	Gumbel Maximum	Normal	Weibull 3P
2	0.5	321	324	330	392	468	306
10	0.1	756	824	836	1,073	1,062	926
20	0.05	1,085	1,188	1,156	1,333	1,231	1,274
50	0.02	1,762	1,900	1,698	1,670	1,420	1,793
100	0.01	2,554	2,690	2,216	1,923	1,547	2,225
200	0.005	3,715	3,791	2,839	2,174	1,663	2,686

Table 3. Floods [m³/s] of different return periods using different methods for peaks above threshold.

			Peaks above threshold					
ARI	*ARI* × *k*	Exceedance Probability (p) = 1/(*ARI* × *k*)	GEV	LP 3	LN (3P)	Gumbel Maximum	Normal	Weibull 3P
2	4.519	0.221	359	378	389	603	655	446
10	22.593	0.044	801	916	833	1,108	1,009	1,049
20	45.185	0.022	1,180	1,353	1,124	1,316	1,126	1,381
50	112.963	0.009	1,996	2,247	1,615	1,581	1,258	1,866
100	225.926	0.004	3,271	3,571	2,198	1,821	1,367	2,358
200	451.852	0.002	5,032	5,316	2,819	2,025	1,452	2,814

Table 4. Floods [m³/s] of different return periods using empirical methods.

	Empirical Methods	
Return period T (years)	Hydest	Modified Hydest
2	216	240
10	438	531
20	535	665
50	670	858
100	778	1016
200	892	1186

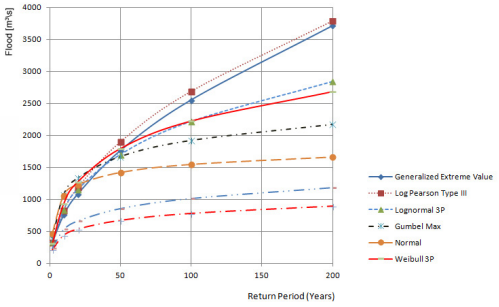

Fig. 3a. Plot of return period vs. flood for different distributions using annual maximum floods.

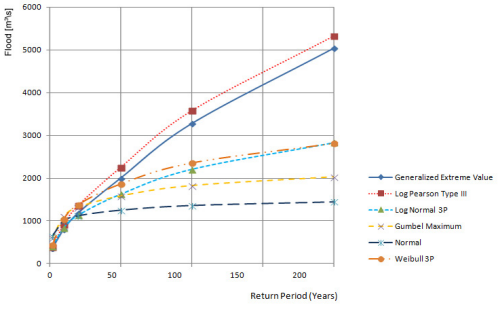

Fig. 3b. Plot of return period vs. flood for different distributions using peaks above threshold.

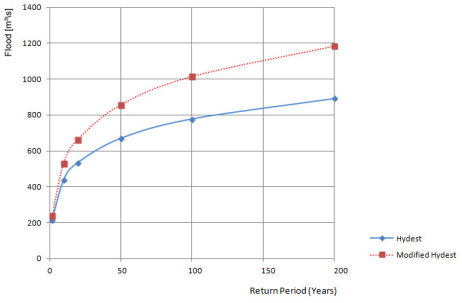

Fig. 3c. Plot of return period vs. flood using empirical methods.

Sixty-one peaks above threshold flood over a period of 27 years were taken to predict floods for various return periods. There is no particular rule for establishing the trim level for partial frequency analysis, so we took the lowest annual maximum value as our trim level, and floods greater or equal to that value were fed into probabilistic distribution models. The data were evaluated with the probability distribution functions mentioned above to determine the flood discharges for return periods of 2, 10, 20, 50, 100, and 200 years. Comparisons of the different frequency analysis methods and empirical methods are shown in Tables 2, 3, and 4.

Estimated floods are presented in Tables 2, 3, and 4 for comparative analysis. Figures 3a, 3b, and 3c also provide information about floods of different return periods using various methods. It has been found that the estimated flood values from different methods diverge for higher return periods. The best fits of distribution functions are shown by ranking in Tables 5 and 6. When designing hydraulic structures for a river like Modi Khola, the choice of distribution to estimate the flood for different return periods should be based on the fit of the distribution to the discharge data. From Table 4, we found that Hydest and Modified Hydest estimated smaller floods than other frequency analysis methods.

To fit the probability distribution functions with the flood data at a certain significance level (α) × 100%, the test statistics and critical values were analyzed. The test statistics for different kinds of tests: Kolmogorov Smirnov (K-S), Anderson Darling (A-D), and chi-squared (χ^2) should be less than the critical value corresponding to significance level α.

The following tables give the details of the probabilistic analysis carried out for annual maximum floods and peaks above threshold.

Each distribution was assigned a rank, the first rank indicating the best fitting distribution, and the last indicating the worst fitting

Table 5. Fitness of hydrologic distributions for annual maxima.

Test	Distribution	GEV	LP 3	LN (3P)	Gumbel Maximum	Normal	Weibull 3P
K-S	Test Statistic	0.0893	0.10369	0.10661	0.28203	0.28361	0.20639
	Critical value at α = 0.05	0.25438	0.25438	0.25438	0.25438	0.25438	0.25438
	Rank	1	2	3	5	6	4
	Decision at 5% significance level	Accept	Accept	Accept	Reject	Reject	Accept
A-D	Test Statistic	0.30003	0.47387	0.37112	2.9499	3.8913	4.8144
	Critical value at α = 0.05	2.5018	2.5018	2.5018	2.5018	2.5018	2.5018
	Rank	1	3	2	4	5	6
	Decision at 5% significance level	Accept	Accept	Accept	Reject	Reject	Reject
χ^2	Test Statistic	0.20178	0.66937	1.7897	6.2978	5.3965	N/A
	Critical value at α = 0.05	5.9915	5.9915	5.9915	5.9915	5.9915	N/A
	Rank	1	2	3	5	4	N/A
	Decision at 5% significance level	Accept	Accept	Accept	Reject	Accept	Reject

Table 6. Fitness of hydrologic distributions for peaks above threshold.

Test	Distribution	GEV	LP 3	LN (3P)	Gumbel Maximum	Normal	Weibull 3P
K-S	Test Statistic	0.06286	0.08828	0.08642	0.34283	0.32045	0.19077
	Critical value at α = 0.05	0.17091	0.17091	0.17091	0.17091	0.17091	0.17091
	Rank	1	3	2	6	5	4
	Decision at 5% significance level	Accept	Accept	Accept	Reject	Reject	Reject
A-D	Test Statistic	0.2523	15.441	0.56032	9.5651	11.419	2.8666
	Critical value at α = 0.05	2.5018	2.5018	2.5018	2.5018	2.5018	2.5018
	Rank	1	6	2	4	5	3
	Decision at 5% significance level	Accept	Reject	Accept	Reject	Reject	Reject
χ^2	Test Statistic	3.366	N/A	6.7201	27.89	21.765	14.735
	Critical value at α = 0.05	11.07	N/A	11.07	7.8147	7.8147	9.4877
	Rank	1	N/A	2	5	4	3
	Decision at 5% significance level	Accept	Reject	Accept	Reject	Reject	Reject

among the distributions used for comparison. The N/A value indicates that the distribution is not applicable for the given data at the 5% significance level and hence rejected. From Tables 5 and 6, generalized extreme value and log Normal (3P) functions are accepted at a 95% confidence interval.

5. CONCLUSION

The frequency analysis of annual maximum and peak discharges above threshold for identifying the best fit probability distribution was performed using normal, Gumbel maximum, log Pearson type III, log Normal (3P), generalized extreme value, Hydest, Modified Hydest and Weibull 3P distributions. Most of the research on flood flow estimations has been conducted at gauged locations, with very little research for ungauged locations. Estimating flood discharges at different locations in an ungauged catchment requires a hydrologically similar reference catchment, the choice of which is a challenge.

For our study basin, based on K-S, A-D and χ^2 tests, we found that GEV and LN (3P) are well fitted compared to other hydrological distributions. Selection of the suitable distribution also depends upon financial considerations as well as risk optimization. Designing hydraulic structures based on the design floods from the GEV distribution may not be cost-effective because of the large predicted flood values for larger return periods, so the LN (3P) can be suggested as an alternative. This study indicates that at least GEV and LN (3P) distributions are better suited for flood frequency analysis of an ungauged basin where the geographical and hydrological features are similar to that of the study basin.

Nevertheless, the limited data available for both spatial and temporal resolution for the gauged basin should be acknowledged, and the hydrological similarities between the catchments should be carefully assessed; these characteristics can vary drastically from one place to another. A cross-check of transferred data should be done where another similar catchment is available to enhance the credibility of the data while selecting the appropriate method. Hydest and Modified Hydest are commonly used in Nepal for preliminary assessment of the hydrology of ungauged basins.

The methodology we used in this study can be adopted to study the hydrology of an ungauged site in the basin where the hydrological and meteorological stations are very sparse. Because of epistemic as well as aleatory uncertainties, we cannot exactly quantify the hydrological characteristics of even the gauged river basins. Moreover, for ungauged basins, epistemic uncertainty is significantly high. Therefore, we should be skeptical about our probabilistic analysis while selecting the appropriate distributions, and thus a comparative analysis of hydrological distributions for different tests is recommended. Moreover, choosing a probability distribution function does not depend only on its goodness of fit but also on the optimization of hydraulic structures based on safety and cost. Therefore, this study helps in estimating return floods for various return years in ungauged basins and in selecting design flood for engineering structures, in developing hydrology models, agriculture, flood management, river training works, and environmental studies.

REFERENCES

- Alam S., Khan M.S.M.K., Rahat S.H., 2016, A study on selection of probability distributions of extreme hydrologic parameters for the peripheral river system of Dhaka city, [in:] Proceedings of Academics World 15th International Conference, Bangkok, Thailand, 29-34
- Archfield S.A., Vogel R.M., 2010, Map correlation method: selection of a reference streamgage to estimate daily streamflow at ungaged catchments, Water Resources Research, 46, 1-15, DOI: 10.1029/2009WR008481

- Bobee B., Cavidas G., Ashkar F., Bernier J., Ramussen P., 1993, Towards a systematic approach to comparing distributions used in flood frequency analysis, Journal of Hydrology, 142 (1-4), 121-136, DOI: 10.1016/0022-1694(93)90008-W
- Gianfagna C.C., Johnson C.E., Chandler D.G., Hofmann C., 2015, Watershed area ratio accurately predicts daily streamflow in nested catchments in the Catskills, New York, Journal of Hydrology: Regional Studies, 4, 583-594, DOI: 10.1016/j.ejrh.2015.09.002
- Izinyon O.C., Ihimekpen N., Igbinoba G.E., 2011, Flood frequency analysis of Ikpoba River catchment at Benin City using Log Pearson Type III distribution, Journal of Emerging Trends in Engineering and Applied Sciences, 2 (1), 50-55
- Ojha G.S.P., Berndtsson R., Bhunya P., 2008, Engineering hydrology, Oxford University Press, New Delhi, India
- Rahman A.S., Rahman A., Zaman M.A., Haddad K., Ahsan A., Imteaz M., 2013, A study on selection of probability distribution for at-site flood frequency analysis in Australia, Natural Hazards, 69, 1803-1813, DOI: 10.1007/s11069-013-0775-y
- Reich B.M., 1961, Short duration rainfall intensity in South Africa, South African Journal of Agricultural Science, 4 (4), 589-614
- Reich B.M., 1963, Short-duration rainfall-intensity estimates and other design aids for regions of sparse data, Journal of Hydrology, 1 (1), 3-28, DOI: 10.1016/0022-1694(63)90029-5
- Rijal S.P., 2007, Land holding and livelihoods: a synthesis from Modi Khola watershed, Nepal, The Third Pole, 5 (7), 43-51, DOI: 10.3126/ttp.v5i0.1952
- Sapkota A., Pandit H.P., Shrestha R., 2016, Hydraulic and sediment handling performance assessment of Rani Jamara Kulariya Irrigation Project (RJKIP) by conjunctive use of 1D and 3D simulation models, Naresuan University Engineering Journal, 11 (1), 1-6, DOI: 10.14456/nuej.2016.1
- Singh U.K., Kumar B., 2018, Climate change impacts on hydrology and water resources of Indian river basins, Climate World Environment, 13 (1), 32-43
- Tao D.Q., Nguyena V.T.V., Bourque A., 2002, On selection of probability distributions for representing extreme precipitations in Southern Quebec, [in:] Annual Conference of the Canadian Society for Civil Engineering, Montreal, Quebec, Canada, 1-8
- Wickramaarachchi T.N., 2016, Frequency analysis of flood discharge in Gin River at Tawalama, Sri Lanka, [in:] 7th International Conference on Water Resources and Environment Research, ICWRER 2016, Kyoto, Japan, 7, 1-6

Meteorology Hydrology and Water Management
Volume 8 | Issue 2

Assessing the effects of water withdrawal for hydraulic fracturing on surface water and groundwater – a review

Gopal Chandra Saha
Wilfrid Laurier University, 75 University Ave W, Waterloo, ON, Canada, e-mail: gsaha@wlu.ca

Michael Quinn
Mount Royal University, 4825 Mt Royal Gate SW, Calgary, AB, Canada

DOI: 10.26491/mhwm/131229

ABSTRACT. The interaction between groundwater and surface water plays an important role in the function of riparian ecosystems and sustainable water resource management. Hydraulic fracturing, an unconventional oil and gas well stimulation method, has increased dramatically in North America in an effort to exploit previously inaccessible shale oil and gas reserves. Hydraulic fracturing often requires several thousand cubic meters of water to fracture the source formations. Use of such a high volume of water has raised considerable public concern over the sustainability of this activity and the potential impacts on surface water and groundwater. This paper provides a review of the published literature addressing the effects of water withdrawal for hydraulic fracturing on surface water and groundwater. The potential effects of such withdrawal are: decreased volume of water in rivers, streams, lakes and aquifers; alteration of natural flow regimes; regional water shortages during periods of drought; creating conflicts with other water users in water-stressed regions; inadequate downstream water availability; reduced downstream water quality for human uses, due to less water availability for dilution; and degradation of habitat and aquatic ecosystem function, impacting local wildlife. This review demonstrates that relatively little attention has been paid to quantify and understand these interactions, and suggests that there is a significant need for further research in this area to address the currently limited availability of data.

KEYWORDS: Groundwater, surface water, hydraulic fracturing, water withdrawal, shale oil and gas production.

SUBMITTED: 5 April 2020 | **REVISED:** 12 November 2020 | **ACCEPTED:** 7 December 2020

1. INTRODUCTION

The interaction between groundwater and surface water is a significant component of the function of riparian ecosystems and sustainable water resources management (Kalbus et al. 2006). During wet periods, surface water can recharge groundwater, and during dry periods, groundwater provides a major source of water to the surface water flow. Therefore, groundwater and surface water are closely linked components of the hydrologic system. The development and utilization of any one component can affect the other, hence it is essential to understand and quantify the exchange processes between these two components for developing sustainable water resources management plans (Sophocleous 2002; Su et al. 2018).

Multi-stage hydraulic fracturing is an unconventional oil and gas well stimulation method of shale oil and gas production (ALL Consulting 2012). In most cases, water is used in hydraulic fracturing to 'frack' the geologic formations due to its efficiency, availability and low-cost. This technique facilitates extraction of oil and gas from vast shale reserves, which were previously considered inaccessible or unprofitable (Entrekin et al. 2011). In hydraulic fracturing, a fluid, either a liquid (most often water) or a gas, is pumped down with a suspended proppant (usually sand or ceramic beads) and additives (various chemicals which increase the performance of the fluid) under high pressure into the well, to cause the surrounding rock to fracture or crack (Oil and Gas Info 2019). When fracture pressures are abated, the proppant remains to keep the fractures open and allow oil and gas to be produced in the well. Figure 1 shows a schematic diagram of a hydraulically fractured well with horizontal drilling, where water is abstracted from surface water and groundwater sources for hydraulic fracturing. The volume of water used as fracturing fluid by the oil and gas industry varies significantly depending on the geological context. For example, in the Upper Peace Region of northwestern Alberta, Canada, the average water use per well was 3,671 m^3 in 2013-2014 (Saha 2016). In 2016, the median water use per well in the Marcellus region (Pennsylvania and West Virginia) and the Permian Basin (Texas and New Mexico) was 27,950 m^3 and 42,500 m^3, respectively (Kondash et al. 2018). Meanwhile the average water consumption per well in the Vaca Muerta Play, Argentina in 2016, was 22,538 m^3 (Rosa, D'Odorico 2019). Furthermore, in 2011-2017, the median water use per well in the Weiyuan play of the Sichuan Basin, China, was 36,014 m^3 (Wu et al. 2019).

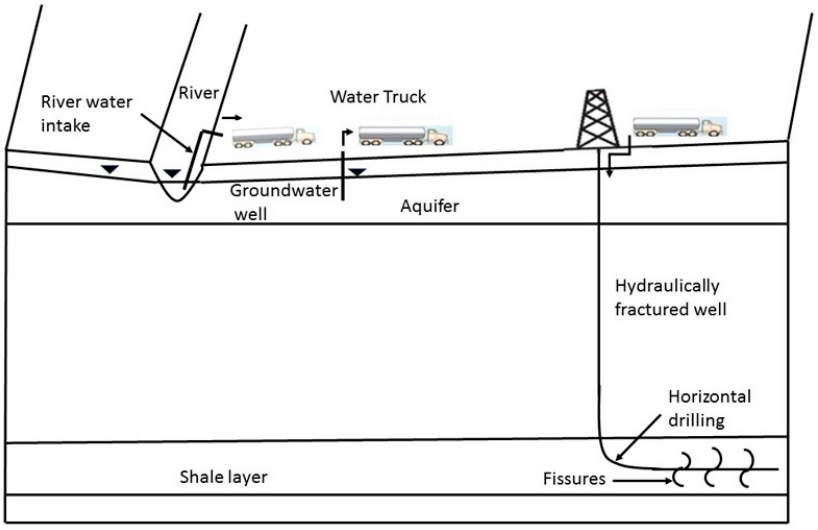

Fig. 1. A schematic diagram of a hydraulically fractured well with horizontal drilling, and water collection from surface water and groundwater sources for hydraulic fracturing. Figure is not drawn to a scale.

Although multi-stage hydraulic fracturing reduces the amount of natural landscape disturbance per well compared to conventional vertical drilling (ALL Consulting 2012), there is considerable public concern regarding the sustainability of this activity, because of its requirement for large volumes of water and given limited water resources (e.g. groundwater and surface water). Most often, the water is collected from surface water (i.e. rivers, lakes and wetlands), groundwater, or a combination of both. As a result, there is a need to understand the interaction between groundwater and surface water following water withdrawal for hydraulic fracturing. The objectives of this review are: a) to understand how the interaction between groundwater and surface water are affected by the impacts of water withdrawal for hydraulic fracturing, based on previously published literature, and; b) to identify future potential research in this area, required to better understand and quantify these interactions and to develop sustainable water resources management plans in shale gas and oil play regions.

2. MATERIALS AND METHODS

Firstly, a search for relevant previously published literature in Google Scholar was completed, using the phrase "The effects of hydraulic fracturing on" with a variety of other keywords, such as "groundwater-surface water (GW-SW) interaction, stream flow, groundwater flow, stream water level, and groundwater table". Only publications written in the English language were considered during the review process. Secondly, the results of each publication (i.e. qualitative and quantitative) was reviewed, selecting publications that highlighted the effects of water withdrawal for hydraulic fracturing on either stream flow, groundwater table, environmental flow or surface water and groundwater availability. In total, 29 suitable publications were identified (stream flow (18), groundwater table (7), environmental flow (2), and surface water and groundwater availability (2)). In addition, publications which highlighted other environmental issues associated with hydraulic fracturing have been cited as part of this review, to demonstrate the comprehensive negative impacts of hydraulic fracturing on the environment, society and human health.

3. RESULTS AND DISCUSSION

3.1. SURFACE WATER AND GROUNDWATER CHANGES, UNDER THE EFFECTS OF WATER WITHDRAWAL FOR HYDRAULIC FRACTURING

Since 2010, the concerns related to hydraulic fracturing have been focused on various environmental issues, such as stray gas migration to shallow groundwater (Osborn et al. 2011; Vengosh et al. 2014) and to the atmosphere (Howarth et al. 2011), possible hydraulic connectivity between deep shale formations and shallow aquifers (Warner et al. 2012), water use (Nicot, Scanlon 2012; Carlson, Stelfox 2014), air quality (Colborn et al. 2014), seismicity (Holland 2011; Keranen et al. 2014), and the potential for contamination from hydraulic fracturing fluid and/or produced brines containing toxic substances during drilling,

transport, and disposal (Dresel, Rose 2010; Rowan et al. 2011; Gregory et al. 2011). The results from these studies revealed that hydraulic fracturing has the potential for pollution of surface water, groundwater and the air, for causing earthquakes, creating conflict among competing water users and health related issues. Among these identified impacts, the potential for pollution of surface water and groundwater due to hydraulic fracturing has been paramount in public discourse and peer-reviewed journal articles (Osborn et al. 2011; Myers 2012; Barbot et al. 2013; Fontenot et al. 2013; Gordalla et al. 2013; Olmstead et al. 2013; Vengosh et al. 2013; Vidic et al. 2013; Warner et al. 2013; Brittingham et al. 2014; Vengosh et al. 2014; Gallegos, Varela 2015; Kuwayama et al. 2015). A moderate number of articles qualitatively addressed the potential impacts of hydraulic fracturing on water resources due to extensive water withdrawal from nearby water sources (Kargbo et al. 2010; Entrekin et al. 2011; Brittingham et al. 2014; Vengosh et al. 2014; Gallegos, Varela 2015; Kuwayama et al. 2015), and the combined effects of this withdrawal with other activities related to hydraulic fracturing (Rahm, Riha 2012). The potential impacts from such withdrawal include: decreased volumes of water in rivers, streams, lakes and aquifers (Rahm, Riha 2012; Brittingham et al. 2014; Vengosh et al. 2014; Gallegos, Varela 2015; Kuwayama et al. 2015); alteration of natural flow regimes (Entrekin et al. 2011; Rahm, Riha 2012; Brittingham et al. 2014); regional water shortages during periods of drought (Entrekin et al. 2011; Vengosh et al. 2014); creating conflicts among competing users in regions of water-stress (Cooley, Donnelly 2012); inadequate downstream water availability (Entrekin et al. 2011; Rahm, Riha 2012); reduced quality of water downstream for human use, due to less water availability for dilution (Entrekin et al. 2011; Brittingham et al. 2014; Vengosh et al. 2014) and; degradation of habitat (Rahm, Riha 2012; Brittingham et al. 2014) and aquatic ecosystem function (Kargbo et al. 2010; Entrekin et al. 2011; Brittingham et al. 2014), essential for wildlife. Very few studies/articles were found that quantified the impacts of water withdrawal for hydraulic fracturing, representing a significant gap in the literature.

Due to the importance of water resources, quantifying the effects of water withdrawal for hydraulic fracturing has received increased research attention over the last 7 years. The variables assessed in the selected literature included the impacts on annual stream flow (Cothren et al. 2013; Best, Lowry 2014; Sharma et al. 2015), daily stream flow (Shank, Stauffer 2015; Barth-Naftilan et al. 2015; Sullivan et al. 2015), monthly stream flow (MacQuarrie 2018; Entrekin et al. 2018), stream low flow (Sharma et al. 2015; Shrestha et al. 2016; Lin et al. 2018), environmental stream flow components (i.e. high flow, low flow and extremely low flow) (Cothren et al. 2013; Buchanan et al. 2017), annual surface water and groundwater availability (Sullivan et al. 2015; Vandecasteele et al. 2015), and annual groundwater table/level (Best, Lowry 2014; Sullivan et al. 2015; Lin et al. 2018). Studies were primarily conducted using: hydrological models, such as the SWAT (Soil and Water Assessment Tool) model (Cothren et al. 2013; Sharma et al. 2015; Shrestha et al. 2016) and the MODFLOW (Modular 3-Dimensional Finite-Difference Groundwater Flow) model (Best, Lowry 2014); regression models, such as the CIRF (Conditional Inference Random Forest) model (Buchanan et al. 2017); or a range of indices such as a withdrawal index (Shank, Stauffer 2015; Barth-Naftilan et al. 2015), surface water use intensity index (Sullivan et al. 2015; MacQuarrie 2018; Entrekin et al. 2018) or water exploitation index (Vandecasteele et al. 2015).

Based on the search and review of the published literature, quantitative research most commonly focused on the impacts of water withdrawal for hydraulic fracturing on surface water. Of these, most studies considered surface water withdrawal from streams only, the key findings of which are presented in Table 1. Overall, these studies found that the total amount of water withdrawal for hydraulic fracturing was very low compared to stream flow. The magnitude of this proportion varied inversely with stream size (i.e. order) and watershed area. For example, Shank and Stauffer (2015) found daily water withdrawal for shale gas development ranged from 0.04% to 6.8% of average daily flow in the Susquehanna River Basin (71,251 km^2), United States of America (USA), with the largest values associated with the headwater (i.e. upstream or lower order) streams, because of the relatively lower stream flow compared to that of higher order streams (i.e. downstream). Sullivan et al. (2015) also found similar results in the Susquehanna River Basin, USA. Barth-Naftilan et al. (2015) found daily permitted water withdrawal was less than 5% of median flow of streams that lie within comparatively large watersheds (>1000 km^2) in Pennsylvania's Marcellus Shale Play, USA. Meanwhile, MacQuarrie (2018) found monthly water withdrawal for shale gas development was 6% of mean monthly stream flow during winter months (November-February) in a sub-basin (835 km^2) of the Duvernay Formation (approximately 130,000 km^2) in Alberta, Canada, while for other sub-basins with larger areas, that value was lower. Furthermore, Cothren et al. (2013) found the water quantity used for hydraulic fracturing was approximately 0.05% of the overall discharge of the study area (127,300 km^2) in the Fayetteville Shale Play in Arkansas, USA. Therefore, the effects of water withdrawal for hydraulic fracturing on stream flow depend not only proportionally on the amount of water withdrawn, but also inversely on the stream size and watershed area.

In addition, the effects of water withdrawal for hydraulic fracturing on stream flow depends on the temporal and spatial stream flow in the watershed. For example, Cothren et al. (2013) found no difference between the annual water balance components of the baseline scenario (with no water withdrawn for hydraulic fracturing) and the generated scenarios (with water withdrawn for hydraulic fracturing) at basin scale (127,300 km^2) in the Fayetteville Shale Play in Arkansas, USA. However, on the monthly time-step and sub-basin scale, they found significant changes in stream flow during low flow months. Sharma et al. (2015) found at the local scale (i.e. sub-basin), water withdrawal from streams had little (less than 1.5%) impact on mean seasonal and annual flow in the Muskingum watershed (20,720 km^2) of eastern Ohio, USA. However, modest impacts were found on the 7-day minimum monthly flow (low flow), especially at the local scale and in lower order streams, which had a variable impact between 5.2% and 10.6%, in comparison to baseline and generated scenarios. They also found the impacts of water withdrawal from streams is greater on the 7-day minimum monthly flow than on the mean monthly, seasonal and annual stream flow, because of the lower value of the 7-day minimum monthly flow. In the same watershed, Shrestha et al. (2016) found that the headwater streams in the sub-watersheds were heavily affected, with significant decrease in 7-day low flow. Best and Lowry (2014) found under the maximum density of well development, stream flow was reduced by up to 13% in a localized region with narrow valleys and streams with lower annual discharge, whereas stream flow reduction still remained under 3% throughout most of the stream network in a study area (3,390 km^2), in the Marcellus Shale Play in New York, USA.

Table 1. The key findings from the quantitative studies related to the impacts of water withdrawal for hydraulic fracturing on water resources.

Key finding	Justification
The effects of water withdrawal from streams for hydraulic fracturing on stream flow are dependent not only proportionally on the volume of water withdrawn, but also inversely on stream size and watershed area.	Shank and Stauffer (2015) found that daily water withdrawal ranged from 0.04% to 6.8% of average daily flow in the Susquehanna River Basin (71,251 km^2), USA. The largest values are associated with the headwater (i.e. upstream or lower order) streams, and vice versa. Barth-Naftilan et al. (2015) found daily permitted water withdrawal were less than 5% of median flow of streams in the comparatively large watersheds (>1000 km^2) in Pennsylvania's Marcellus Shale Play, USA. Similar results were found in Cothren et al. (2013), and MacQuarrie (2018).
The effects of water withdrawal from streams for hydraulic fracturing on stream flow are dependent on both temporal and spatial components of stream flow in the watershed.	Cothren et al. (2013) did not find any difference between the annual water balance components of the baseline scenario (with no withdrawal of water for hydraulic fracturing) and the generated scenarios (with water withdrawn for hydraulic fracturing) at basin scale (127,300 km^2) in the Fayetteville Shale Play, in Arkansas, USA. However, they found significant changes in stream flow during low flow months on the monthly time-step and sub-basin scale. Sharma et al. (2015) found that at the local scale (sub-basin), water withdrawal from streams had little (<1.5%) impact on mean seasonal and annual flow in the Muskingum watershed (20,720 km^2) of eastern Ohio, USA. However, modest (5.2% to 10.6%) impacts were found on the 7-day minimum monthly flow (low flow) especially at the local scale and in lower order streams, in comparison with baseline and generated scenarios. Similar results were found in Best and Lowry (2014), Shrestha et al. (2016), and Entrekin et al. (2018).
The effects of water withdrawal from streams for hydraulic fracturing on environmental flow of lower order streams with small watersheds are significant during low flow periods.	Buchanan et al. (2017) found under the least intense withdrawal scenario (i. e. daily water withdrawal 1,210 m^3) 21% of reference headwaters and creeks (drainage areas less than 99 km^2) experienced approximately 50% reduction in stream flow during low-flow periods in the Marcellus Shale formation (170,000 km^2), USA, whereas for larger rivers, little change was found. Cothren et al. (2013) also found stream flow decreased during November 2007 and January 2008 (low flow months) by 34% and 67%, respectively, in one of the sub-basins with a large number of wells located upstream in the Fayetteville Shale Play, in Arkansas, USA. Similar results were found by Shrestha et al. (2016) in the headwater streams in the sub-watersheds of the Muskingum watershed, USA.
The effects of water withdrawal from groundwater for hydraulic fracturing on groundwater level are local, and groundwater level decreases proportionally to the amount of water withdrawal from the groundwater pumping well.	Best and Lowry (2014), Sullivan et al. (2015), Vandecasteele et al. (2015), and Lin et al. (2018) found notable groundwater level decreases near the pumping wells.

Entrekin et al. (2018) found estimated daily water usage for hydraulic fracturing exceeded the monthly low-flow withdrawal threshold in 48-79% of the catchments (mainly in smaller catchments) during dry months (June-November) in 2011-2014, in the Fayetteville Shale Play (total area: 127,300 km^2, consists of catchments ranged in size from 47 to 1,959 km^2) in Arkansas, USA. Lin et al. (2018) found during low flow conditions, the small-to-medium sized streams in the Bakken Shale Play (35,000 km^2) in North Dakota, USA, had more stream flow during 2008-2014 than 2000-2007, due to greater rainfall than normal. Therefore, the Bakken Shale Play oil development had little impact on stream flow. Using a water exploitation index, Vandecasteele et al. (2015) evaluated the potential impacts of shale gas development in northern Poland. They found that in 2028 under the high scenario (i.e. water consumption per well 19,000 m^3), 0.83% of the hydraulic fracturing water would come from surface water, while 22.42% would come from groundwater sources. It was concluded that water for shale gas extraction in northern Poland should be withdrawn from surface waterbodies, in order to reduce stress on groundwater. Alternatively, in 2011, Sullivan et al. (2015) found 77.5% and 21.9% of hydraulic fracturing water was taken from surface water (i.e. rivers and stream) and groundwater, respectively, in the Susquehanna River Basin, USA. It indicated that groundwater should be used for hydraulic fracturing to reduce impact on surface water in this basin.

Water withdrawal from streams for hydraulic fracturing has significant effects on environmental flow (i.e. instream flow needs) of lower order streams with small watersheds, during periods of low flow. According to the Brisbane Declaration (2007), environmental flow is defined as "the quantity, timing, and quality of water flows required to sustain freshwater and estuarine ecosystems and the human livelihoods and well-being that depend on these ecosystems." Buchanan et al. (2017) revealed water withdrawal for shale gas development alters natural flow regimes, especially streams draining small watersheds (less than 99 km^2) during low-flow periods in the Marcellus Shale formation (170,000 km^2), USA. They found under the least intense withdrawal scenario (i. e. daily water withdrawal 1,210 m^3) 21% of reference headwaters and creeks (drainage areas less than 99 km^2) experienced approximately 50% reduction in summer flow (low flow months), whereas for larger rivers little change was found. Cothren et al. (2013) found at one of the sub-basins with a large number of wells located upstream in the Fayetteville Shale Play in Arkansas, USA, stream flow decreased during November 2007 and January 2008 (low flow months) by 34% and 67%, respectively. Similar results were found in the headwater streams in the sub-watersheds of the Muskingum watershed, USA (Shrestha et al. 2016). Therefore, lower order streams in a smaller sub-basin (sub-watershed) are at greater risk to be impacted negatively by water withdrawal for hydraulic fracturing during intervals of low flow or water scarcity, such as during winter months or periods of drought (Vandecasteele et al. 2015; MacQuarrie 2018). Our searches revealed scant published literature on the impacts of water withdrawal for hydraulic fracturing on other types of surface water bodies, such as lakes or wetlands. Water withdrawal from such sources requires additional attention, as lakes and wetlands can ease the negative impact of flooding and droughts by storing large amounts of water which is then released during shortages. They also replenish groundwater, improve water quality of downstream watercourses, and preserve the biodiversity and habitat of the surrounding area.

Similarly, we found very little research on the impacts of water withdrawal for hydraulic fracturing on groundwater. Studies which did assess the effects on groundwater, found that groundwater level decreased locally and proportionally to the amount of water withdrawn from the groundwater pumping well (Best, Lowry 2014; Sullivan et al. 2015; Vandecasteele et al. 2015; Lin et al. 2018). For example, Lin et al. (2018) found regional groundwater level decreased by 0.3-1.5 m in three shallow aquifers, where a large number of hydraulically fractured wells used groundwater from those aquifers during fracturing operation in the Bakken Shale Play, USA. However, one study using the MODFLOW model indicated that groundwater level (for the study area of 3,390 km^2) did not experience any detectable change when water was withdrawn from the stream network (Best, Lowry 2014). This finding is likely a result of the coarser model resolution which consisted of 193 rows and 281 columns of 250 m × 250 m cells. However, finer grid resolution (e.g. 10 m by 10 m grid cells) of the model domain could detect groundwater levels changes (i.e. declines) near to the surface water withdrawal locations.

Based on our literature search, very few research studies have used hydrological models to quantify the effects of water withdrawal on water resources. These studies often made

Table 2. Assumptions made in hydrological models of reviewed studies due to missing information, to quantify the impacts of water withdrawal for hydraulic fracturing on water resources.

Study	Type of water source	Location of water withdrawal	Amount of water per well	Timing of water withdrawal
Cothren et al. (2013)	Stream (surface water)	From the nearest stream to each hydraulically fractured well	18,927.0 m^3	3,785.4 m^3 of water was uniformly withdrawn during 5 consecutive months
Best, Lowry (2014)	Stream (surface water) and groundwater	For surface water withdrawal: from the nearest stream to each hydraulically fractured well; For groundwater withdrawal: from the closest municipal well and private well to each hydraulically fractured well	11,356.2 m^3	All water withdrawals were distributed over the entire year
Sharma et al. (2015)	Stream (surface water)	No information reported	The amount of water for each hydraulically fractured well reported in www.fracfocus.org was used for each hydraulically fractured well	No information reported
Shrestha et al. (2016)	Stream (surface water)	No information reported	The amount of water for each hydraulically fractured well reported in www.fracfocus.org was used for each hydraulically fractured well	No information reported

a range of assumptions due to missing information (i.e. location of water withdrawal, type of water source, amount of water per well, and timing of water withdrawal), which are detailed in Table 2. They simulated annual stream flow, stream low flow, environmental steam flow components (i.e. high flow, low flow and extremely low flow) and annual groundwater table/level under the influence of water withdrawal for hydraulic fracturing. On the other hand, studies which used regression models (e.g. CIRF model) simulated only environmental stream flow components (i.e. high flow, low flow and extremely low flow). Furthermore, studies which used a withdrawal index, surface water use intensity index, or water exploitation index, estimated the proportion of the water withdrawn from stream for hydraulic fracturing relative to the stream flow in relation to the orders of streams and the overall discharge of the study area.

3.2. POTENTIAL OPPORTUNITIES FOR FUTURE RESEARCH

This review has identified missing information and gaps in the current understanding of GW-SW interaction associated with the effects of water withdrawal for hydraulic fracturing. The following research areas are considered as potential opportunities for future study:

How the mechanism and quantity of water withdrawal from surface water (i.e. streams) and groundwater sources for hydraulic fracturing might affect groundwater discharge (i.e. base flow), surface water and groundwater levels, and groundwater contributions to stream flow in shale gas and oil play areas. In line with this, questions for consideration should include: What are the temporal patterns of those impacts throughout the year and what are the spatial patterns of those impacts in a shale gas and oil play area? Since previous studies have demonstrated that water withdrawal from streams has little impact on stream flow in comparatively large watersheds, further research should be done at a small scale (e.g. streams with small catchment areas) to better understand localized GW-SW interaction and quantify the impacts of water withdrawal from surface water (streams) and groundwater for hydraulic fracturing. In addition, models should use a finer grid resolution (e.g. 10 m by 10 m grid cells) to understand and visualize those impacts on groundwater level changes, near to the surface water withdrawal locations in stream.

What are the temporal and spatial patterns of the impacts of water withdrawal for hydraulic fracturing on other surface water bodies, especially lakes and wetlands?

What are the potential impacts of water withdrawal for hydraulic fracturing on other water users, such as agriculture, mining, manufacturing industries, municipal water supply, especially in regions with limited water resources?

Do we need to improve the definition of passby flow for lower order streams, especially during periods of low flow because the relative reduction in stream flow is higher in those streams due to water withdrawal? Passby flow is defined as the minimum stream flow that must be allowed to pass through a prescribed point of stream at any time, during which a water withdrawal is occurring from that point (Liu et al. 2018). When the natural flow is below the threshold passby flow at a prescribed point of stream, water withdrawal must be stopped from that point, and the entire natural flow must be allowed to pass through that point of stream.

Can pressure changes in hydraulic fracturing activate fracture connections to change flow to or from streams/lakes/wetlands, which might affect GW-SW interaction? This research should be conducted at a small scale to understand and quantify any variation.

Addressing these questions would provide comprehensive information needed to develop regional water budgets, which will help regional water managers to develop sustainable water resources management plans in shale gas and oil play regions. For example, the temporal (i.e. monthly, seasonal, annual) changes in groundwater contributions to stream flow could determine the temporal status of groundwater resources and site conditions for groundwater-dependent terrestrial ecosystems (Naumburg et al. 2005). Determination of the monthly, seasonal and annual variations in the dependency of stream flow on groundwater, together with temporal surface water flow, would provide useful information to set monthly, seasonal and annual water extraction limits from the rivers, lakes and groundwater, and aid allocation to stakeholders for future water supply. In addition, a better understanding of GW-SW interactions will help water managers to take proper actions to maintain healthy aquatic and terrestrial ecosystems. For example, suspending water licenses for water withdrawal from local water sources during periods of low flow and drought, recycling water for hydraulic fracturing, promoting hydraulic fracturing during high flow and water level in rivers, streams and lakes, building water reservoirs, and encouraging the use of alternative fracturing fluids (e.g. frac oil; a combination of frac oil and nitrogen; a combination of frac oil and carbon dioxide, or; a combination of frac oil, acid water and hydrochloric acid) in regions with limited water resources during periods of low flow and drought.

The oil and gas industry currently uses a range of conservation practices for hydraulic fracturing to manage water resources, which mainly fall into three categories: 1) using lower quality water from non-traditional sources, 2) recycling and reusing produced and flowback waters, and 3) building infrastructure for transporting water (American Petroleum Institute 2017). Here, produced water means the water naturally present in the geologic formation, flowing to the surface along with oil and gas when those are pumped from the well (Freyman 2014), and flowback water refers to the water injected into the well as a fracturing fluid comes back to the surface after the end

of hydraulic fracturing. The choice to use each practice(s) is based on a variety of factors, such as local water stresses, individual business needs, and the particular requirements for specific geologic formations. In Canada, the oil and gas industry uses deep saline and non-potable groundwater (Encana 2013), water reservoir and lined water storage pits (Chevron Canada 2019), water resource hub that recycle produced water (Encana 2013), water treatment plants (Encana 2019), recycling and reusing produced and flowback waters (BC Oil & Gas Commission 2012). In the USA, recycling and reusing of produced and flowback waters is very common (U.S. Chamber of Commerce Foundation 2019), as well as buying effluent water from local municipalities (Freyman 2014).

There are significant challenges to overcome in order to address the identified research gaps. The major challenge results from limited data with which to assess the effects of water withdrawal for hydraulic fracturing on GW-SW interaction. For example, the limited number of groundwater monitoring wells and surface water monitoring gauges is one concerning issue. This problem is more significant in Canadian shale gas and oil play regions (i.e. Alberta and British Columbia) than in the USA. For example, in the Duvernay Formation (approximately 130,000 km^2) in Alberta, Canada, there are publicly available records for only 60 active groundwater monitoring wells, accessible from Alberta provincial groundwater monitoring wells database (http://environment.alberta.ca/apps/GOWN/), and 10 surface water monitoring stations, which are maintained by the Water Survey of Canada (https://wateroffice.ec.gc.ca/).

In addition, monitoring stations of surface water bodies are primarily in streams and rivers, with very few in lakes and wetland areas. Furthermore, datasets that cover a wide spatial distribution of hydraulically fractured wells are not available for longer time periods (e.g. 10 years). For example, in the USA, this information has been available in the national hydraulic fracturing chemical registry called "fracfocus.org" since April 11, 2011 (United States Environmental Protection Agency 2015). Whereas in Canada, this data is accessible from a publicly available chemical disclosure registry called "fracfocus.ca" since January 1, 2012 in British Columbia, and December 19, 2012 in Alberta (Rivard et al. 2014). Another issue arises from a lack of data on the timing of water withdrawal for each well, the type of water source for hydraulic fracturing, and the locations of the water source in many shale gas and oil play regions. Having more comprehensive and readily available data would greatly assist in addressing the identified research gaps more accurately, through use of more detailed hydrological models.

Currently, there are no specific regulations in the USA or Canada specific to water withdrawal for hydraulic fracturing activities. Richardson et al. (2013) conducted a survey of regulations in 31 states where sources of shale gas and oil are available or might be available, and found that several states had discussed rules and restrictions for water withdrawal specific to shale gas and oil industry, however only in draft form. It was found that none had passed such legislation, and so these 31 states regulate water withdrawal (both surface water and groundwater) under general regulations. Meanwhile, 13 states (Texas, Utah, Colorado, Nebraska, Wyoming, Kansas, Oklahoma, New Mexico, California, Arkansas, Maryland, Pennsylvania and North Dakota) require water permits for all water withdrawal activities. 4 states (Michigan, New York, Georgia and New Jersey) require water permits only for water withdrawal over a specific threshold at 378.54 m^3 per day or more**.** Similarly, Montana, South Dakota, Mississippi and Kentucky require permits over 190.78 m^3, 98.12 m^3, 75.70 m^3 and 37.85 m^3 per day, respectively. Virginia has the highest threshold, requiring permits for water withdrawal of 1,135.62 m^3 per day or more. More stringently, 3 states (Indiana, Ohio, and Vermont) require permit, registration and reporting over a specific threshold. While Indiana requires permit, registration and reporting of withdrawal over 378.54 m^3 per day, Ohio and Vermont require registration and reporting for water withdrawal over 378.54 m^3 and 75.70 m^3 per day, respectively, but also require permits only when water withdrawal is more than 7,570.82 m^3 and 218 m^3 per day, respectively. West Virginia, Illinois, Alabama, Tennessee, and North Carolina do not require any permits, but mandate registration and reporting for water withdrawal for over 26.50 m^3, 378.54 m^3, 378.54 m^3, 37.85 m^3 and 378.54 m^3 per day, respectively. Comparably, Louisiana does not provide any permits, but requires registration and reporting for all water withdrawals.

In Canada, there are also no water withdrawal regulations specific to hydraulic fracturing. For example, in Alberta and British Columbia where the majority of hydraulic fracturing activities occur, the oil and gas operators have to submit their water license applications along with their requested water demand for a specific year (e.g. in British Columbia 3 years projection period). The request for water demand will consider the numbers of wells to be completed in a specific period, how much water will be required, if there will be any recycling and which sources (i.e. groundwater and/or surface water) and locations will be used for hydraulic fracturing activities. The corresponding authorities (Alberta Energy Regulator in Alberta, and British Columbia Oil and Gas Commission in British Columbia) determine the outcome of applications depending on available water resources. Alternatively in Saskatchewan and Manitoba, water licenses are required for industrial activities when water withdrawal is over 4,933.92 m^3, and 25 m^3 per day, respectively.

4. CONCLUSIONS

This review discussed and evaluated the context and effects of water withdrawals for hydraulic fracturing on surface water and groundwater resources, based on previously published literature. It was found that water withdrawal for hydraulic fracturing has negative impacts on the volume of water resources, and that most of the quantitative research focused on surface water sources, particularly focusing on water withdrawal from streams only. The key findings of those quantitative studies include: 1) the effects of water withdrawal from streams for hydraulic fracturing on stream flow depend not only proportionally on the volume of water withdrawn, but also inversely on the stream size and watershed area; 2) the effects of water withdrawal from streams for hydraulic fracturing on stream flow depend on both temporal and spatial components of stream flow in the watershed; 3) during periods of low flow, water withdrawal from streams for hydraulic fracturing have significant effect on environmental flow of lower order stream in small watershed, and; 4) groundwater level decreases locally and proportionally to the volume of water withdrawn from the groundwater pumping well for hydraulic fracturing. This review also demonstrates that there is a lack of published research that quantifies changes in the GW-SW interaction under the effects of water withdrawal for hydraulic fracturing. Based on this, suggestions for further research are made, alongside identifying the current data limitations that constrain robust analysis. In particular, the effects of water withdrawal on lakes and wetlands during periods of low flow, and in areas of groundwater flow, require further investigation. Natural gas production using hydraulic fracturing is expected to increase globally to meet future energy demands. Given the extensive use of water, a much better understanding of the effects on watersheds and hydrologic function, is required. The development of sustainable water resource management plans calls for a much better understanding of GW-SW interactions.

REFERENCES

- ALL Consulting, 2012, The modern practices of Hydraulic fracturing: a focus on Canadian resources, prepared for Petroleum Technology Alliance Canada and Science and Community Environmental Knowledge Fund, Tulsa, Oklahoma, 229 pp.
- American Petroleum Institute, 2017, Hydraulic fracturing. Unlocking America's natural gas resources, available online at https://www.api.org/~/media/Files/Oil-and-Natural-Gas/Hydraulic-Fracturing-primer/Hydraulic-Fracturing-Primer.pdf (data access 07.12.2020)
- Barbot E., Vidic N.S., Gregory K.B., Vidic R.D., 2013, Spatial and temporal correlation of water quality parameters of produced waters from Devonian-age shale following hydraulic fracturing, Environmental Science & Technology, 47 (6), 2562-2569, DOI: 10.1021/es304638h
- Barth-Naftilan E., Aloysius N., Saiers J.E., 2015, Spatial and temporal trends in freshwater appropriation for natural gas development in Pennsylvania's Marcellus Shale Play, Geophysical Research Letter, 42 (15), 6348-6356, DOI: 10.1002/2015GL065240
- BC Oil & Gas Commission, 2012, Water use in oil and gas activities. 2012 Annual Report., available online at https://www.bcogc.ca/files/reports/Technical-Reports/annual-water-report-2012.pdf (data access 07.12.2020)
- Best L.C., Lowry C.S., 2014, Quantifying the potential effects of high-volume water extractions on water resources during natural gas development: Marcellus Shale, NY, Journal of Hydrology: Regional Studies, 1, 1-16, DOI: 10.1016/j.ejrh.2014.05.001
- Brisbane Declaration, 2007, The Brisbane Declaration: environmental flows are essential for freshwater ecosystem health and human well-being, Declaration of the 10th International River symposium and International Environmental Flows Conference, Brisbane, Australia, 3-6 September 2007, available online at http://riverfoundation.org.au/wp-content/uploads/2017/02/THE-BRISBANE-DECLARATION.pdf (data access 11.12.2020)
- Brittingham M.C., Maloney K.O., Farag A.M., Harper D.D., Bowen Z.H., 2014, Ecological risks of shale oil and gas development to wildlife, aquatic resources and their habitats, Environmental Science & Technology, 48 (19), 11034-11047, DOI: 10.1021/es5020482
- Buchanan B.P., Auerbach D.A., McManamay R.A., Taylor J.M., Flecker A.S., Archibald J.A., Fuka D.R., Walter M.T., 2017, Environmental flows in the context of unconventional natural gas development in the Marcellus Shale, Ecological Applications, 27 (1), 37-55, DOI: 10.1002/eap.1425
- Carlson M., Stelfox B., 2014, The cumulative effects of hydraulic fracturing in Alberta's eastern slopes, prepared for the project: CWN Hydraulic Fracturing and Water-Landscape Impacts, 40 pp.
- Chevron Canada, 2019, Water management Chevron's approach to protecting this critical natural resource, available online at https://canada.chevron.com/environment/water-management (data access 07.12.2020)
- Colborn T., Schultz K., Herrick L., Kwiatkowski C., 2014, An exploratory study of air quality near natural gas operations, Human and Ecological Risk Assessment: An International Journal, 20 (1), 86-105, DOI: 10.1080/10807039.2012.749447
- Cooley H., Donnelly K., 2012, Hydraulic fracturing and water resources: Separating the frack from the fiction, Pacific Institute, Oakland, CA, USA, 35 pp., available online at http://pacinst.org/wp-content/uploads/sites/21/2014/04/fracking-water-sources.pdf (data access 07.12.2020)
- Cothren J., Thoma G., Diluzio M., Limp F., 2013, Integration of water resource models with Fayetteville Shale decision support and information system, Final Technical Report, University of Arkansas and Blackland Texas A&M Agrilife, DE-FC2609FE0000804, 161 pp.,. available online at https://core.ac.uk/download/pdf/188994778.pdf (data access 07.12.2020)
- Dresel P., Rose A., 2010, Chemistry and origin of oil and gas well brines in Western Pennsylvania, Pennsylvania Geological Survey, 4th series Open-File Report OFOG 10-01.0; 48 pp.
- Encana, 2013, 2013 Sustainability report, Calgary, Alberta, available at http://www.encana.com/pdf/sustainability/corporate/reports/sustainability-report-2013.pdf (07.12.2020)
- Encana, 2019, Debolt facility provides alternative to surface water sources, available online at https://www.encana.com/news-stories/our-stories/environment-debolt-facility.html (data access 07.12.2020)
- Entrekin S., Evans-White M., Johnson B., Hagenbuch E., 2011, Rapid expansion of natural gas development poses a threat to surface waters, Frontiers in Ecology and the Environment, 9 (9), 503-511, DOI: 10.1890/110053
- Entrekin S., Trainor A., Saiers J., Patterson L., Maloney K., Fargione J., Kiesecker J., Baruch-Mordo S., Konschnik K., Wiseman H., Nicot J.-P., Ryan J.N., 2018, Water stress from high-volume hydraulic fracturing potentially threatens aquatic biodiversity and ecosystem services in Arkansas, United States, Environmental Science & Technology, 52 (4), 2349-2358, DOI: 10.1021/acs.est.7b03304
- Fontenot B.E., Hunt L.R., Hildenbrand Z.L., Carlton D.D., Oka H., Walton J.L., Hopkins D., Osorio A., Bjorndal B., Hu Q.H., Schug K.A., 2013, An evaluation of water quality in private drinking water wells near natural gas extraction sites in the Barnett Shale formation, Environmental Science & Technology, 47 (17), 10032-10040, DOI: 10.1021/es4011724
- Freyman M., 2014, Hydraulic fracturing & water stress: Water Demand by the Numbers- Shareholder, Lender & Operator Guide to Water Sourcing, Ceres Report, available online at https://www.oilandgasbmps.org/viewpub.php?id=674 (data access 07.12.2020)
- Gallegos T.J., Varela B.A., 2015, Trends in hydraulic fracturing distributions and treatment fluids, additives, proppants, and water volumes applied to wells drilled in the United States from 1947 through 2010 – Data analysis and comparison to the literature, U.S. Geological Survey Scientific Investigations, Report 2014-5131, 15 pp., available online at https://pubs.usgs.gov/sir/2014/5131/ (data access 07.12.2020)
- Gordalla B.C., Ewers U., Frimmel F.H., 2013, Hydraulic fracturing: a toxicological threat for groundwater and drinking-water?, Environmental Earth Science, 70, 3875-3893, DOI: 10.1007/s12665-013-2672-9
- Gregory K.B., Vidic R.D., Dzombak D.A., 2011, Water management challenges associated with the production of shale gas by hydraulic fracturing, Elements, 7, 181-186, DOI: 10.2113/gselements.7.3.181
- Holland A., 2011, Examination of possibly induced seismicity from hydraulic fracturing in the Eola Field, Garvin County, Oklahoma, Oklahoma Geological Survey, Open-File Report, OF1-2011, 31 pp., available online at http://www.ogs.ou.edu/pubsscanned/openfile/OF1_2011.pdf (data access 07.12.2020)
- Howarth R.W., Santoro R., Ingraffea A., 2011, Methane and the greenhouse-gas footprint of natural gas from shale formations, Climatic Change, 106, 679-690, DOI: 10.1007/s10584-011-0061-5
- Kalbus E., Reinstorf F., Schirmer M., 2006, Measuring methods for groundwater-surface water interactions: a review, Hydrology and Earth System Science, 10, 873-887, DOI: 10.5194/hess-10-873-2006
- Kargbo D.M., Wilhelm R.G., Campbell D.J., 2010, Natural gas plays in the Marcellus Shale: challenges and potential opportunities, Environmental Science & Technology, 44, 5679-5684, DOI: 10.1021/es903811p
- Keranen K.M., Weingarten M., Abers G.A., Bekins B.A., Ge S., 2014, Sharp increase in central Oklahoma seismicity since 2008 induced by massive wastewater injection, Science, 345 (6195), 448-451, DOI: 10.1126/science.1255802

- Kondash A.J., Lauer N.E., Vengosh, A., 2018, The intensification of the water footprint of hydraulic fracturing, Science Advances, 4 (8), eaar5982, DOI: 10.1126/sciadv.aar5982
- Kuwayama Y., Olmstead S., Krupnick A., 2015, Water quality and quantity impacts of hydraulic fracturing, Current Sustainable Renewable Energy Reports, 2, 17-24, DOI: 10.1007/s40518-014-0023-4
- Lin Z., Lin T., Lim S.H., Hove M.H., Schuh W.M., 2018, Impacts of Bakken Shale oil development on regional water uses and supply, Journal of the American Water Resources Association, 54 (1), 225-239, DOI: 10.1111/1752-1688.12605
- Liu C., Zhang Z., Balay J.W., 2018, Posterior assessment of reference gages for water resources management using instantaneous flow measurements, Science of the Total Environment, 634, 12-19, DOI: 10.1016/j.scitotenv.2018.03.312
- MacQuarrie A., 2018, Case study analysis on the impacts of surface water allocations for hydraulic fracturing on surface water availability of the Upper Athabasca River, Master's Thesis, Royal Roads University, 117 pp., available online at https://viurrspace.ca/handle/10613/5688 (data access 07.12.2020)
- Myers T., 2012, Potential contaminant pathways from hydraulically fractured shale to aquifers, Groundwater, 50 (6), 872-882, 10.1111/j.1745-6584.2012.00933.x
- Naumburg E., Mata-Gonzalez R., Hunter R., Mclendon T., Martin D., 2005, Phreatophytic vegetation and groundwater fluctuations: A review of current research and application of ecosystem response modeling with an emphasis on Great Basin vegetation, Environmental Management, 35, 726-740, DOI: 10.1007/s00267-004-0194-7
- Nicot J.P., Scanlon B.R., 2012, Water use for Shale – Gas production in Texas, U.S., Environmental Science & Technology, 46 (6), 3580-3586, DOI: 10.1021/es204602t
- Oil and Gas Info, 2019, All about fracking, available online at https://oilandgasinfo.ca/all-about-fracking/ (data access 07.12.2020)
- Olmstead S.M., Muehlenbachs L.A., Shih J., Chu Z., Krupnick A.J., 2013, Shale gas development impacts on surface water quality, [in:] Proceedings of the National Academy of Sciences of the United States of America, 10 (13), 4962-4967
- Osborn S.G., Vengosh A., Warner N.R., Jackson R.B., 2011, Methane contamination of drinking water accompanying gas-well drilling and hydraulic fracturing, [in:] Proceedings of the National Academy of Sciences of the United States of America, 108 (20), 8172-8176
- Rahm B.G., Riha S.J., 2012, Toward strategic management of shale gas development: regional, collective impacts on water resources, Environmental Science & Policy, 17, 12-23, DOI: 10.1016/j.envsci.2011.12.004
- Richardson N., Gottlieb M., Krupnick A., Wiseman H, 2013, The state of state shale gas regulation, Resources For The Future Report, available online at https://www.rff.org/publications/reports/the-state-of-state-shale-gas-regulation/ (data access 07.12.2020)
- Rivard C., Lavoie D., Lefebvre R., Sejourne S., Lamontagne C., Duchesne M., 2014, An overview of Canadian Shale gas production and environmental concerns, International Journal of Coal Geology, 126, 64-76, DOI: 10.1016/j.coal.2013.12.004
- Rosa L., D'Odorico P., 2019, The water-energy-food nexus of unconventional oil and gas extraction in the Vaca Muerta Play, Argentina, Journal of Cleaner Production, 207, 743-750, DOI: 10.1016/j.jclepro.2018.10.039
- Rowan E., Engle M., Kirby C., Kraemer T., 2011, Radium content of oil- and gas-field produced waters in the northern Appalachian Basin (USA): summary and discussion of data, U.S. Geological Survey Scientific Investigations Report 513, 31 pp., DOI: 10.3133/sir20115135
- Saha G.C., 2016, Investigation of temporal dynamics of hydraulic fracturing and water use: a case study from northwestern Alberta, Canada, [in:] Under Western Skies 2016, September 27-30, Calgary, Canada
- Shank M.K., Stauffer Jr. J.R., 2015, Land use and surface water withdrawal effects on fish and macroinvertebrate assemblages in the Susquehanna River basin, USA, Journal of Freshwater Ecology, 30 (2), 229-248, DOI: 10.1080/02705060.2014.959082
- Sharma S., Shrestha A., McLean C.E., Martin S.C., 2015, Hydrologic modelling to evaluate the impact of hydraulic fracturing on stream low flows: challenges and opportunities for a simulation study, American Journal of Environmental Sciences, 11 (4), 199-215, DOI: 10.3844/ajessp.2015.199.215
- Shrestha A., Sharma S., McLean C.E., Kelly B.A., Martin S.C., 2016, Scenario analysis for assessing the impact of hydraulic fracturing on stream low flows using the SWAT model, Hydrological Sciences Journal, 62 (5), 849-861, DOI: 10.1080/02626667.2016.1235276
- Sophocleous M., 2002, Interactions between groundwater and surface water: the state of the science, Journal of Hydrogeology, 10, 52-67, DOI: 10.1007/s10040-001-0170-8
- Su X.S., Cui G., Wang H., Dai Z.X., Woo Nam-Chil., Yuan W.Z., 2018, Biogeochemical zonation of sulfur during the discharge of groundwater to lake in desert plateau (Dakebo Lake, NW China), Environmental Geochemistry and Health, 40 (3), 1051-1066, DOI: 10.1007/s10653-017-9975-9
- Sullivan K., Cyterski M., Kraemer S., Knightes C., Price K., Kim K., Prieto L., Gabriel M., Sidle R., 2015, Case study analysis of the impacts of water acquisition for hydraulic fracturing on local water availability, U.S. Environmental Protection Agency, Washington, DC, EPA/600/R-14/179, available online at https://www.epa.gov/sites/production/files/2015-07/documents/hf_water_acquisition_report_final_6-3-15_508_km.pdf (data access 07.12.2020)
- U.S. Chamber of Commerce Foundation, 2019, Recycling water in hydraulic fracturing, available online at https://www.uschamberfoundation.org/recycling-water-hydraulic-fracturing (data access 07.12.2020)
- United States Environmental Protection Agency, 2015, Analysis of Hydraulic Fracturing Fluid Data from the FracFocus Chemical Disclosure Registry 1.0, Office of Research and Development, Washington, DC, EPA/601/R-14/003, available online at https://www.epa.gov/hfstudy/analysis-hydraulic-fracturing-fluid-data-fracfocus-chemical-disclosure-registry-1-pdf (data access 07.12.2020)
- Vandecasteele I., Marí Rivero I., Sala S., Baranzelli C., Barranco R., Batelaan O., Lavalle C., 2015, Impact of shale gas development on water resources: a case study in Northern Poland, Environmental Management, 55, 1285-1299, DOI: 10.1007/s00267-015-0454-8
- Vengosh A., Warner N., Jackson R., Darrah T., 2013, The effects of shale gas exploration and hydraulic fracturing on the quality of water resources in the United States, Procedia Earth and Planetary Science, 7, 863-866, DOI: 10.1016/j.proeps.2013.03.213
- Vengosh A., Jackson R.B., Warner N., Darrah T.H., Kondash A., 2014, A critical review of the risks to water resources from unconventional shale gas development and hydraulic fracturing in the United States, Environmental Science & Technology, 48 (15), 8334-8348, DOI: 10.1021/es405118y
- Vidic R.D., Brantley S.L., Vandenbossche M., Yoxtheimer D., Abad J.D., 2013, Impact of shale gas development on regional water quality, Science, 340, 6134, DOI: 10.1126/science.1235009
- Warner N.R., Christie C.A., Jackson R.B., Vengosh A., 2013, Impacts of shale gas wastewater disposal on water quality in Western Pennsylvania, Environmental Science & Technology, 47(20), 11849-11857, DOI: 10.1021/es402165b
- Warner N.R., Jackson R.B., Darrah T.H., Osborn S.G., Down A., Zhao K., White A., Vengosh A., 2012, Geochemical evidence for possible natural migration of Marcellus Formation brine to shallow aquifers in Pennsylvania, [in:] Proceedings of the National Academy of Sciences of the United States of America, 109 (30), 11961-11966, DOI: 10.1073/pnas.1121181109
- Wu X., Xia J., Guan B., Yan X., Zou L., Liu P., Yang L., Hong S., Hu, S., 2019, Water availability assessment of shale gas production in the Weiyuan Play, China, Sustainability, 11 (3), 940, DOI: 10.3390/su11030940

Reviewers Cooperating with Editorial Board of Meteorology Hydrology and Water Management magazine in 2020

Robert Banasiak
Nejc Bezak
Marek Błaś
Mariano Bresciani
Jakub Fuska
Liudmyla Gorbachova
Ferda Imanov
Petr Janal
Radosław Juszczak
Tomasz Kałuża
Justas Kažys
Valeriy Khokhlov
Janusz Kindler
Krzysztof Kochanek
Leszek Kolendowicz
Andrzej Kotowski
Jacek Kurnatowski
Ainis Lagzdins
Henny van Lanen
Ondrej Ledvinka
Tomáš Lepeška
Alicja Lisowska
Artur Magnuszewski
Michał Marosz
Zoya Mateeva
Tomasz Okruszko
Juraj Parajka
Marek Półrolniczak
Artur Radecki-Pawlik
Stanisław Rolbiecki
P.K. Singh
Tomasz Stuczyński
Łukasz Szałata
Tomasz Tymiński
Stanisław Węglarczyk
Ramos Yvette

THANK YOU

METEOROLOGY HYDROLOGY AND WATER MANAGEMENT
IMGW-PIB Science Journal since 2013

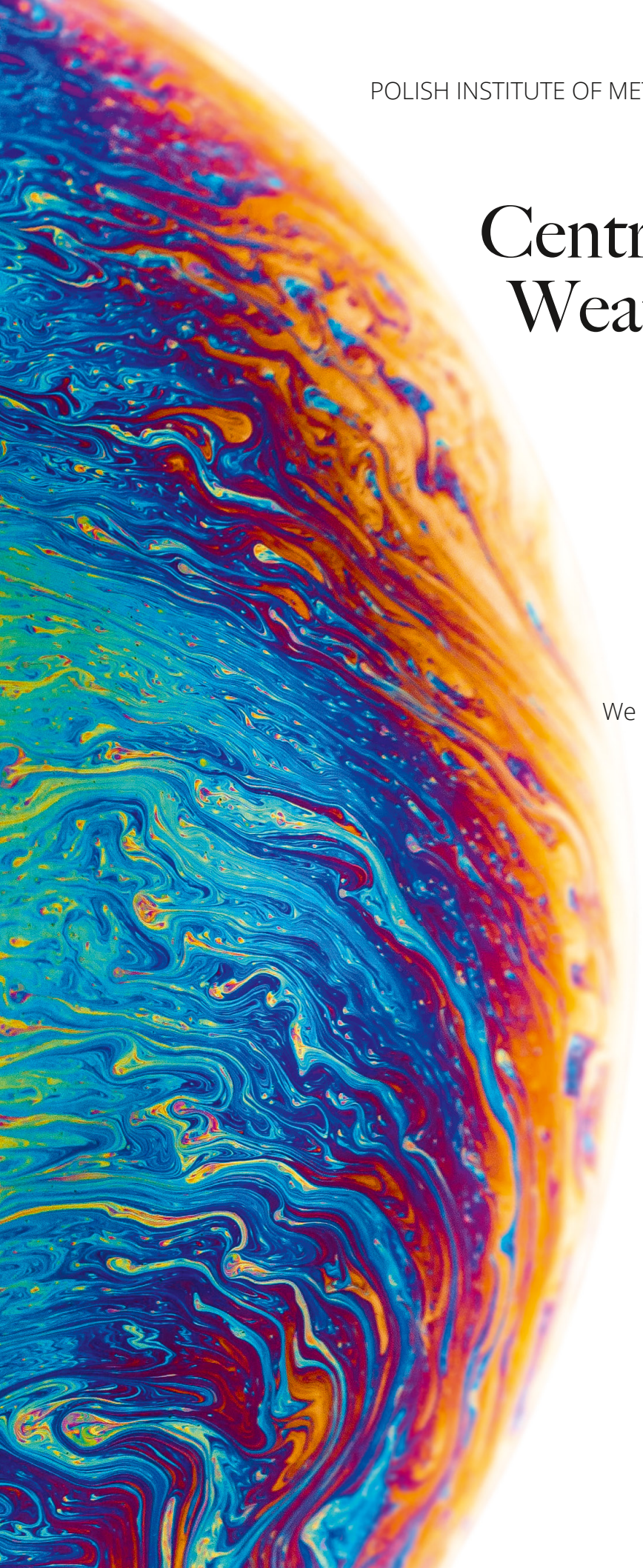

POLISH INSTITUTE OF METEOROLOGY AND WATER MANAGEMENT
– NATIONAL RESEARCH INSTITUTE

Centre of Numerical Weather Prediction

We built Center based on science knowledge and power of supercomputers, allowing much finer numerical resolution and fewer approximations in the operational atmospheric models.

We use accurate methods of data assimilation, which result in improved initial conditions for the models.

imgw.pl
meteo.imgw.pl
mhmm.com
obserwator.imgw.pl